Dynamisch gedrag van oscillatornetwerken

Dynamic Behavior of Oscillator Networks

Jonathan A. A. Rogge

Promotor: prof. dr. ir. D. Aeyels
Proefschrift ingediend tot het behalen van de graad van
Doctor in de Ingenieurswetenschappen: Toegepaste Natuurkunde

Vakgroep Elektrische Energie, Systemen, en Automatisering
Voorzitter: Prof. dr. ir. J. Melkebeek
Faculteit Ingenieurswetenschappen
Academiejaar 2005–2006

Dynamic Behavior of Oscillator Networks
Jonathan A. A. Rogge

Supervisor:
prof. dr. ir. Dirk Aeyels

Address:
Onderzoeksgroep SYSTeMS
Vakgroep Elektrische Energie, Systemen, en Automatisering (TW08)
Universiteit Gent
Technologiepark Zwijnaarde 914
B-9052 Zwijnaarde
België

This book was typeset using LaTeX.

ISBN
NUR
Wettelijk depot

Acknowledgments

During the five years that I spent working on my PhD, I met many people, who – directly or indirectly – had an influence on the present dissertation. This seems the perfect opportunity to express my gratitude to these people.

Foremost I would like to thank Dirk Aeyels, my supervisor, for his scientific guidance, the many fine hours of cooperation and the spirited discussions. I also thank Rodolphe Sepulchre and Brian Anderson, who took a particular interest in my research and offered some interesting suggestions.

Many thanks to my colleagues and former colleagues for the interesting conversations on science and other topics and for the inspiring atmosphere in the office: Gert, René, Jacques, Patrick, Luc, George, Matthias, Filip ($\times 2$), Erik, Mila, Guido, Tite, Valery and Margot. I'd also like to thank all my friends, who were there when I needed them and with whom I spent many enjoyable hours: Rogier & Marloes, Tim, Jeroen, Cedric, Valdo & Ibi, Elena, Helga & Johan, Frederik & Tilly, Kristel, Paul, Michiel, Sabine, Bellie, Trixie, Greet,...

I thank my parents for their unconditional love and everlasting support. And finally, thank you, Jana, for making the picture complete.

This dissertation presents research results of the Belgian Programme on Interuniversity Attraction Poles, initiated by the Belgian Federal Science Policy Office. The scientific responsibility rests with its author.

Jonathan A. A. Rogge
Gent

Contents

The dream was always running ahead of me. To catch up, to live for a moment in unison with it, that was the miracle.

Anais Nin (1903 - 1977)

Nederlandstalige Samenvatting

Systemen van onderling gekoppelde oscillatoren zijn alomtegenwoordig in de natuur. Voorbeelden hiervan omvatten congregaties van flikkerende vuurvliegjes en het synchrone kloppen van pacemakercellen in het hart. Interessante ingenieurstoepassingen zijn antennegroeperingen, die b.v. in draadloze communicatie worden gebruikt, en rijen van gekoppelde Josephsonjuncties, die o.a. in hersenscanners en atmosferische pollutiecontrole worden toegepast. De gemeenschappelijke kenmerken van de bovengenoemde systemen worden adequaat gemodelleerd door het Kuramotomodel. Dit model is gebaseerd op twee vereenvoudigende veronderstellingen:

- Elke oscillator wordt beschreven door een scalaire dynamica op de eenheidscirkel. De evolutie van elke oscillator kan dan gevisualiseerd worden als een punt dat op de eenheidscirkel beweegt. Een oscillatie komt overeen met een rotatie over 2π op de cirkel.

- De interactie tussen oscillatoren is zwak.

Deze veronderstellingen laten een eenvoudig model toe dat alle kenmerken van het originele systeem behoudt.

Het Kuramotomodel dient als uitgangspunt van dit proefschrift. We voeren een wiskundige analyse van twee types *eindige* netwerken van interagerende oscillatoren uit:

- globale koppeling: elke oscillator is aan alle andere oscillatoren in het netwerk gekoppeld,

- unidirectionele ringkoppeling: de oscillatoren worden gekoppeld in een ring; elke oscillator beïnvloedt precies één andere oscillator en de koppelingen zijn hetzij allemaal in wijzerzin, hetzij allemaal in tegenwijzerzin gericht.

Globale koppeling

In de literatuur is de analyse van oneindige netwerken (of populaties) van globaal gekoppelde oscillatoren goed gekend. Oneindige netwerken vertonen *partiële synchronisatie*: één groep oscillatoren *fasevergrendelt* (d.w.z. alle oscillatoren van de groep oscilleren aan dezelfde frequentie met constante onderlinge faseverschillen), terwijl de faseverschillen tussen de oscillatoren van de resterende groep variëren in de tijd. De stabiliteitseigenschappen van partiële synchronisatie zijn tot op heden niet mathematisch aangetoond. Dit brengt ons ertoe om de eindige tegenhanger van het oneindige globaal gekoppelde netwerk te onderzoeken. Ten eerste zijn netwerken die uit een eindig aantal interagerende deelsystemen bestaan belangrijker om te bestuderen aangezien alle netwerken in de reële wereld eindig zijn. Ten tweede brengt onze analyse kwalitatieve verschillen en gelijkenissen tussen eindige en oneindige oscillatornetwerken naar voren.

Alvorens met de analyse van eindige oscillatornetwerken van start te gaan, bekijken we eerst **lineair interagerende scalaire systemen** (ook *agenten* genoemd) waarbij we de interconnectietopologie vrij laten:

$$\dot{x}_i = \omega_i + \sum_{j \in \mathcal{N}_i} (x_j - x_i), \quad i \in \mathcal{N} \triangleq \{1, \ldots, N\}, \tag{1}$$

waarbij $x_i, \omega_i \in \mathbb{R}$, $\forall i \in \mathcal{N}$ en met $\mathcal{N}_i$ de verzameling agenten die de i-de agent rechtstreeks beïnvloeden. Dit type netwerken vertoont *toestandsvergrendeling*: $x_i(t) - x_j(t) = c_{ij} \in \mathbb{R}$, $\forall t \in \mathbb{R}$, $\forall i, j \in \mathcal{N}$. De interconnecties tussen de agenten kunnen voorgesteld worden d.m.v. een geöriënteerde graf waarvan de knopen de agenten voorstellen, en de takken de interacties zijn. We bewijzen het volgende theorema:

Theorema 1. *Elke begintoestand van systeem (1) convergeert naar een toestandsvergrendelde oplossing als en slechts als het netwerk een globaal achterwaarts bereikbare knoop bezit.*

Een netwerk bezit een globaal achterwaarts bereikbare knoop als men vanuit deze knoop alle andere knopen langs takken van het netwerk kan bereiken. Verder dient opgemerkt dat het geïnterconnecteerde lineaire systeem (1) een translatiesymmetrie bezit die zich onder andere manifesteert in een nuleigenwaarde in de systeemmatrix. Deze nuleigenwaarde is structureel en heeft geen invloed op de stabiliteit van het systeem: als alle overige eigenwaarden een negatief reëel deel bezitten is het systeem asymptotisch stabiel. Dat systeem (1) deze eigenschap bezit, wordt aangetoond in Hoofdstuk 4.

De vergelijkingen die een **eindig globaal gekoppeld oscillatornetwerk** beschrijven, zijn

$$\dot{\theta}_i = \omega_i + \frac{K}{N} \sum_{j=1}^{N} \sin(\theta_j - \theta_i), \qquad i \in \mathcal{N}, \tag{2}$$

waarbij $\theta_i \in S^1 \triangleq \mathbb{R} \mod 2\pi$ de *fase* en $\omega_i \in \mathbb{R}$ de *natuurlijke frequentie* van de i-de oscillator is. De parameter $K \geq 0$ wordt de *koppelsterkte* genoemd.

We starten de analyse van (2) met een behandeling van eindige populaties van globaal gekoppelde *identieke* oscillatoren. We bekomen een karakterisering van de fasevergrendelde oplossingen door gebruik te maken van het concept "complexe ordeparameter". Wanneer de fase van elke oscillator door een punt op de eenheidscirkel in het complexe vlak wordt voorgesteld, is de complexe ordeparameter eenvoudigweg het zwaartepunt van alle fases.

Theorema 2. *Elke fasevergrendelde oplossing van systeem (2) met identieke oscillatoren behoort tot de klasse van elementaire oplossingen (d.i. het faseverschil tussen elk paar oscillatoren neemt de waarde nul of π aan), of de amplitude van de overeenkomstige ordeparameter is nul.*

Deze twee voorwaarden sluiten elkaar niet uit: er bestaan elementaire oplossingen met een amplitude van de ordeparameter gelijk aan nul.

De stabiliteit van het systeem wordt bepaald door gebruik te maken van de gradiëntstructuur van het systeem. We bewijzen dat elke begintoestand die zich niet op de stabiele manifold van één van de instabiele evenwichtspunten bevindt, naar de oorsprong van het systeem convergeert. Dit impliceert dat de gesynchroniseerde oplossing (d.i. alle faseverschillen gelijk aan nul) bijna-overal-asymptotisch stabiel is.

Vervolgens bekijken we het geval waarbij de natuurlijke frequenties van de oscillatoren *niet identiek* zijn. In tegenstelling tot het identieke geval, waar fasevergrendeling een stabiel gedrag is voor alle koppelsterktes verschillend van nul, bestaat fasevergrendeling niet onder een kritieke waarde K_T van de koppelsterkte. We stellen een algoritme op om de waarde van K_T te berekenen en geven een nodige en voldoende voorwaarde voor het bestaan van fasevergrendeling. De constante amplitude r_∞ van de ordeparameter, die met een bepaalde fasevergendelde oplossing overeenkomt, voldoet aan een consistentievoorwaarde:

$$r_\infty = \frac{1}{N} \sum_{j=1}^{N} \pm \sqrt{1 - \left(\frac{\omega_j - \omega_m}{K r_\infty} \right)^2}, \tag{3}$$

waarbij ω_m de gemiddelde natuurlijke frequentie voorstelt. Uitdrukking (3) stelt een verzameling van 2^N vergelijkingen voor: elke term in de sommatie kan zowel met een plus- als een minteken voorkomen. Elk van deze vergelijkingen wordt apart beschouwd om een of meerdere oplossingen r_∞ te bepalen.

Ons belangrijkste resultaat is de totstandbrenging van stabiliteit van *elke* fasevergrendelde oplossing voor algemene frequentiedistributies:

Theorema 3. *Als de amplitude r_∞ voldoet aan (3) met mintekens bij sommige termen, dan is de overeenkomstige fasevergrendelde oplossing van (2)* lokaal instabiel

in de veranderlijken θ_i, $i \in \mathcal{N}$.

Theorema 4. *De fasevergrendelde oplossing van (2) waarvan* r_∞ *voldoet aan (3) met enkel plustekens, is* lokaal asymptotisch stabiel *als en slechts als aan de volgende extra voorwaarde is voldaan:*

$$\sum_{j=1}^{N} \frac{1 - 2(\frac{\omega_j - \omega_m}{K r_\infty})^2}{\sqrt{1 - (\frac{\omega_j - \omega_m}{K r_\infty})^2}} > 0.$$

Wanneer de koppelsterkte groter is dan K_T is er één lokaal stabiele fasevergrendelde oplossing aanwezig in het systeem. In de limiet $K \to \infty$, convergeren de faseverschillen van deze oplossing naar nul, wat tot synchronisatie van de populatie leidt.

Als de koppelsterkte waarden aanneemt die kleiner zijn dan K_T, maar groter dan een drempelwaarde K_P, vertoont een globaal gekoppeld netwerk *partiële meevoering*: sommige oscillatoren *voeren* elkaar *mee*, d.i. hun onderlinge faseverschil is begrensd, en de resterende oscillatoren gedragen zich ongekoppeld. De volgende resultaten over partiële meevoering worden verkregen voor het drie-oscillatornetwerk:

Theorema 5. *De aanvang van partiële meevoering* K_P *van een drie-oscillatornetwerk voldoet aan* $K_P \in (1.5\Delta\omega, 1.7044\Delta\omega]$, *met* $\Delta\omega = \min W$, *waarbij* $W = \{\omega_{ij} \mid \omega_{ij} = |\omega_i - \omega_j|,\ i \neq j\}$.

Theorema 6. *Bewijs van het bestaan van partiële meevoering: zij* $\omega_1 < \omega_2 < \omega_3$ *en* $|\omega_2 - \omega_1| = \min W$. *Als* $K > 4.065(\omega_2 - \omega_1)$, *dan is* $\theta_2 - \theta_1$ *begrensd.*

Theorema 7. *Als de natuurlijke frequenties voldoen aan* $\omega_1 = \omega_2$, *dan bestaan er oplossingen met* $(\theta_2 - \theta_1)(t) = 0$, $\forall t \in \mathbb{R}$ *en deze oplossingen zijn lokaal stabiel.*

Unidirectionele ringkoppeling

De vergelijkingen die unidirectionele ring-gekoppelde oscillatornetwerken beschrijven, zijn

$$\dot{\theta}_i = \omega_i + K \sin(\theta_{i+1} - \theta_i), \quad i \in \mathcal{N},$$

met $\theta_{N+1} \equiv \theta_1$ en $K > 0$. Analoog aan het geval van globale koppeling, maken we een onderscheid tussen ringen van identieke oscillatoren en ringen van niet-identieke oscillatoren.

Voor ringen van identieke oscillatoren bepalen we alle fasevergrendelde oplossingen expliciet. Elke fasevergrendelde oplossing behoort tot precies één van de volgende klassen:

- de klasse van de lopende-golfoplossingen, d.i. gelijke faseverschillen tussen opeenvolgende oscillatoren,

- de klasse van elementaire oplossingen,
- de gesynchroniseerde oplossing.

Fasevergendeling doet zich voor als stabiel gedrag voor elke koppelsterkte verschillend van nul.

Ringen van niet-identieke oscillatoren bezitten pas fasevergrendelde oplossingen voor koppelsterktes boven een kritieke waarde, die we opnieuw aanduiden met K_T. We construeren een algoritme dat alle fasevergrendelde oplossingen bepaalt. In tegenstelling tot globale koppeling worden deze niet verkregen via een consistentievoorwaarde op de amplitude van de ordeparameter, maar via een consistentievoorwaarde op de groepssnelheid Ω van de fasevergrendelde oplossing. Zodra de waarde van Ω gekend is, kunnen de overeenkomstige faseverschillen gemakkelijk berekend worden.

We voeren een stabiliteitsanalyse uit die alle fasevergrendelde oplossingen in klassen onderverdeelt. Elke klasse heeft haar specifieke stabiliteitseigenschappen. De stabiliteitseigenschappen worden bepaald door middel van een nieuwe uitbreiding van de stelling van Gershgorin. Definieer de faseverschillen $\phi_i \triangleq (\theta_i - \theta_{i-1}),\ i = 2, \ldots, N$ en $\phi_1 \triangleq (\theta_1 - \theta_N)$. Gebruik makend van deze definitie, worden de stabiliteitsresultaten samengevat in Tabel 1. De stabiliteitsanalyse toont aan dat verscheidene lokaal stabiele fase-

Tabel 1: Samenvatting van de stabiliteitstheorema's.

Fasevergrendelde oplossing met	Stabiliteit
geen faseverschillen $\in [\pi/2, 3\pi/2]$	stabiel
één faseverschil $\in (\pi/2, 3\pi/2)$ en $\sum_{j=1}^{N} \prod_{k=1,\ k\neq j}^{N} \cos\phi_k > 0$	stabiel
één faseverschil $\in (\pi/2, 3\pi/2)$ en $\sum_{j=1}^{N} \prod_{k=1,\ k\neq j}^{N} \cos\phi_k < 0$	instabiel
twee of meer faseverschillen $\in (\pi/2, 3\pi/2)$ en $\sum_{j=1}^{N} \prod_{k=1,\ k\neq j}^{N} \cos\phi_k \neq 0$	stabiel
één of meer faseverschillen $\in (\pi/2, 3\pi/2)$ en identieke oscillatoren	instabiel

vergendelde oplossingen gelijktijdig aanwezig kunnen zijn in de toestandsruimte van het systeem. Dit geldt voor zowel identieke als niet-identieke oscillatoren. Merk op dat in het geval van *globale* koppeling er slechts één stabiele fasevergrendelde oplossing aanwezig was voor $K > K_T$.

In het geval van identieke oscillatoren duiden we deze coëxistentie expliciet aan: voor elke strikt positieve koppelsterkte, bestaan er stabiele lopendegolfoplossingen samen met de stabiele gesynchroniseerde oplossing. Welk gedrag het systeem vertoont, hangt af van de begintoestand.

Zelfregeling van voertuigpelotons

Geïnspireerd door de resultaten verkregen in de unidirectionele ring van gekoppelde oscillatoren, beslissen we om deze interconnectietopologie op het onderzoeksdomein van voertuigpelotons toe te passen. Een voertuigpeloton

is een lint van voertuigen dat zich aan een constante snelheid met constante tussenafstanden tussen opeenvolgende voertuigen voortbeweegt. We bestuderen verscheidene controlestrategieën voor linten van voertuigen resulterend in een voertuigpeloton. Alle strategieën hebben een zelforganizerende eigenschap gemeenschappelijk; geen enkel voertuig fungeert als leider of aanvoerder van de groep voertuigen. De koppelstructuren die we bekijken zijn uni - of bidirectionele ringkoppelingen. In de unidirectionele ring meet elk voertuig de afstand met zijn directe voorbuur en het eerste voertuig in het lint ontvangt informatie over de positie van het laatste voertuig. In het bidirectionele geval ontvangt elk voertuig informatie over de positie van zowel voor- als achterbuur; het eerste en laatste voertuig wisselen informatie over hun posities uit en brengen zo een ringsstructuur op het controleniveau tot stand. We bewijzen dat het resulterende gedrag van deze systemen een voertuigpeloton is. In het geval van de unidirectionele ringkoppeling wordt het systeem beschreven door

$$\ddot{x}_i + p\dot{x}_i = \omega_i + K(x_{i-1} - x_i - L_i), \quad i \in \mathcal{N}, \tag{4}$$

waar x_i de positie van het i-de voertuig is, $p \geq 0$ een parameter is die de wrijvingscoëfficiënt per eenheidsmassa vertegenwoordigt, $K > 0$ de koppelsterkte is en $\omega_i > 0$, $L_1 \leq 0$, $L_i \geq 0$, $i = 2, \ldots, N$ reële constanten zijn. De massa van elk voertuig is gelijkgesteld aan één . We bewijzen het volgende theorema:

Theorema 8. *Het systeem (4) is asymptotisch stabiel voor voldoend kleine koppelsterktes, namelijk* $K < \frac{p^2}{2\cos^2(\pi/N)}$.

Het concept van *lintstabiliteit* van een peloton wordt besproken en toegepast op de voorgestelde interconnectie. Een lint van voertuigen wordt lintstabiel genoemd wanneer storingen verkleinen wanneer ze zich door het lint voertuigen voortplanten. We presenteren enkele simulaties die erop wijzen dat het systeem zich met betrekking tot lintstabiliteit goed gedraagt.

Voor bidirectionele ringkoppeling tonen we aan dat het peloton stabiel is als de waarden van de koppelsterkte in voorwaartse en achterwaartse richting voldoende dicht bij elkaar liggen. Dit leidt o.a. tot een sneller uitstervend overgangsverschijnsel. Verder bezit het peleton een gewenst gedrag bij pannes. Veronderstel dat er een defect bij een van de voertuigen optreedt; dit voertuig krijgt een ondergrens op zijn snelheid opgelegd die groter is dan de evenwichtsnelheid van het peleton. Simulaties tonen aan dat het peloton zich aan dit defect aanpast door aan de snelheid van het falende voertuig te rijden, zonder dat dit met botsingen gepaard gaat. Het peleton vertoont een gelijkaardig gedrag wanneer een van de voertuigen een bovengrens op zijn snelheid bezit en de evenwichtsnelheid van het peleton niet kan aannemen. Het peleton past zich aan deze “zwakste schakel” aan.

English Summary

Systems of mutually coupled oscillators are ubiquitous in nature. Examples include congregations of flashing fireflies and the synchronous beating of pacemaker cells in the heart. Interesting engineering applications can be found in antenna arrays, used in e.g. wireless communication, and arrays of Josephson junctions, applied in e.g. brain scanners and atmospheric pollution monitoring. The common characteristics of the above systems are adequately modelled by the Kuramoto model. The model is based on two simplifying assumptions:

- Each oscillator is described by a scalar dynamics on the unit circle. The evolution of each oscillator can then be visualized as a point moving on the unit circle. One oscillation corresponds to a rotation over 2π on the circle.
- The interactions between oscillators are weak.

These assumptions allow for a simple model retaining all the characteristics of the original system.

The Kuramoto model serves as the starting point of the present dissertation. We perform a mathematical analysis of two types of *finite* networks of interacting oscillators:

- all-to-all coupling: each oscillator is coupled to all other oscillators in the network,
- unidirectional ring coupling: the oscillators are coupled in a ring; each oscillator is coupled to exactly one other oscillator and the interconnections are either all directed clockwise or counterclockwise.

All-to-all coupling

In the literature the analysis of an *infinite* network of all-to-all coupled oscillators is well-known. It establishes a behavior called *partial synchronization*: one group of oscillators *phase locks* (i.e. all oscillators of the group oscillate

at the same frequency with constant mutual phase differences), while the phase differences between the oscillators of the remaining group vary with time. Unfortunately, the stability properties of partial synchronization are not established in the analysis.

This leads us to investigate the finite counterpart of the all-to-all coupled network. First, networks consisting of a finite number of interacting subsystems are more relevant to study since all networks in the physical world are finite. Second, our analysis reveals qualitative differences and similarities between finite and infinite populations, from which more insight in the properties of the Kuramoto model may be gained.

Before embarking on the analysis of finite coupled oscillator networks, we shortly examine networks of **linearly coupled agents** with arbitrary interconnection topology:

$$\dot{x}_i = \omega_i + \sum_{j \in \mathcal{N}_i} (x_j - x_i), \quad i \in \mathcal{N} \triangleq \{1, \ldots, N\}, \tag{5}$$

where $x_i, \omega_i \in \mathbb{R}$, $\forall i \in \mathcal{N}$ and with $\mathcal{N}_i$ the set of agents that directly influence the i-th agent. This type of networks exhibits *state-locking*: $x_i(t) - x_j(t) = c_{ij} \in \mathbb{R}$, $\forall t \in \mathbb{R}$, $\forall i, j \in \mathcal{N}$. the interconnections between agents can be represented by a graph with the nodes representing the agents and the arcs representing the interconnections. We prove the following theorem:

Theorem 1. *Every initial state of (5) converges to a state locked solution if and only if the graph corresponding to the system has a globally backward reachable node.*

A network has a globally backward reachable node when starting from this node all other nodes of the network can be reached along arcs. Furthermore the interconnected linear system possesses a translation symmetry which is manifested by a zero-eigenvalue of the system matrix. This zero-eigenvalue is structural and does not influence the stability of the system: if all remaining eigenvalues have a negative real part, then the system is asymptotically stable. System (5) possesses this property, as will be proven in Chapter 4.

The equations describing a **finite all-to-all coupled oscillator network** are

$$\dot{\theta}_i = \omega_i + \frac{K}{N} \sum_{j=1}^{N} \sin(\theta_j - \theta_i), \qquad i \in \mathcal{N}, \tag{6}$$

where $\theta_i \in S^1 \triangleq \mathbb{R} \mod 2\pi$ is the *phase* of the i-th oscillator and $\omega_i \in \mathbb{R}$ is the *natural frequency* of the i-th oscillator. The parameter $K \geq 0$ is called the *coupling strength*.

We start the analysis of (6) with a treatment of finite populations of all-to-all coupled *identical* oscillators. We obtain a characterization of the phase locking solutions (i.e the entire network is phase locking) using the concept

of the *complex order parameter*. When the phase of each oscillator is represented by a point on the unit circle in the complex plane, the complex order parameter is simply the centroid of all the phases.

Theorem 2. *Every phase locking solution belongs to the elementary solutions (i.e. the phase difference between each pair of oscillators assumes either the value zero or π), or the amplitude of the corresponding order parameter is zero.*

These two conditions are not mutually exclusive since some elementary solution have a zero amplitude of the order parameter.

The stability of the system is established by taking advantage of the gradient structure of the system. We prove that each initial state that is not situated on the stable manifold of one of the unstable equilibria converges to an equilibrium point corresponding to synchronization. This implies that the synchronizing solution (all phase differences equal to zero) is asymptotically stable almost everywhere.

Second, we allow the natural frequencies of the oscillators to be *nonidentical*. Contrary to the identical case where phase locking is a stable behavior for all non-zero coupling strengths, phase locking does not exist below a critical value K_T of the coupling strength. We construct an algorithm to compute the value of K_T and obtain a necessary and sufficient condition for the existence of phase locking. The constant amplitude r_∞ of the order parameter, corresponding to a phase locking solution satisfies a consistency condition:

$$r_\infty = \frac{1}{N}\sum_{j=1}^{N} \pm\sqrt{1-\left(\frac{\omega_j-\omega_m}{Kr_\infty}\right)^2}, \tag{7}$$

where ω_m represents the mean natural frequency. Expression (7) represents a set of 2^N equations: each term in the summation can have a plus as well as a minus sign. Each of these equations is considered separately to determine a solution r_∞.

Our main result is the establishment of stability of *each* phase locking solution for general frequency distributions:

Theorem 3. *If the amplitude r_∞ satisfies (7) containing minus signs, the corresponding phase locking solution of (6) is* locally unstable *in the variables $\theta_i, i \in \mathcal{N}$,*

Theorem 4. *The phase locking solution of (6) with the amplitude r_∞ satisfying (7) containing only plus signs is* locally asymptotically stable *if and only if the extra condition*

$$\sum_{j=1}^{N} \frac{1-2(\frac{\omega_j-\omega_m}{Kr_\infty})^2}{\sqrt{1-(\frac{\omega_j-\omega_m}{Kr_\infty})^2}} > 0,$$

is satisfied.

When the coupling strength is larger than K_T there is one locally stable phase locking solution present. For $K \to \infty$ the phase differences of the stable phase locking solution tend to zero, yielding synchronization of the network.

If the coupling strength assumes values smaller than K_T, but larger than a threshold value K_P, all-to-all coupled networks exhibit *partial entrainment*: some oscillators *entrain* each other, i.e. their mutual phase difference is bounded, while the remaining oscillators behave as if they were uncoupled. The following results about partial entrainment are obtained for the three oscillator network:

Theorem 5. *The onset of partial entrainment K_P of a three oscillator network satisfies $K_P \in (1.5\Delta\omega, 1.7044\Delta\omega]$, with $\Delta\omega = \min W$, where $W = \{\omega_{ij} \mid \omega_{ij} = |\omega_i - \omega_j|,\ i \neq j\}$.*

Theorem 6. *Proof of existence: let $\omega_1 < \omega_2 < \omega_3$ and $|\omega_2 - \omega_1| = \min W$. If $K > 4.065(\omega_2 - \omega_1)$ then $\theta_2 - \theta_1$ is bounded.*

Theorem 7. *If the natural frequencies are such that $\omega_1 = \omega_2$, then there exist solutions with $(\theta_2 - \theta_1)(t) = 0,\ \forall t \in \mathbb{R}$ and these solutions are locally stable.*

Unidirectional ring coupling

The equations describing unidirectional ring coupled networks, are:

$$\dot{\theta}_i = \omega_i + K \sin(\theta_{i+1} - \theta_i), \quad i \in \mathcal{N},$$

with $\theta_{N+1} \equiv \theta_1$ and $K > 0$. Similar to the case of all-to-all coupling, we make a distinction between rings of identical oscillators and rings of nonidentical oscillators. For rings of identical oscillators we determine all phase locking solutions explicitly. Each phase locking solution belongs to exactly one of the following classes:

- the class of travelling wave solutions, i.e. equal phase differences between consecutive oscillators,
- the class of elementary solutions,
- the synchronized solution.

Phase locking arises as a stable behavior for every non-zero coupling strength. Rings of nonidentical oscillators only possess phase locking solutions for coupling strengths above a critical value, again denoted by K_T. We produce an algorithm determining all phase locking solutions. Contrary to all-to-all coupling they are not obtained through a consistency condition on the amplitude of the order parameter, but via a consistency condition on

the group velocity Ω of the phase locking solution. Once the value of Ω is obtained, the corresponding phase differences are readily calculated.

We perform a stability analysis such that all phase locking solutions are classified into classes, each with its own stability properties. The stability properties are obtained by means of a novel extension of Gershgorin's theorem. Define the phase differences $\phi_i \in S^1 : \phi_i \triangleq (\theta_i - \theta_{i-1}) \bmod 2\pi,\ i = 2, \ldots, N$ and $\phi_1 \triangleq (\theta_1 - \theta_N) \bmod 2\pi$. Using this definition, the stability results are summarized in Table 2. The stability analysis shows that several

Table 2: Summary of the stability theorems.

Phase locking solution with	Stability
no phase differences $\in [\pi/2, 3\pi/2]$	stable
one phase difference $\in (\pi/2, 3\pi/2)$; $\sum_{j=1}^{N} \prod_{k=1,\ k\neq j}^{N} \cos\phi_k > 0$	stable
one phase difference $\in (\pi/2, 3\pi/2)$; $\sum_{j=1}^{N} \prod_{k=1,\ k\neq j}^{N} \cos\phi_k < 0$	unstable
two or more phase differences $\in (\pi/2, 3\pi/2)$; $\sum_{j=1}^{N} \prod_{k=1,\ k\neq j}^{N} \cos\phi_k \neq 0$	unstable
one or more phase differences $\in (\pi/2, 3\pi/2)$ and identical oscillators	unstable

locally stable phase locking solutions can coexist in the state space of the system, in the case of identical as well as nonidentical oscillators. Recall that in the all-to-all coupled case there exists only one stable phase locking solution for $K > K_T$. For a ring of identical oscillators this coexistence is made explicit by proving the existence and stability of travelling wave solutions together with the existence of the stable synchronized solution for all non-zero coupling strengths. Which type of behavior the system exhibits depends on the initial conditions.

Self-regularization of vehicle platoons

Inspired by the results obtained in the unidirectional ring of oscillators, we decide to apply this interconnection topology to the research domain of vehicle platoons. A vehicle platoon is a string of vehicles moving at a constant velocity with constant interdistances between consecutive vehicles. We study several control strategies for strings of vehicles resulting in a vehicle platoon. All strategies have a self-organizing property in common; there is no leader/master vehicle present. The coupling structures are uni- or bidirectional ring couplings. In the unidirectional ring, each vehicle measures the distance with its immediate forward neighbor and the lead vehicle in the platoon receives information on the position of the last vehicle in the platoon. In the bidirectional case each vehicle receives information on the position of both forward and backward neighboring vehicles; the first and last vehicle in the string exchange information on their positions as well, establishing a ring structure on the control level. We prove that the resulting behavior of the system is a vehicle platoon.

In the case of unidirectional ring coupling the system equations are

$$\ddot{x}_i + p\dot{x}_i = \omega_i + K(x_{i-1} - x_i - L_i), \quad i \in \mathcal{N}, \tag{8}$$

where x_i represents the position of the i-th vehicle, $p \geq 0$ is a parameter representing the friction/drag coefficient per unit mass, $K > 0$ is the coupling strength and $\omega_i > 0$, $L_1 \leq 0$, $L_i \geq 0$, $i = 2, \ldots, N$ are real constants. The mass of each vehicle is taken equal to one. We prove the following theorem:

Theorem 8. *System (8) is asymptotically stable for sufficiently small coupling strengths, namely* $K < \frac{p^2}{2\cos^2(\pi/N)}$.

The concept of *string stability* of a platoon is discussed and applied to the proposed interconnection. A string of vehicles is called string stable if disturbances are attenuated as they propagate down the string. We present some simulations supporting the claim that the system is well-behaved with respect to string stability.

For the bidirectional ring case it is shown that the platoon is stable if the coupling strengths in forward and backward direction are sufficiently close to each other. This yields an improvement over the unidirectional ring case, since the coupling strengths may be large, resulting in a fast decay of the transient behavior. Furthermore, the platoon has a desired response to malfunctions. Assume one of the vehicles receives a lower bound on its velocity, that is larger than the equilibrium velocity. Simulations show that the platoon will adapt to the malfunctioning vehicle without collisions. Similarly, when one of the vehicles has an upper bound on its velocity, that is smaller than the equilibrium velocity, the platoon will adapt to this weakest link by assuming the maximum velocity attainable by the malfunctioning vehicle.

Chapter 1

Introduction

The subject of this dissertation is related to the Kuramoto model, its properties and its applications. The model, dating from 1975, describes a set, or *population*, of interacting oscillators. An oscillator is a periodic process with a fixed frequency, its so-called natural frequency. Moreover the oscillators are self-sustained, i.e. when perturbed they return to their original frequency. The Kuramoto model is proposed as an explanation of the phenomenon of *synchronization*: in many diverse systems it is observed how interacting oscillators start to oscillate at the same frequency even though they do not possess identical natural frequencies.

Chapter 2 of this dissertation serves as an introductory chapter. It gives an overview of different research domains where the problems of synchronization and interacting oscillators appear. They range from antenna arrays driven by voltage controlled oscillators in radio engineering and Josephson junction arrays in laser physics, over interacting oscillating chemical reactions, to synchronously flashing fireflies and synchronously beating cardiac pacemaker cells in biology. This clearly illustrates the relevance and the multidisciplinary character of the research related to the Kuramoto model.

The mathematical model proposed by Kuramoto to explain the behavior of oscillator populations is introduced in Chapter 3. The model is derived from basic principles and it consists of a system of coupled nonlinear differential equations. The second part of the chapter reviews the analysis of the Kuramoto model as performed by Yoshiki Kuramoto himself. The analysis is restricted to populations of an *infinite* number of oscillators. This restriction allows for the use of mathematical techniques from statistical physics facilitating the mathematical analysis. Unfortunately, the choice of an infinite number of oscillators makes it difficult to perform a full stability analysis. Up to this day a complete picture of the stability of the Kuramoto model has not been obtained. We decided to circumvent this problem by investigating *finite* oscillator populations described by the Kuramoto model. Although the

model is in principle equally applicable to finite populations, an analysis of finite populations had not been conducted before. In this thesis a complete analysis of finite populations was performed for the first time, together with a full stability analysis of their *phase locking behavior*. A population is called phase locking if all oscillators oscillate at the same frequency with constant mutual phase differences. It is shown that the behavior of finite populations is qualitatively different from infinite populations. An extensive comparison between both cases is included. The analysis of finite populations forms the core of the dissertation and is described in Chapter 4 to Chapter 6.

Chapter 4 is introductory to the analysis of the nonlinear models to be investigated in subsequent chapters. It presents the linear counterpart of the Kuramoto model. Contrary to the Kuramoto model, where the interconnection is all-to-all, i.e. each oscillator is coupled to all other oscillators, the interconnection topology is arbitrary. It is shown that the interconnection topology plays a determining role in the behavior of a group of linearly interacting systems.

The analysis of finite oscillator populations is divided into two parts. The first part, Chapter 5, considers populations of *identical* oscillators, i.e. all oscillators having the same natural frequency. This turns the dynamical system describing the interacting oscillators into a gradient system on the torus, simplifying the analysis. It is proven that populations of identical oscillators always synchronize. Moreover, some properties of the phase locking solutions are established which have not appeared in the literature.

The second part of our finite analysis is found in Chapter 6, which investigates the problem of *nonidentical* oscillators. If the interaction between the oscillators is stronger than some critical value K_T, the oscillators phase lock. Existence of this behavior is mathematically proven and we provide a full stability analysis. An algorithm is provided to compute the value of K_T. If the mutual coupling is not sufficiently strong to cause phase locking, the behavior can still display some degree of order and the population is then said to exhibit *partial entrainment*. This type of behavior is not observed in the Kuramoto analysis of infinite populations. We analyzed partial entrainment for the simple case of three interacting oscillators. All results on phase locking and partial entrainment in Chapter 6 are original and have been published in [3, 5]. To conclude, Chapter 6 contains a comparison between our finite analysis and the infinite analysis of Kuramoto as described in Chapter 3.

The Kuramoto model is characterized by its all-to-all coupling. In Chapter 7 a novel interconnection topology is considered, where the oscillators are interconnected in a unidirectional ring. We are the first to give a complete analysis of such interconnections [73, 74]. Analysis techniques introduced in Chapter 6 are applied to determine the phase locking solutions, to prove their existence and to establish their stability properties. The ring coupling is applicable to the research area of antenna arrays, as presented in Chapter 8. A paper summarizing the results of Chapter 4 to Chapter 7 has appeared

in [4].

Chapter 9 does not treat networks of oscillators. However, it transposes the unidirectional ring coupling to another domain of application, namely vehicle platoons. A vehicle platoon is a string of vehicles driving at a constant velocity with constant interdistances between consecutive vehicles. Traditionally, vehicle platoons are formed through leader-follower control: the leader vehicle of the platoon is steered independently; all other vehicles are controlled to follow the leader. Inspired by the results and techniques of Chapter 6 and Chapter 7, we decided to interconnect the vehicles in such a way that no leader is present: the same control law is applied to each vehicle. Just as phase locking arises through self-organization between the oscillators, we now aspire to obtain a structured vehicle platoon through self-regularization between the autonomous vehicles: the vehicles are coupled at the control level into a uni- or bidirectional ring in order to form a vehicle platoon. We investigate the conditions under which a vehicle platoon is formed and establish its stability properties. In the unidirectional case, we found the platoon to be stable only for sufficiently small coupling strengths. This contrasts with the situation of coupled oscillators, where phase locking is stable for sufficiently *large* coupling strengths. The results of this chapter appeared in [75,76].

The final chapter contains a concluding overview of the contents of the dissertation.

Chapter 2

Self-Sustained Oscillators

The building blocks of the interconnected systems under investigation in this dissertation are *self-sustained oscillators*. The present chapter serves as an overview of different research domains where such oscillators are subject of investigation. This overview does not pretend to be exhaustive. It focusses on those domains where *networks* of oscillators are important research topics.

2.1 Oscillators in Physics and Engineering

In the field of engineering, oscillators serve many distinct purposes. Originally they played a major role in the development of radio communication, where they received the name *voltage controlled oscillators (VCOs)*. In 1915 Edwin Armstrong devised the first electronic oscillator [7]. It consisted of an electric circuit containing an Audion, a type of vacuum tube constructed by Lee de Forest. The oscillator was a key element in the so-called superheterodyne principle discovered by Armstrong. The superheterodyne principle became a superior technique to tune a receiver to a desired radio signal and it is still used in modern day radio receivers. Armstrong's discovery meant the start of the invention of a series of highly performing oscillators. After its invention in the late 40's, the transistor replaced the vacuum tube as the active element in VCOs and significantly changed the practical oscillator topologies. The new transistors were smaller and consumed less power than vacuum tubes, with lower operating voltage requirements and ultimately lower cost. With the introduction of wireless communication in the 90's, VCOs became even more miniaturized and new designing techniques were introduced, an example of which being topologies with *multiple* oscillators. Furthermore, designers were gaining a better understanding of VCO theory, building upon mathematical models from the past, such as Van der Pol's and Leeson's equations. This is presented in detail in Chapter 8, where an

example of multiple VCOs steering an antenna is presented.

A second engineering application using (coupled) self-sustained oscillators is found in laser physics. The oscillators used in this application are *Josephson junctions*, conceived by Brian Josephson in 1962 [40]. A Josephson junction consists of two superconductors connected by a very thin layer of oxide. A superconductor is a metal, metal alloy or other composite material which, below a specific temperature, provides an extremely low level of resistance to the passage of electrical current, therefore making it possible to transfer electricity with minimal energy loss. The configuration of the Josephson junction enables an electric current to flow through the thin oxide layer without resistance, which is surprising since oxide is an insulator. Moreover, the current flows through the layer even when there is no voltage difference between the two superconductors. When a constant voltage is applied to the junction, a nonconstant alternating current is produced, turning the junction into an oscillator with frequencies of up to 10^{11} Hz. Nowadays, *arrays* of Josephson junctions are used in many modern technologies, from brain scanners to atmospheric pollution monitoring. Arrays have the advantage over single junctions that their power can be increased to practically useful levels. A single junction produces only a microwatt of power, too small for any practical application. However, if the oscillators are coupled in an array and then synchronized, their combined power is proportional to the square of the number of junctions. In [35] an analysis is given of a one-dimensional array of N junctions shunted by a load. Each junction $j \in \{1, \ldots, N\}$ is determined by its wave-function phase difference across the junction $\phi_j \in S^1$. For a precise definition of this quantity ϕ_j, the reader is referred to [90]. In [35] it was proven that the *synchronized state*, also called the *in-phase state*, i.e. $\phi_i(t) = \phi_j(t),\ \forall i, j \in \{1, \ldots, N\},\ \forall t \in \mathbb{R}$, is stable when the load is inductive and unstable when it is capacitive. Moreover, in subsequent research a new type of behavior of the array was discovered, the so-called *splay state* of the array [65], defined as $\phi_k(t) = \phi_1(t+(k-1)T/N),\ \forall k \in \{1, \ldots, N\},\ \forall t \in \mathbb{R}$, where $T > 0$ represents the oscillation period. This type of behavior is sometimes also called "the anti-phase state" and "ponies on a merry-go-round". In the present dissertation it is referred to as *the travelling wave solution* (cfr. Chapter 7). Because of permutation symmetry in the system, multiple splay states are possible, e.g. a 5-junction array yields 24 splay states. This yielded the theoretical possibility to build computer memories with arrays of Josephson junctions [86]. Such a computer has never been built because it was considered not to be commercially competitive with future generations of semi-conductor based computers. The concepts of synchronized state and splay state introduced here play a major role in the present dissertation.

2.2 Chemical Oscillators

The systematic study of oscillating chemical reactions is of considerably recent origin. In this section, we present a brief overview of the history of nonlinear chemical dynamics.

2.2.1 Bray Reaction

The first chemical oscillator to be described was the reaction of iodate, iodine and hydrogen peroxide studied by William C. Bray in 1921 [12]. Nonetheless, for the next fifty years, chemists would write that the oscillations found by Bray were an artifact of dust or bubbles, although Bray had explicitly addressed these possible objections by using carefully filtered and stirred solutions at room temperature. Bray's work was revived in the 1970's by Noyes and coworkers who, through careful experiments and mathematical modelling, succeeded in convincing the chemical community that the Bray reaction represented a genuine chemical oscillator [80].

2.2.2 The Belousov-Zhabotinsky (BZ) Reaction

The beginning of modern nonlinear chemical dynamics can be traced to Boris Pavlovich Belousov (1893-1970). He investigated a solution of bromate, citric acid and ceric ions and expected to see the monotonic conversion of yellow Ce+4 into colorless Ce+3. Instead, the solution repeatedly cleared and then became yellow again! Belousov also noted that, unstirred in a graduated cylinder, the solution exhibited propagating waves of yellow. He submitted a manuscript in 1951, but it was rejected and did not get published. Belousov's only publication on this reaction appeared in the abstracts of a conference on radiation biology in 1958. A manuscript that Belousov wrote in 1951 describing his work was posthumously published in Russian in 1981 and in English translation in 1985 [27].

In 1961, Anatol Zhabotinsky, a graduate student in biophysics at Moscow State University, began looking at the same system. Although Zhabotinsky did not have Belousov's 1958 paper, he did have access to the original recipe. A conference was held in Prague in 1968 on Biological and Biochemical Oscillators, and Zhabotinsky presented some of his results. This meeting motivated many researchers in Eastern Europe to study this so-called Belousov-Zhabotinsky reaction, and the publication of the proceedings in English [18] brought the BZ reaction to the attention of several Western chemists.

2.2.3 The Brusselator

Real chemical systems oscillate within a finite range of parameters, and they have a single mode (amplitude and frequency) of oscillation, to which they return if the system is perturbed. Is it possible to construct a reasonable model that has these features? The first chemically "respectable" model was proposed by Prigogine and Lefever in 1968 and named the "Brusselator" [72]. It mimics the reactions of two disinfectants and an acid used in the manufacture of pharmaceutical products. The theoretical chemical reactions are given by

$$\begin{aligned} A &\to X, \\ 2X + Y &\to 3X, \\ B + X &\to D + Y, \\ Y &\to E. \end{aligned} \tag{2.1}$$

The Brusselator has often been studied as a flow reactor where the substances A and B are fed in continuously to maintain their concentrations and the substances D and E are taken out. The flow reactor allows scientists to focus on the two key ingredients that vary, namely X and Y. The system of equations that models the Brusselator (for certain choices of time, temperature, and concentrations of the substances A and B) is:

$$\begin{aligned} \dot{u} &= 1 + au^2v - (b+1)u, \\ \dot{v} &= bu - au^2v, \end{aligned} \tag{2.2}$$

where u is the concentration of X, v is the concentration of Y and $a, b \in \mathbb{R}$. By analysis and numerical simulation of the differential equations, Prigogine and Lefever demonstrated that their model shows homogeneous oscillations and propagating waves like those seen in the BZ system. The Brusselator was extremely important because it showed that a chemically reasonable mechanism could exhibit self-organization and oscillations.

2.2.4 The Oregonator

In 1969, Richard Field started a cooperation with Richard Noyes at the University of Oregon in Eugene. Field and Noyes were fascinated by the oscillations of the BZ reaction and set out to determine the mechanism of this remarkable behavior. Together with Körös they were eventually able to explain the qualitative behavior of the BZ reaction using the same principles of chemical kinetics and thermodynamics that govern "ordinary" chemical reactions. They published their mechanism, now known as the FKN-mechanism, in a classic paper in 1972 [28, 66].

Arthur Winfree, a biologist with an interest in spatial and temporal patterns, had attended the Prague conference where Zhabotinsky had presented

his results on the BZ reaction. Winfree decided to pursue the study of pattern formation in the BZ reaction. In 1972, the cover of Science magazine featured Winfree's photo of *spiral wave patterns* in the BZ reaction [95]. Field and Noyes immediately saw how to understand the development of such patterns with the aid of the FKN-mechanism, and they published an explanation the same year [29]. Furthermore, they managed to simplify the FKN-mechanism, which had about twenty elementary steps and chemical species. They obtained a model that had only three variable concentrations yet maintained all the essential features of the full BZ reaction. The model was called the "Oregonator" [30]:

$$\begin{aligned} \dot{x} &= k_1 a y - k_2 x y + k_3 a x - k_4 x^2, \\ \dot{y} &= -k_1 a y - k_2 x y + \frac{1}{2} k_5 z, \\ \dot{z} &= 2 k_3 a x - k_5 z, \end{aligned} \tag{2.3}$$

with $k_i,\ i = 1, \ldots, 5$ rate constants of the chemical equations underlying the differential equations, and $a = [BrO_3^-]$, $x = [HBrO_2]$, $y = [Br^-]$ and $z = [Ce^{4+}]$. The square brackets denote concentrations of the chemical reagents. A thorough analysis of the Oregonator is described in [64].

2.2.5 Coupled Oscillators

In 1975, Marek and Stuchl were the first to present experimental results on the behavior of two interacting chemical oscillators [56]. The investigated system consisted of two connected flow-through continuous stirred tank reactors, in each of which the BZ reaction was taking place. The reactors were connected by a perforated plate and interaction between both reactors was achieved by fluid flowing through the holes of the plate. The frequency of each oscillation was controlled by changing the reaction temperature in the corresponding reactor. Phenomena such as synchronization of oscillations at a common frequency, synchronization at multiples of a common frequency, and amplitude amplification (i.e. every third or fourth oscillation, the amplitude of the slower oscillator is amplified) were observed, depending on the degree of interaction and the differences in the original oscillation frequencies. Mathematical modelling of the above phenomena however failed due to insufficient knowledge of a kinetic model.

Shortly after, in 1978, Fujii and Sawada slightly refined the experiment and added a (simplified) mathematical model which partially explained their observations [31]. The mathematical model was an adaptation of a model by Yoshiki Kuramoto, which people later came to know as the *Kuramoto model*. The important observation in [31], explained by the Kuramoto model, was that for coupling strengths larger than a critical value, the phase difference between both BZ oscillations became constant in time. This type

of system behavior is called *phase locking*. It will be discussed in detail in the subsequent chapters.

In 1992 Yoshimoto et. al. [102] investigated *three* coupled BZ-reactions in order to find more experimental indications of the validity of the mathematical models proposed in the literature to describe coupled oscillator systems. Contrary to the previous experimental set-ups, the three reactors were interconnected by tubes. The flow rates through the connecting tubes were controlled by peristaltic pumps. By changing the flow rate, the coupling strengths between the oscillators were adjusted. Again, phase locking was retrieved as possible behavior, but compared to the two-oscillator systems a novel type of behavior was observed, called *phase death*. A group of interconnected oscillators is said to exhibit phase death, when all oscillators stop oscillating. Phase death is a behavior which cannot be retrieved with the Kuramoto model, which indicates the area of validity of the model is restricted. However, the model is capable of explaining most other types of behavior encountered in the experiments.

2.3 Biological Oscillators

In 1958 "Nonlinear problems in random theory" by Norbert Wiener was published [93]. In this book the professor from MIT presented research he had conducted together with Professor Rosenblith, concerning the nature of the electroencephalogram and in particular of the alpha rhythm in the brain. They modelled the 8 to 12 Hz oscillations from the electroencephalograph by a system of random nonlinear oscillators excited by a random input. The oscillators represented a population of spontaneously active neurons, mutually synchronizing to generate a global oscillation. Although this picture of the brain did not turn out to be convincing to neurophysiologists, it became a paradigm for many other biological systems and at the same time Wiener was the first who dared to tackle the problem of analyzing *large* groups of interacting nonlinear systems.

Inspired by the work of Wiener, Arthur Winfree, a PhD-student at Princeton University, published a paper called "Biological Rhythms and the behavior of populations of coupled oscillators" in 1967. Winfree collected numerous examples from different biological disciplines and asserted that the idea of Wiener was generally applicable to these examples. Winfree's paper signified the start of research concerned with the mathematical analysis of synchronization in phase oscillators, one of the topics of the present dissertation.

At the time of Winfree's paper recent progress had been made in understanding the origin of the beating of the heart. Experiments indicated that the pacemaker nodes of the chicken heart were populations of many spontaneously beating cells, mutually synchronizing so that eventually the whole

population behaved as a single oscillator [34]. (In the 1960's, this picture was refined and it was shown that not synchronization, but phase locking takes place in the heart [42].)

The phenomenon of synchronization had also been observed in a completely different biological system, namely congregations of fireflies in South-East Asia. In the mid-1960's John Buck and his wife Elisabeth, both biologists, travelled to Thailand to observe the interactions between fireflies [15]. The males of some species tend to flash at regular intervals, but the flashing event can be triggered or delayed by the sight of a neighbor flashing. The Bucks witnessed the synchronization of huge groups of fireflies, flashing in unison at a frequency of twice per second. Trying to unravel the mechanism behind the synchronization, Buck conducted some laboratory studies with the fireflies. In one experiment, one firefly was flashed at with an artificial light and its response was measured. The experiment led to conclude that an individual firefly shifts the timing of its flashes when receiving a stimulus. The size and the direction of the shift depend on when in the cycle the stimulus is received. This indicated that the flash rhythm is regulated by an internal resettable oscillator and that each firefly in a congregation of fireflies can shift the timing of other fireflies' flashes. At the same time its own flashes get shifted by the other fireflies, eventually leading to synchronization of the entire group.

A third class of self-sustained oscillators in biology are the so-called biological clocks or circadian rhythms. In 1729 the French scientist Jean-Jacques D'Ortous de Mairan published a monograph on the daily leaf movements of the mimosa plant. The mimosa plant belongs to the group of plants that raise their leaves in the morning and lower them in the evening, each day at the same time. It was assumed that this happened under the influence of sunlight. De Mairan placed a mimosa plant in a dark cabinet and made observations at regular intervals. He observed that the plant continued to raise and lower its leaves, but with a period that slowly drifted away from the 24-hour period. This finding suggested that the movement was not a simple response to sunlight but that it was controlled by an internal clock. De Mairan's observation is considered as the first discovery of a circadian rhythm. In the 1950's the study of biological rhythms became an independent scientific discipline, called chronobiology, of which Colin Pittendrigh and Jurgen Aschoff are considered the pioneers. Pittendrigh conducted studies on the influence of temperature on the circadian rhythmicity in fruit flies. Interesting to note is that he was Winfree's supervisor. Jurgen Aschoff examined circadian rhythms in humans. Subjects were placed in an underground bunker and allowed to turn lights on or off according to their own internal rhythms. Aschoff tracked their sleep-wake cycles and body temperature and concluded that humans, like the plants investigated by de Mairan, have endogenous circadian cycles.

One of the most interesting features of circadian rhythms is that their pe-

riods are not equal to 24 hours, but slightly smaller or larger. Without any external stimulus biological clocks are slowly drifting away from the day-night cycle. However, the synchrony of organisms with their external environments suggests that biological clocks are able to get *entrained* by external time-cues, such as the light-dark cycle. Researchers discovered that the organism's response to an external stimulus differs depending on the phase in the organism's cycle at which the stimulus is applied. For example, exposure to light during the early part of an individual's "normal" dark period generally results in a phase delay, whereas exposure during the late part of its normal dark period causes a phase advance. Such a response can be graphically displayed by a so-called *phase-response curve*. The scientific use of the phase response curve is discussed in Section 3.4.

2.4 Conclusions

The above sections make it clear that systems of interacting oscillators are ubiquitous in nature, with many possessing interesting engineering applications (e.g. arrays of Josephson junctions and antenna arrays). Important types of behavior are *synchronization*, i.e. all oscillators possess the same phase at each time instant, and, more generally, *phase locking*, i.e. all oscillators oscillate at the same frequency with constant mutual phase differences. We mentioned that a useful mathematical model of populations of mutually coupled oscillators has been proposed by Kuramoto. The next chapter presents a description of the Kuramoto model and a review of its analysis as performed by Kuramoto himself.

Chapter 3

The Kuramoto Model

3.1 Large populations of Oscillators

Consider a population of N all-to-all coupled oscillators, i.e. each oscillator is coupled to all other oscillators. Each oscillator can be modelled by a nonlinear continuous-time system possessing an isolated attractive limit cycle (for definitions of basic concepts of systems theory the reader is referred to Appendix A). Let M be the order of the corresponding nonlinear differential equation. The population as a whole is then modelled by an (NM)-dimensional vector field. The combination of the nonlinearity of the vector field with the high dimensionality of the system renders its analysis mathematically hard to solve.

In order to construct a tractable model of a population of mutually coupled oscillators, Winfree proposed two simplifying assumptions. A first simplification consists in the introduction of the concept of "phase". The limit cycle of each oscillator can be regarded as a 1-dimensional manifold embedded in $\mathbb{R}^M$. The evolution of the state on the limit cycle can then be replaced by a dynamics of a single scalar variable representing the position of the state on the limit cycle. This position can be represented by a point on the unit circle S^1. The point on the unit circle corresponding to the state of the oscillator on the limit cycle is called *the phase of the oscillator*. The introduction of the phase variable will be made mathematically precise in the next section.

Secondly, the interactions between oscillators are assumed at all times weak enough so that the sequence of states traversed by each oscillator does not get significantly altered: the state of the oscillator stays close to the limit cycle at all times. This enables us to maintain the phases of the oscillators as the system variables of the interconnected system.

Combining both assumptions allows for a considerable reduction of the model's dimension from NM to N. The model obtained via this reduction is

called the *Kuramoto model*.

3.2 The Kuramoto Model

Although Winfree carried out some mathematical analysis, mostly treating the synchronizing behavior of the oscillator population (which will be discussed in a next chapter), he did not obtain a differential equation with the phases as variables describing the overall behavior of the population. A detailed mathematical description appeared in 1984, when the Japanese physicist Yoshiki Kuramoto published a book on his research of coupled oscillators [45]. The book gathered previously published partial results on the topic. In this section an adaptation of Kuramoto's reduction of the cooperative dynamics of an oscillator community to a phase dynamics as described in [46] is presented.

3.2.1 Preliminary Definitions from Differential Geometry

The following definitions are adopted from [1], [11] or [77].

Definition 1. *A* topological space (M, τ) *(often abbreviated to M) is a set M together with a system τ of subsets of M satisfying*

- $\emptyset \in \tau$ *and* $M \in \tau$.
- $U_1, U_2 \in \tau \Rightarrow U_1 \cap U_2 \in \tau$.
- *The union of any number of elements of τ belongs to τ.*

Definition 2. *A topological space is* Hausdorff (separated) *if any two distinct points possess disjoint neighborhoods.*

Definition 3. *A mapping f is said to belong to* class C^p *if f has continuous derivatives up to order p.*

A homeomorphism *is a bijection f which is bicontinuous (i.e. f and f^{-1} are continuous).*

A C^p-diffeomorphism *is a bijection f with f and f^{-1} of class C^p, $p \geq 1$. (When $p = \infty$ we simply say* diffeomorphism.*)*

Definition 4. *Each pair (U, ϕ), where U is an open subset of a topological space M and $\phi : U \to V \subset \mathbb{R}^n$ is a homeomorphism, is called a* coordinate neighborhood *or* (coordinate) chart.

To $m \in U$ we assign the n coordinates $x^1(m), \ldots, x^n(m)$ of its image $\phi(m)$. The function $x^i : m \mapsto x^i(m)$ is the i-th coordinate function.

Definition 5. *A* manifold *is a Hausdorff topological space M together with a countable collection of coordinate charts (U_i, ϕ_i) which satisfy the following properties:*

1. *The coordinate charts cover M:*

$$\cup_j U_j = M.$$

2. *The coordinate charts are* compatible, *i.e. on the overlap of any pair of coordinate charts $U_i \cap U_j$ the composite map*

$$\phi_j \circ \phi_i^{-1} : \phi_i(U_i \cap U_j) \to \phi_j(U_i \cap U_j),$$

is a diffeomorphism.

In the remainder of this section M represents a manifold and $m \in M$.

Definition 6. *Let $I \subset \mathbb{R}$ be an interval. A* curve at m *is a C^1-map $c : I \to M; t \mapsto c(t)$ with $0 \in I$ and $c(0) = m$.*

Definition 7. *Let c_1 and c_2 be two curves at m and (U, ϕ) a chart with $m \in U$. Then c_1 and c_2 are called* tangent at m with respect to ϕ *if and only if $\frac{d(\phi \circ c_1)}{dt}(0) = \frac{d(\phi \circ c_2)}{dt}(0)$.*

It can be proven that tangency of curves at $m \in M$ is independent of the charts used. The concept of tangency induces an equivalence relation on the space of all curves at m. Two curves are called equivalent if they are tangent. An equivalence class of tangent curves at m is denoted by $[c]_m$ where c is a representative of the class.

Definition 8. *The* tangent space $T_m M$ to M at m *is the set of equivalence classes of curves at m:*

$$T_m M := \{[c]_m : c \text{ is a curve at } m\}.$$

An element of $T_m M$ is also called a tangent vector to m.

Definition 9. *The* tangent bundle of M *is defined as*

$$TM := \cup_{m \in M} T_m M,$$

and the tangent bundle projection *is $\tau_M : TM \to M; [c]_m \mapsto \tau_M([c]_m) := m$.*

Definition 10. *Let N be a manifold. If $f : M \to N$ is of class C^1, the* tangent mapping $T_m f$ of f *is defined by*

$$T_m f : T_m M \to T_{f(m)} N;\ T_m f([c]_m) := [f \circ c]_{f(m)}.$$

The tangent TF of f is defined by

$$Tf : TM \to TN;\ Tf([c]_m) = Tf|_{T_m M}([c]_m) = T_m f([c]_m).$$

By construction the following diagram commutes:

$$\begin{array}{ccc} TM & \xrightarrow{Tf} & TN \\ {\scriptstyle \tau_M}\downarrow & & \downarrow{\scriptstyle \tau_N} \\ M & \xrightarrow[f]{} & N \end{array}$$

Definition 11. *A* vector field X on M *is a mapping* $X : M \to TM$ *such that* $m \mapsto X(m) \in T_mM$, $\forall m \in M$. *The set of all vector fields on* M *is denoted by* $\mathcal{X}(M)$.

Definition 12. *The* C^∞*-curve* $c : I \subset \mathbb{R} \to M$ *is an* integral curve *of* X *if*

$$T_{t_0}c\left(\left.\frac{d}{dt}\right|_{t_0}\right) = X(c(t_0)), \quad \forall t_0 \in I, \tag{3.1}$$

where $\left.\frac{d}{dt}\right|_{t_0}$ *is the vector forming the natural basis of* $T_{t_0}\mathbb{R}$.

Definition 13. *Let* $\varphi : M \to N$ *be a* C^∞*-diffeomorphism and* X *a vector field on* M. *The* push forward of X by φ *is defined by*

$$\varphi_* X := T\varphi \circ X \circ \varphi^{-1} \in \mathcal{X}(N).$$

Definition 14. *Let* $\varphi : M \to N$ *be a* C^∞*-mapping. The vector fields* $X \in \mathcal{X}(M)$ *and* $Y \in \mathcal{X}(N)$ *are called* φ-related *if* $T\varphi \circ X = Y \circ \varphi$.

Note that if φ is a diffeomorphism and X and Y are φ-related, then $Y = \varphi_* X$. In general X can be φ-related to more than one vector field on N. φ-relatedness means that the following diagram commutes:

$$\begin{array}{ccc} TM & \xrightarrow{T\varphi} & TN \\ {\scriptstyle X}\uparrow & & \uparrow{\scriptstyle Y=\varphi_* X} \\ M & \xrightarrow[\varphi]{} & N \end{array}$$

Definition 15. *If* (U, ϕ) *is a chart on* M, ϕ *induces an isomorphism* $T_m\phi : T_mM \to T_{\phi(m)}\mathbb{R}^n$. *With* $a = \phi(m)$, *the map* $(T_m\phi)^{-1}$ *maps* $T_a\mathbb{R}^n$ *isomorphically onto* T_mM.

The images $E_i := (T\phi)^{-1}(\frac{\partial}{\partial x^i}), i = 1, \ldots, n$, *where* $\frac{\partial}{\partial x^1}, \ldots, \frac{\partial}{\partial x^n}$ *is the natural basis of* $T_a\mathbb{R}^n$ *for each* $a \in \phi(U) \subset \mathbb{R}^n$, *determine at* $m = \phi^{-1}(a) \in M$ *a basis* $E_1(m), \ldots, E_n(m)$ *of* T_mM. *The set* $\{E_1, \ldots, E_n\}$ *is called the set of* coordinate frames.

With $f : M \to \mathbb{R}$, we define

$$E_i(m)(f) := \frac{\partial f_\phi}{\partial x^i}(\phi(m)),$$

with $f_\phi := f \circ \phi^{-1}$. It can then be proven (for details cfr. [11]) that each tangent vector $X(m)$ can be written as

$$X(m) = \sum_{j=1}^{n} X(m)(x^j) E_j(m).$$

We decide not to give a definition of $X(m)(x^j)$, since this would lead us too far into the theory of differential geometry. For the purposes of this dissertation it suffices to state that $X(m)(x^j) \in \mathbb{R}$. In the remainder of the text $X(m)(x^j)$ is denoted by $X^j(m)$.

3.2.2 The Unperturbed Oscillator

Let the dynamics of a single oscillator be described by

$$\dot{x} = f(x), \qquad x \in \mathbb{R}^n,\ f : \mathbb{R}^n \to \mathbb{R}^n. \tag{3.2}$$

This system is assumed to have precisely one isolated asymptotically orbitally stable periodic solution $p : \mathbb{R} \to \mathbb{R}^n;\ t \mapsto p(t)$, with period T. The trajectory of this solution is a stable limit cycle Γ. We also assume that p possesses the asymptotic phase property (cfr. Appendix A).

Define the unit circle $S^1 \subset \mathbb{R}^2$ as

$$S^1 := \{(x, y) : x^2 + y^2 = 1\}.$$

The unit circle can be given the structure of a one-dimensional manifold by constructing an atlas of two compatible charts.

Consider a constant vector field X_ω on S^1, written in local coordinates (with coordinate chart (U, φ)) as

$$X_\omega(s) = \omega \frac{\partial}{\partial \varphi},\ \forall s \in U, \omega \in \mathbb{R}. \tag{3.3}$$

Now, the C^∞-diffeomorphism Ψ is constructed:

$$\Psi : \Gamma \subset \mathbb{R}^n \to S^1; \quad x \mapsto \Psi(x) \text{ and } X_\omega = \Psi_* \left(f|_\Gamma \right). \tag{3.4}$$

Each point of the limit cycle Γ is identified with a point on S^1, and the vector field f of the oscillator restricted to the limit cycle is Ψ-related to the constant vector field X_ω on the unit circle.

Definition 16. *The image $\Psi(x)$ is called* the phase *of the state $x \in \Gamma$.*

Each solution $t \mapsto x(t)$ of (3.2) is an integral curve of the vector field f, since the manifold on which the system (3.2) is defined, is the Euclidean space $\mathbb{R}^n$ (cfr. [11] p.132). Define the function $y : \mathbb{R} \to S^1$ as follows:

$$t \mapsto y(t) := \Psi(p(t)), \tag{3.5}$$

with $t \mapsto p(t)$ the periodic solution of system (3.2).

Theorem 9. *The curve $y = \Psi \circ p$ is an integral curve of X_ω.*

Proof. For each $t_0 \in \mathbb{R}$ it holds that

$$\begin{aligned} T_{t_0} y \left(\left. \frac{\mathrm{d}}{\mathrm{d}t} \right|_{t_0} \right) &= T_{p(t_0)} \Psi \left(T_{t_0} p \left(\left. \frac{\mathrm{d}}{\mathrm{d}t} \right|_{t_0} \right) \right), \\ &= T_{p(t_0)} \Psi \left(f(p(t_0)) \right), \\ &= \left(T\Psi \circ f \right) \left(p(t_0) \right), \\ &= \left(X_\omega \circ \Psi \right) \left(p(t_0) \right), \\ &= X_\omega \left((\Psi \circ p)(t_0) \right), \\ &= X_\omega \left(y(t_0) \right). \end{aligned} \tag{3.6}$$

□

Written in coordinates (using a chart (U, φ)),

$$\frac{\mathrm{d}(\varphi \circ y)}{\mathrm{d}t}(t) = \omega, \quad \forall t \in \mathbb{R}.$$

Hence, $\varphi \circ y$ is a solution of the differential equation

$$\dot{\theta} = \omega. \tag{3.7}$$

Equation (3.7) is called *the phase dynamics of the unperturbed oscillator* and ω is *the natural frequency of the oscillator*. The proof of Theorem 9 shows that using Ψ the dynamics on the limit cycle Γ can be identified with the scalar dynamics (3.7).

As a next step it is investigated how a perturbation of the original dynamics (3.2) can be translated into a perturbation of the phase dynamics (3.7). In order to take perturbations of (3.2) into account, it is required to extend the definition of the phase to an open region $\mathcal{A} \subset \mathbb{R}^n$ containing the limit cycle Γ. Let p_0 be a fixed point on the limit cycle Γ. For each $c \in \mathbb{R} \mod T$, define the set

$$S_c := \{x \in \mathbb{R}^n \mid \lim_{t \to \infty} (|\phi(t + c, x) - p(t, p_0)|) = 0\}, \tag{3.8}$$

with $\phi(t + c, x)$ the solution of (3.2) starting at x at time $-c$. The set S_c is the set of all points in $\mathbb{R}^n$ with the same *asymptotic phase* c (cfr. Appendix A). It can be proven that the set S_c is a $(n-1)$-manifold. Such a manifold S_c on which the asymptotic phase is constant is called an *isochron* [46]. Each isochron is completely determined by the vector field f. Figure 3.1 shows the phase portrait of a three-dimensional limit-cycle oscillator. The limit cycle is indicated by a bold line. In three-dimensional state space isochrons are two-dimensional surfaces. Some isochrons are indicated on the figure by dotted curves (not by surfaces not to overload the picture).

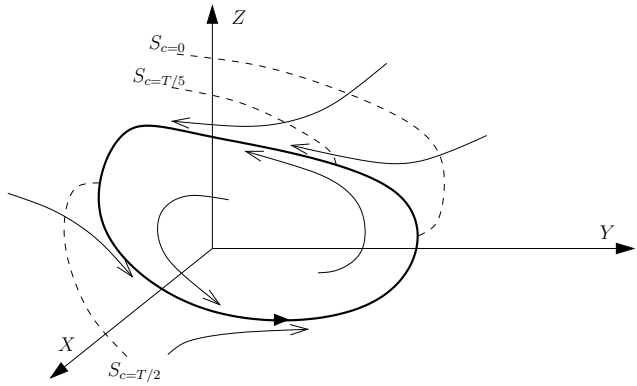

Figure 3.1: The phase portrait of a limit cycle oscillator in three-dimensional state space.

Theorem 10. *The flow of (3.2) translates isochrons into isochrons.*

Proof. Consider the isochron S_c at time $t = 0$. After a time $t_1 \in \mathbb{R}$, the flow has mapped the isochron into the set

$$X := \{x \in \mathbb{R}^n \mid x = \phi(t_1, y) \wedge \lim_{t\to\infty} (|\phi(t + c, y) - p(t, p_0)|) = 0\}.$$

Since $\phi(t, x) = \phi(t, \phi(t_1, y)) = \phi(t + t_1, y),\ \forall t \in \mathbb{R}$, it follows that

$$\phi(t + c, y) = \phi(t + c - t_1, x), \forall t \in \mathbb{R}.$$

The set X can then be written as

$$X = \{x \in \mathbb{R}^n \mid \lim_{t\to\infty} (|\phi(t + c - t_1, x) - p(t, p_0)|) = 0\}.$$

This is the definition of the isochron with asymptotic phase equal to $c - t_1$. This concludes the proof. □

Now define the function $\Theta :\ \mathcal{A} \subset \mathbb{R}^n \to S^1,\ x \mapsto \Theta(x)$ such that for each $c \in \mathbb{R} \mod T$

$$\Theta(x_c) := \Psi(x_{0c}),\ \forall x_c \in S_c \cap \mathcal{A},$$

with $x_{0c} := S_c \cap \Gamma$. Define the function $t \mapsto x_0(t)$ as

$$x_0(t) = \Psi^{-1}\left(\Theta(x(t))\right),\ \forall t \in \mathbb{R}, \tag{3.9}$$

with $t \mapsto x(t)$ a solution of (3.2) with $x(t) \in \mathcal{A}$. Since

- $x(t)$ and $x_0(t)$ are located on the same isochron for each time instant t,

- the flow of (3.2) maps isochrons into isochrons,
- $x_0(t) \in \Gamma$, $\forall t \in \mathbb{R}$,

it holds that $x_0 \equiv p$. Let the function $z : \mathbb{R} \to S^1$ be defined as:

$$z(t) := \Theta(x(t)), \quad \forall t \in \mathbb{R}. \tag{3.10}$$

Then

$$\begin{aligned} T_{t_0} z \left(\frac{\mathrm{d}}{\mathrm{d}t}\Big|_{t_0} \right) &= T_{x(t_0)}\Theta \left(T_{t_0} x \left(\frac{\mathrm{d}}{\mathrm{d}t}\Big|_{t_0} \right) \right), \\ &= T_{x_0(t_0)}\Psi \left(T_{t_0} x_0 \left(\frac{\mathrm{d}}{\mathrm{d}t}\Big|_{t_0} \right) \right), \\ &= T_{p(t_0)}\Psi \left(T_{t_0} p \left(\frac{\mathrm{d}}{\mathrm{d}t}\Big|_{t_0} \right) \right), \\ &= X_\omega \left(z(t_0) \right), \end{aligned} \tag{3.11}$$

showing z is an integral curve of X_ω. The mappings Ψ and Θ allow an identification of the n-dimensional dynamics of the oscillator in a neighborhood $\mathcal{A}$ of the limit cycle Γ with the scalar dynamics $\dot{\theta} = \omega$ on the unit circle.

3.2.3 The Externally Perturbed Oscillator

In the previous section a coordinate-free treatment of the unperturbed oscillator has been presented. In order not to make the matter unnecessarily involved the following sections describe the dynamics in (local) coordinates (with respect to a coordinate chart (U, φ)). Not to overload notation, define $\hat{z} := \varphi \circ z$, $\hat{\Theta} := \varphi \circ \Theta$ and $\hat{\Psi} := \varphi \circ \Psi$ (see Figure 3.2), and introduce the shorthand notation $\frac{\partial \hat{\Theta}}{\partial x} := [\frac{\partial \hat{\Theta}}{\partial x_1} \ \cdots \ \frac{\partial \hat{\Theta}}{\partial x_n}]^T$. Before the problem of the externally perturbed oscillator is tackled, we show the coordinate version of (3.11): for $x(t) \in \mathcal{A}$, $\forall t \in \mathbb{R}$,

$$\begin{aligned} \frac{\mathrm{d}\hat{z}}{\mathrm{d}t}(t) &= \sum_{i=1}^{n} \frac{\partial \hat{\Theta}}{\partial x_i}(x(t)) \frac{\mathrm{d}x_i}{\mathrm{d}t}(t), \\ &= \sum_{i=1}^{n} \frac{\partial \hat{\Theta}}{\partial x_i}(x(t)) f_i(x(t)), \\ &= \left(\frac{\partial \hat{\Theta}}{\partial x} \cdot f \right)(x(t)), \\ &= \omega, \quad \forall t \in \mathbb{R}. \end{aligned} \tag{3.12}$$

This should be regarded as a (partial) transcription of (3.11): the last line in (3.12) does not follow logically from the penultimate line, but is a direct

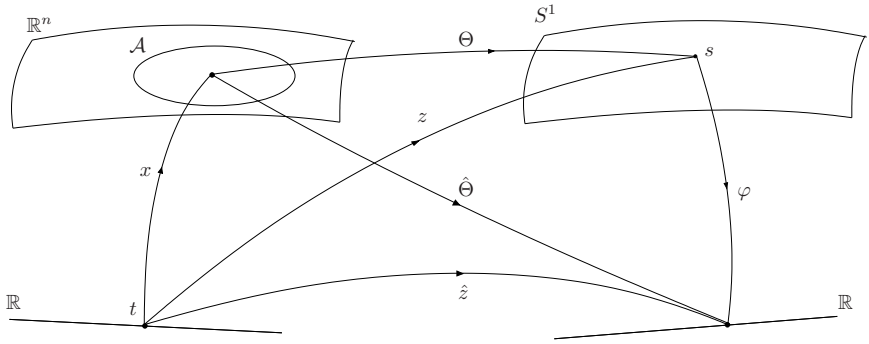

Figure 3.2: Depiction of the relation between the functions considered in Section 3.2.3.

transcription of the last line of (3.11). From (3.12) follows the important result that

$$\left(\frac{\partial\hat{\Theta}}{\partial x}\cdot f\right)(x(t)) = \omega, \quad \forall t \in \mathbb{R}. \tag{3.13}$$

The system equations of an externally perturbed oscillator are

$$\dot{x} = f(x) + \epsilon\, q(x,t), \qquad 0 < \epsilon \ll 1, \tag{3.14}$$

with $q : \mathbb{R}^{n+1} \to \mathbb{R}^n$; $(x,t) \mapsto q(x,t)$ representing the external perturbation and with $\epsilon \in \mathbb{R}$ the strength of the perturbation. Using the chain rule and (3.13),

$$\begin{aligned}\frac{\mathrm{d}\hat{z}}{\mathrm{d}t}(t) &= \left(\frac{\partial\hat{\Theta}}{\partial x}\cdot f\right)(x(t)) + \epsilon\frac{\partial\hat{\Theta}}{\partial x}(x(t))\cdot q(x(t),t),\\ &= \omega + \epsilon\frac{\partial\hat{\Theta}}{\partial x}(x(t))\cdot q(x(t),t).\end{aligned} \tag{3.15}$$

In order to obtain a closed expression in $\hat{z}$ the following assumption is introduced: the distance between the states $x(t)$ and $x_0(t)$ defined by (3.9), is considered to be proportional to the strength of the perturbation:

$$\exists h(t) \in \mathbb{R}^n : x(t) = x_0(t) + \epsilon h(t), \quad \forall t \in \mathbb{R}. \tag{3.16}$$

Now (3.15) can be rewritten as

$$\frac{\mathrm{d}\hat{z}}{\mathrm{d}t}(t) = \omega + \epsilon\,\frac{\partial\hat{\Theta}}{\partial x}(x_0(t)+\epsilon h(t))\cdot q(x_0(t)+\epsilon h(t),t).$$

Performing a Taylor series expansion in x, where second and higher order terms in ϵ are neglected, leads to:

$$\frac{\mathrm{d}\hat{z}}{\mathrm{d}t}(t) = \omega + \epsilon\,\frac{\partial\hat{\Theta}}{\partial x}(x_0(t))\cdot q(x_0(t),t) + O(\epsilon^2). \tag{3.17}$$

Because $x_0(t) \in \Gamma, \forall t \in \mathbb{R}$ and because of the definitions (3.10) and (3.9),

$$x_0(t) = \hat{\Psi}^{-1}(\hat{z}(t)). \tag{3.18}$$

Equation (3.17) can then be rewritten as

$$\frac{\mathrm{d}\hat{z}}{\mathrm{d}t}(t) = \omega + \epsilon \frac{\partial \hat{\Theta}}{\partial x}(\hat{\Psi}^{-1}(\hat{z}(t))) \cdot q(\hat{\Psi}^{-1}(\hat{z}(t)), t) + O(\epsilon^2).$$

implying that, up to first order, $\hat{z}$ is a solution of the differential equation

$$\dot{\theta} = \omega + \epsilon \frac{\partial \hat{\Theta}}{\partial x}(\hat{\Psi}^{-1}(\theta)) \cdot q(\hat{\Psi}^{-1}(\theta), t). \tag{3.19}$$

Equation (3.19) is called *the phase dynamics of the perturbed oscillator*.

3.2.4 Two Mutually Coupled Oscillators

In this section we consider the dynamics of two nearly identical mutually coupled oscillators. For sufficiently weak coupling the influence of the first oscillator on the second oscillator can be considered a perturbation of the second oscillator and vice versa. The differential equations are:

$$\begin{cases} \dot{x}_1 = f_1(x_1) + \epsilon\, V(x_1, x_2), \\ \dot{x}_2 = f_2(x_2) + \epsilon\, V(x_2, x_1). \end{cases} \tag{3.20}$$

with $x_i(t) \in \mathbb{R}^n$ the state of the i-th oscillator and $V : \mathbb{R}^n \times \mathbb{R}^n \to \mathbb{R}^n$ the coupling function. External perturbations are not considered in this section. The near-identity of the oscillators is expressed as follows:

$$f_i(x_i) = f(x_i) + \epsilon\, g_i(x_i), \quad 0 < \epsilon \ll 1, \quad i = 1, 2.$$

The vector field of each oscillator deviates slightly from a common vector field f. The differential equation (3.20) changes into

$$\dot{x}_i = f(x_i) + \epsilon\Big(V(x_i, x_j) + g_i(x_i)\Big), \quad i, j = 1, 2, \quad i \neq j.$$

Define $\hat{z}_i : \mathbb{R} \to \mathbb{R}$ as

$$\hat{z}_i(t) := \hat{\Theta}(x_i(t)), \quad i = 1, 2. \tag{3.21}$$

Then

$$\begin{aligned} \frac{\mathrm{d}\hat{z}_i}{\mathrm{d}t}(t) &= \left(\frac{\partial \hat{\Theta}}{\partial x_i} \cdot f\right)(x_i(t)) + \epsilon \frac{\partial \hat{\Theta}}{\partial x_i}(x_i(t)) \cdot \Big(V(x_i(t), x_j(t)) + g_i(x_i(t))\Big), \\ &= \omega + \epsilon \frac{\partial \hat{\Theta}}{\partial x_i}(x_i(t)) \cdot \Big(V(x_i(t), x_j(t)) + g_i(x_i(t)))\Big), \end{aligned}$$

for $i, j = 1, 2,\ i \neq j$. Similar to the treatment in the previous section, an approximation is introduced:

$$\exists h_i(t) \in \mathbb{R}^n : x_i(t) = x_{i0}(t) + \epsilon h_i(t), \quad \forall t \in \mathbb{R},\ i = 1, 2, \tag{3.22}$$

where

$$x_{i0}(t) := \hat{\Psi}^{-1}(\hat{z}_i(t)). \tag{3.23}$$

Then

$$\frac{\mathrm{d}\hat{z}_i}{\mathrm{d}t}(t) = \omega + \epsilon \frac{\partial \hat{\Theta}}{\partial x_i}(x_{i0}(t) + \epsilon h_i(t)) \cdot \Big(V(x_{i0}(t) + \epsilon h_i(t), x_{j0}(t) + \epsilon h_j(t)) + g_i(x_{i0}(t) + \epsilon h_i(t))\Big),$$

for $i, j = 1, 2,\ i \neq j$. A Taylor series expansion in x is performed where terms of second order and higher are neglected:

$$\frac{\mathrm{d}\hat{z}_i}{\mathrm{d}t}(t) = \omega + \epsilon \frac{\partial \hat{\Theta}}{\partial x_i}(x_{i0}(t)) \cdot \Big(V(x_{i0}(t), x_{j0}(t)) + g_i(x_{i0}(t))\Big),$$

for $i, j = 1, 2,\ i \neq j$. From (3.21) and (3.23) it follows that $(\hat{z}_1(t), \hat{z}_2(t))$ is a solution of

$$\dot{z}_i = \omega + \epsilon \frac{\partial \hat{\Theta}}{\partial x_i}(\hat{\Psi}^{-1}(z_i)) \cdot \Big(V(\hat{\Psi}^{-1}(z_i), \hat{\Psi}^{-1}(z_j)) + g_i(\hat{\Psi}^{-1}(z_i))\Big), \tag{3.24}$$

for $i, j = 1, 2,\ i \neq j$. The system equations (3.24) can be further simplified using averaging techniques. This technique cannot be applied to the equations as such. It is necessary to define an equivalent dynamics on the real line, with a time-periodic vector field. Define the continuous function $\tilde{z}_i : \mathbb{R} \to \mathbb{R},\ t \mapsto z_i(t)$:

$$\begin{aligned} \tilde{z}_i(t) \mod 2\pi = \hat{z}_i(t), \forall t \in \mathbb{R}, \\ \tilde{z}_i(0) = \hat{z}_i(0) \in [0, 2\pi) \end{aligned} \tag{3.25}$$

and let $\tilde{\Psi}^{-1} : \mathbb{R} \to \mathbb{R}^n$ be defined as

$$v \mapsto \tilde{\Psi}^{-1}(v) := \hat{\Psi}^{-1}(v \mod 2\pi).$$

Define to simplify the notation

$$\begin{aligned} Z : \mathbb{R} \to \mathbb{R}^n, &\qquad v \mapsto Z(v) := \frac{\partial \theta}{\partial x}(\tilde{\Psi}^{-1}(v)), \\ W : \mathbb{R}^2 \to \mathbb{R}^n, &\qquad (v, w) \mapsto W(w, w) := V(\tilde{\Psi}^{-1}(v), \tilde{\Psi}^{-1}(w)), \\ G_i : \mathbb{R} \to \mathbb{R}^n, &\qquad v \mapsto G_i(v) := g_i(\tilde{\Psi}^{-1}(v)). \end{aligned}$$

and introduce the continuous functions $\psi_i : \mathbb{R} \to \mathbb{R}$ by

$$\tilde{z}_i(t) = \omega t + \psi_i(t),$$
$$\psi_i(0) \in [0, 2\pi).$$

The functions ψ_i can be interpreted as phase disturbances. Now consider the following system equations:

$$\dot{\psi}_i = \epsilon\, Z_i(\omega t + \psi_i) \cdot \Big(W(\omega t + \psi_i, \omega t + \psi_j) + G_i(\omega t + \psi_i)\Big). \tag{3.26}$$

with $i, j = 1, 2,\ i \neq j$. These dynamics are constructed in such a way that ψ is a solution of (3.26) if and only if the corresponding function $\hat{z}$ is a solution of (3.24).

The system of equations (3.26) is of the form

$$\dot{x} = \epsilon f(t, x, \epsilon), \quad 0 < \epsilon \ll 1,$$

with $f(t, x, \epsilon) : \mathbb{R}^{n+2} \to \mathbb{R}^n$ periodic in t with period T. By averaging techniques [43], solutions of this system can be approximated by solutions of the system

$$\dot{x} = \epsilon \frac{1}{T} \int_0^T f(\tau, x, 0) d\tau,$$

if the function f is continuous and bounded, and has bounded derivatives up to the second order with respect to its arguments, for $(t, x, \epsilon) \in [0, \infty) \times D \times [0, \epsilon_0]$, with $D = \{x \in \mathbb{R}^n \mid \|x\| < r,\ r \in \mathbb{R}\}$.

Applying the averaging techniques to (3.26) yields an approximating dynamics

$$\begin{aligned}\dot{\psi}_i = {} & \epsilon \frac{1}{2\pi} \int_0^{2\pi} \mathrm{d}\lambda Z(\lambda + \psi_i) \cdot G_i(\lambda + \psi_i) \\ & + \epsilon \frac{1}{2\pi} \int_0^{2\pi} \mathrm{d}\lambda Z(\lambda + \psi_i) \cdot W(\lambda + \psi_i, \lambda + \psi_j), \quad i, j = 1, 2, \quad i \neq j. \end{aligned} \tag{3.27}$$

Consider the expression

$$\frac{1}{2\pi} \int_0^{2\pi} \mathrm{d}\lambda Z(\lambda + \psi_i) \cdot W(\lambda + \psi_i, \lambda + \psi_j), \quad i, j = 1, 2, \quad i \neq j.$$

The substitution $\mu = \lambda + \psi_i$ leads to

$$\frac{1}{2\pi} \int_{\psi_i}^{2\pi + \psi_i} \mathrm{d}\mu Z(\mu) \cdot W(\mu, \mu - (\psi_i - \psi_j)), \quad i, j = 1, 2, \quad i \neq j. \tag{3.28}$$

Since Z and W are periodic functions with period 2π, (3.28) becomes

$$\frac{1}{2\pi} \int_0^{2\pi} \mathrm{d}\mu Z(\mu) \cdot W(\mu, \mu - (\psi_i - \psi_j)), \quad i, j = 1, 2, \quad i \neq j.$$

Similarly, the expression

$$\frac{1}{2\pi}\int_0^{2\pi} \mathrm{d}\lambda Z(\lambda+\psi_i)\cdot G_i(\lambda+\psi_i), \quad i=1,2.$$

can be written as

$$\frac{1}{2\pi}\int_0^{2\pi} \mathrm{d}\lambda Z(\lambda)\cdot G_i(\lambda), \quad i=1,2.$$

Defining the function $\Lambda : \mathbb{R} \to \mathbb{R}$ as

$$v \mapsto \Lambda(v) := \frac{1}{2\pi}\int_0^{2\pi} \mathrm{d}\mu Z(\mu)\cdot W(\mu,\mu-v),$$

and the constant $\gamma_i \in \mathbb{R}$ as

$$\gamma_i := \frac{1}{2\pi}\int_0^{2\pi} \mathrm{d}\lambda Z(\lambda)\cdot G_i(\lambda), \quad i=1,2,$$

equation (3.27) can be written as

$$\dot{\psi}_i = (\omega+\epsilon\,\gamma_i)+\epsilon\,\Lambda(\psi_i-\psi_j), \quad i,j=1,2, \quad i\neq j. \tag{3.29}$$

or in terms of the phase variables $\tilde{z}_i$ on the real line,

$$\dot{\tilde{z}}_i = \omega_i+\epsilon\,\Lambda(\tilde{z}_i-\tilde{z}_j), \quad i,j=1,2, \quad i\neq j. \tag{3.30}$$

with $\omega_i := \omega+\epsilon\,\gamma_i$ the *natural frequency* of the i-th oscillator. Using (3.25), the dynamics (3.30) can be transformed back into a dynamics on the circle since Λ is 2π-periodic: $\hat{z}$ is a solution of the differential equation

$$\dot{\theta}_i = \omega_i+\epsilon\,\Lambda(\theta_i-\theta_j), \quad i,j=1,2, \quad i\neq j. \tag{3.31}$$

3.2.5 N Mutually Coupled Oscillators

The analysis of the previous section can be repeated for a population of N oscillators in a straightforward manner. Let L_i denote the set of oscillators that are coupled to the i-th oscillator. The phase dynamics of the population then is

$$\dot{z}_i = \omega_i+\epsilon\sum_{j\in L_i}\Lambda(z_i-z_j), \quad i\in\mathcal{N}, \tag{3.32}$$

where $\mathcal{N} := \{1,\ldots,N\}$. As a coupling function Λ, Kuramoto proposed the sine function, since it allows for a mathematical analysis of (3.32). This analysis is presented in the next section.

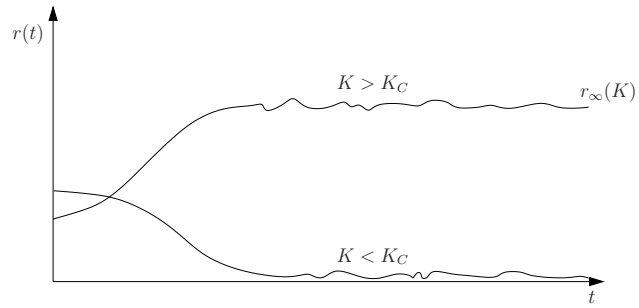

Figure 3.3: Evolution of the amplitude of the order parameter for different values of K in the case of a finite number of oscillators.

3.3 Analysis of the Kuramoto Model with Infinitely Many Oscillators

3.3.1 Kuramoto's Analysis

In [46] and [87] the Kuramoto model describing an *infinite* population of oscillators is analyzed. The analysis is repeated in this section. Before starting a mathematical analysis, Kuramoto performed some simulations. The simulated dynamics are

$$\dot{\theta}_i = \omega_i + \frac{K}{N}\sum_{j=1}^{N}\sin(\theta_j - \theta_i), \qquad i \in \mathcal{N}, \tag{3.33}$$

where $\theta_i \in S^1 := \mathbb{R} \mod 2\pi$, and $\omega_i \in \mathbb{R}$, $\forall i \in \mathcal{N}$. The parameter $K \geq 0$ is called the *coupling strength*. The factor $1/N$ ensures that the model is well behaved as $N \to \infty$. By demanding that the phase θ_i is an element of $\mathbb{R} \mod 2\pi$, equivalence classes are created on the phase values. Two phases belong to the same equivalence class if their difference is a multiple of 2π. Each equivalence class is represented by an element of $[0, 2\pi)$. In the remainder of this dissertation every phase θ_i assumes a value belonging to this set of representatives, by convention. The behavior of the system is visualized through an auxiliary quantity called the complex order parameter Υ, defined as

$$t \mapsto \Upsilon(t) = r(t)e^{i\psi(t)} := \frac{1}{N}\sum_{j=1}^{N} e^{i\theta_j(t)}. \tag{3.34}$$

In Kuramoto's simulations the number of oscillators is taken large and the evolution in time of r is plotted for several values of the coupling strength (cfr. Figure 3.3). For values of K smaller than a certain threshold value K_C, $r(t)$ decays to a tiny jitter of size $O(1/\sqrt{N})$. When K exceeds K_C, $r(t)$ tends

to a constant value $r_\infty(K)$ larger than zero, and keeps fluctuating around this value with fluctuations of size $O(1/\sqrt{N})$. One expects these fluctuations to decrease to zero for $N \to \infty$ and

$$\lim_{t \to \infty} r(t) = r_\infty(K), \quad K > K_C,$$
$$\lim_{t \to \infty} r(t) = 0, \qquad\quad K \leq K_C.$$

Values for $r_\infty(K)$ can be approximated by simulations, leading to the graph of Figure 3.4. The upper branch in the figure has the property that $\lim_{K \to \infty} r_\infty(K) = 1$, which means that for infinitely large coupling strength the oscillators all assume the same phase. This behavior is called *synchronization*. Properties of the upper branch for finite coupling strengths follow from the analysis described below.

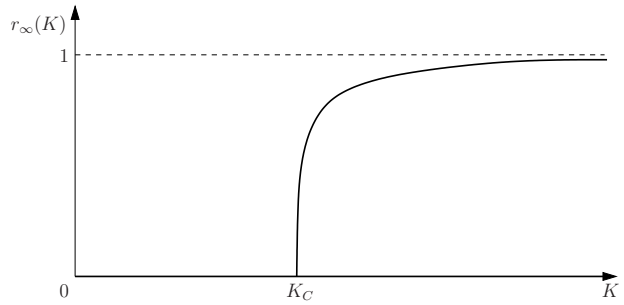

Figure 3.4: Dependence of the steady-state coherence r_∞ on the coupling strength K obtained by simulation.

The simulations suggest that an analysis is more tractable for populations with an infinite number of oscillators, since $r(t)$ converges to a constant instead of fluctuating around some steady state value. This led Kuramoto to investigate system (3.33) with $N \to \infty$. The natural frequencies ω_i are drawn from a prescribed distribution $g : \mathbb{R} \to [0, 1]$ which is assumed to be unimodal and symmetric about its mean frequency Ω.

Definition 17. *A distribution g is called* symmetric about Ω *if* $g(\Omega - \omega) = g(\Omega + \omega)$, $\forall \omega \in \mathbb{R}$.

Definition 18. *The* mean value μ *of a distribution g is defined as*

$$\mu := \int_{-\infty}^{\infty} \omega g(\omega) d\omega. \tag{3.35}$$

It can be proven that for a distribution g symmetric about Ω, $\mu = \Omega$.

Definition 19. *A distribution g which is symmetric about a value Ω is called* unimodal *if it is nowhere increasing on $[\Omega, \infty)$, i.e. $\omega_1 \leq \omega_2 \Rightarrow g(\omega_1) \geq g(\omega_2)$, $\forall \omega_1, \omega_2 > \Omega$.*

The order parameter of an infinite population is defined in [46] as

$$\Upsilon(t) = r(t)e^{i\psi(t)} := \int_0^{2\pi} e^{i\theta} n(\theta, t) \mathrm{d}\theta, \tag{3.36}$$

where $n : S^1 \times \mathbb{R} \to \mathbb{R}$; $(\theta, t) \mapsto n(\theta, t)$ is the number density function; $n(\theta, t)$ stands for the number of oscillators with phase between θ and $\theta + \mathrm{d}\theta$ at time t, normalized by the total number of oscillators. It is important to remark that although (3.33) with $N \to \infty$ represents a population of a *countably* infinite number of oscillators, Kuramoto applied these equations to a population of an *uncountably* infinite number of oscillators, as indicated by his definition of the order parameter. Although not rigorously correct and highly intuitive at times, his approach is described in this section in order to clearly display the line of reasoning which led to his important results. A rigorous description, obtained by Strogatz [87] and mathematically justifying the results obtained by Kuramoto, is presented in the following section.

Before starting the analysis, some possible types of behavior of the population are defined.

Definition 20. *A group of oscillators exhibits* phase locking *when the phase differences between the oscillators are constant in time.*

Definition 21. Partial synchronization *is defined as the state of the population where one group of oscillators phase locks while the phase differences between the oscillators of the remaining group are not constant in time. Furthermore, the amplitude of the order parameter is required to be constant in time.*

Using the order parameter (3.36), the equations (3.33) can be rewritten as

$$\dot{\theta}_i = \omega_i + Kr \sin(\psi - \theta_i), \qquad i \in \mathcal{N}, \tag{3.37}$$

where r and ψ depend on $\theta := [\theta_1 \ \cdots \ \theta_N]^T$. Inspired by the simulations, the existence of solutions with constant r is postulated. Because of the symmetry and convexity of g, the behavior of $\psi(t)$ of these steady state solutions is assumed $\Omega t + \psi(0)$. In general, the assumption on ψ is not needed in the analysis. We could start with an arbitrary function for ψ and at the end of the analysis obtain $\psi(t) = \Omega t + \psi(0)$ from a self-consistency condition [70]. Here, we simply assume Ω to be the frequency of the steady state solution and it will be shown that this indeed solves the problem.

By introducing the rotating frame with frequency Ω, and choosing the origin of this frame correctly, one can set ψ to zero in (3.37) without loss of generality: the time dependent change of coordinates $\tilde{\theta}_i = \theta_i - \Omega t - \psi(0)$ changes (3.37) into

$$\dot{\tilde{\theta}}_i + \Omega = \omega_i + Kr \sin(\psi - \tilde{\theta}_i - \Omega t - \psi(0)), \qquad i \in \mathcal{N}.$$

Since $\psi(t) = \Omega t + \psi(0),\ \forall t \in \mathbb{R}$, this becomes

$$\dot{\tilde{\theta}}_i = \omega_i - \Omega - Kr \sin \tilde{\theta}_i, \qquad i \in \mathcal{N}.$$

The substitution $\tilde{\omega}_i := \omega_i - \Omega$ yields

$$\dot{\tilde{\theta}}_i = \tilde{\omega}_i - Kr \sin \tilde{\theta}_i, \qquad i \in \mathcal{N}, \tag{3.38}$$

with the *shifted natural frequency* $\tilde{\omega}_i$ drawn from the distribution $\tilde{g}$ defined by $\tilde{g}(\omega) := g(\omega + \Omega), \forall \omega \in \mathbb{R}$. This distribution is an even distribution: $\tilde{g}(\omega) = \tilde{g}(-\omega), \forall \omega \in \mathbb{R}$.

If the solution θ is such that for $t \to \infty$ it gives rise to a constant $r(t) = r_\infty$, then the equations (3.38) are effectively uncoupled. Let us take a closer look at these uncoupled equations: each equation is of the form

$$\dot{\theta} = \omega - a\ \sin \theta, \tag{3.39}$$

with $a > 0$. For convenience we assume that $\omega > 0$. The vector field $\omega - a \sin \theta$ is plotted in Figure 3.5 and Figure 3.6. If $a < \omega$ the phase of the oscillator keeps moving on the circle. When $a = \omega$ one fixed point appears at $\theta = \pi/2$ and, although the fixed point is not stable according to the standard stability definition, the phase of the oscillator converges to this point for each initial condition since the vector field is defined on the circle. For $a > \omega$ one stable and one unstable fixed point are present. For almost all initial conditions the oscillator phase converges to the stable fixed point located in the interval $(-\pi/2, \pi/2)$.

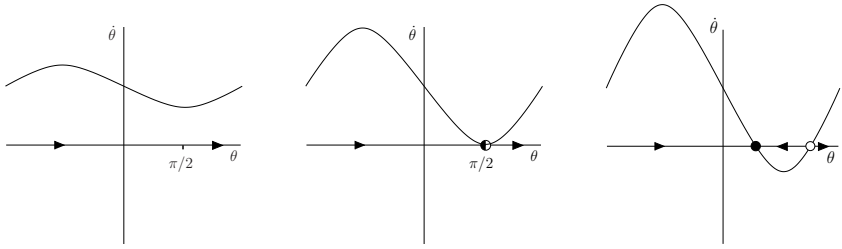

(a) $\omega > a$ (b) $\omega = a$ (c) $\omega < a$

Figure 3.5: Vector field of equation (3.39).

From the above analysis of (3.39) it is concluded that if the equations (3.38) are uncoupled, the population splits into two groups: a group with $|\tilde{\omega}_i| \leq Kr_\infty$ and a group with $|\tilde{\omega}_i| > Kr_\infty$.

- The phase of an oscillator with natural frequency $|\tilde{\omega}_i| \leq Kr_\infty$ converges to the equilibrium point implicitly defined by

  $$\tilde{\omega}_i = Kr_\infty \sin \tilde{\theta}_i, \tag{3.40}$$

  with $|\tilde{\theta}_i| \leq \pi/2$.

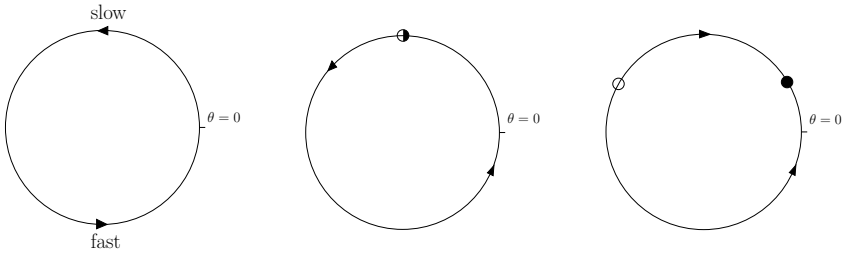

(a) $\omega > a$ (b) $\omega = a$ (c) $\omega < a$

Figure 3.6: Vector field of equation (3.39) displayed on the circle.

- The phase of an oscillator with $|\tilde{\omega}_i| > Kr_\infty$ keeps moving on the circle in a nonuniform manner since the corresponding system equation does not possess equilibrium points. Such behavior is called *drifting*.

The existence of the postulated steady state solution with r constant can only be ensured by imposing a constraint on the phases of the drifting oscillators. Let n_{pl} denote the number density of the **p**hase **l**ocking oscillator group and let n_d denote the number density of the **d**rifting oscillator group. Define Υ_{pl} and Υ_d as the corresponding order parameters:

$$\Upsilon(t) = \Upsilon_{pl}(t) + \Upsilon_d(t) = \int_0^{2\pi} e^{i\theta} n_{pl}(\theta, t)\mathrm{d}\theta + \int_0^{2\pi} e^{i\theta} n_d(\theta, t)\mathrm{d}\theta.$$

Each oscillator belonging to the phase locking group converges to a constant phase in the $\tilde{\theta}$-coordinate implying

$$\exists c_1 \in [0,1], \exists c_2 \in [0, 2\pi) : \Upsilon_{pl}(t) = c_1 e^{i\Omega t + ic_2}.$$

Then the assumption $\Upsilon(t) = r_\infty e^{i\Omega t + i\phi(0)}$ only holds if

$$\exists c_3 \in [0,1], \exists c_4 \in [0, 2\pi) : \Upsilon_d(t) = c_3 e^{i\Omega t + ic_4}. \tag{3.41}$$

If (3.41) is not satisfied, the modulus of the complex number $\Upsilon_{pl}(t) + \Upsilon_d(t)$ will not be constant in time. Therefore Kuramoto demanded that the drifting oscillators form a stationary distribution in $\tilde{\theta}$-space (for each natural frequency separately). This is a sufficient condition for (3.41). Let $\rho(\theta, \omega)\mathrm{d}\theta$ denote the fraction of oscillators with shifted natural frequency ω and with phases in the rotating frame between θ and $\theta + \mathrm{d}\theta$. Kuramoto assumed $\rho(\theta, \omega)$ inversely proportional to the speed at θ (oscillators pile up at slow places and thin out at fast places on the circle):

$$\rho(\theta, \omega) = \frac{C(\omega)}{|\omega - Kr\sin\theta|}, \tag{3.42}$$

with $C(\omega)$ a normalization constant determined by $\int_{-\pi}^{\pi} \rho(\theta,\omega)\mathrm{d}\theta = 1$, which yields

$$C(\omega) = \frac{1}{2\pi}\sqrt{\omega^2 - (Kr)^2}.$$

Let $\tilde{n}_d$ denote the number density of the drifting group in the rotating frame: $\tilde{n}_d(\theta,t) = n_d(\theta + \Omega t + \phi(0), t)$. Then

$$\begin{aligned}\tilde{n}_d(\theta,t) &= \int_{|\omega|>Kr_\infty} \rho(\theta,\omega)\tilde{g}(\omega)\mathrm{d}\omega, \\ &= \int_{|\omega|>Kr_\infty} \frac{\sqrt{\omega^2-(Kr)^2}\tilde{g}(\omega)}{2\pi|\omega - Kr\sin\theta|}\mathrm{d}\omega\end{aligned} \tag{3.43}$$

The number density in the rotating frame $\tilde{n}_{pl}(\theta,t)$ of the phase locking group is obtained via (3.40):

$$\tilde{n}_{pl}(\theta,t) = \tilde{g}(\omega)\left|\frac{\mathrm{d}\omega}{\mathrm{d}\theta}\right| = Kr_\infty\cos\theta\tilde{g}(Kr_\infty\sin\theta).$$

Via the definition (3.36) we obtain the following self-consistency condition:

$$\begin{aligned}r_\infty e^{(i\Omega t + i\phi(0))} &= \int_{-\pi}^{\pi}(n_{pl}(\theta,t) + n_d(\theta,t))e^{i\theta}\mathrm{d}\theta, \\ &= \int_{-\pi}^{\pi}(\tilde{n}_{pl}(\theta,t) + \tilde{n}_d(\theta,t))e^{(i\theta + i\Omega t + i\phi(0))}\mathrm{d}\theta.\end{aligned} \tag{3.44}$$

According to (3.43) the number density $\tilde{n}_d$ is π-periodic in θ and hence does not contribute to the integral (3.44). This is more than we bargained for: not only do we obtain the desired stationarity, but we also get $\Upsilon_d(t) = 0, \forall t \in \mathbb{R}$. Equation (3.44) yields two real equations, namely its real and imaginary part:

$$r_\infty = Kr_\infty\int_{-\pi/2}^{\pi/2}\cos^2\theta\tilde{g}(Kr_\infty\sin\theta)\mathrm{d}\theta, \tag{3.45}$$

$$0 = Kr_\infty\int_{-\pi/2}^{\pi/2}\cos\theta\sin\theta\tilde{g}(Kr_\infty\sin\theta)\mathrm{d}\theta. \tag{3.46}$$

Equation (3.46) is fulfilled due to the symmetry of $\tilde{g}$, which shows that $\psi(t) = \Omega t + \phi(0)$ is a valid assumption. Equation (3.45) determines the amplitude of the order parameter. First, it has a trivial zero solution: $r_\infty(K) = 0,\ \forall K > 0$. The density distributions $\rho(\theta,t,\omega)$ that correspond to $r_\infty = 0$ are in general not stationary. Stability properties of the zero-solution have been established in [87]. A second branch of solutions satisfies

$$1 = K\int_{-\pi/2}^{\pi/2}\cos^2\theta\tilde{g}(Kr_\infty\sin\theta)\mathrm{d}\theta. \tag{3.47}$$

This expression is called the *consistency condition on the amplitude of the order parameter*. This branch corresponds to partially synchronized states and it bifurcates continuously from the branch $r_\infty = 0$ at a value $K = K_C$ obtained by letting $r_\infty \to 0^+$ in the equation above:

$$K_C = \frac{2}{\pi \tilde{g}(0)}.$$

By expanding the integrand in (3.47) in powers of r_∞, we obtain the following expression:

$$r_\infty \approx \sqrt{\frac{16}{\pi K_C^3}} \sqrt{\frac{\alpha}{-\tilde{g}''(0)}}, \qquad \alpha := \frac{K - K_C}{K_C}.$$

The bifurcation is supercritical if $\tilde{g}''(0) < 0$ and subcritical if $\tilde{g}''(0) > 0$. This explains Kuramoto's assumption of unimodality on the frequency distribution, because in the generic case of unimodality, $\tilde{g}''(0) < 0$.

In the special case of a Lorentzian density

$$g(\omega) = \frac{\gamma}{\pi(\gamma^2 + \omega^2)}, \ \omega \in \mathbb{R},$$

with γ a real parameter, Kuramoto integrated (3.47) exactly and obtained:

$$r_\infty(K) = \sqrt{1 - \frac{K_C}{K}}.$$

This expression matches the results of the numerical simulations sketched in figure 3.4.

This way, Kuramoto constructed steady state solutions for (3.33). Notice that he did not prove that those are the only ones and that he did not prove that these solutions are indeed asymptotically stable, as observed in the simulations.

3.3.2 Analysis of the Kuramoto Model by Mirollo and Strogatz

In [62] the discrepancy between the mathematical model representing a countably infinite number of oscillators on one side and the analysis treating an uncountable number of oscillators on the other, was removed. The solution consisted in the introduction of a continuum dynamics. For each natural frequency $\omega \in \mathbb{R}$, imagine a continuum of oscillators distributed on the circle. Let $\rho(\theta, t, \omega)\mathrm{d}\theta$ denote the fraction of oscillators with natural frequency ω that are located between θ and $\theta + \mathrm{d}\theta$ at time t. Then ρ is nonnegative, 2π-periodic in θ and satisfies the normalization

$$\int_0^{2\pi} \rho(\theta, t, \omega)\mathrm{d}\theta = 1, \qquad \forall \omega \in \mathbb{R}, \ \forall t \in \mathbb{R}.$$

Let $v(\theta, t, \omega)$ be the instantaneous velocity of an oscillator with natural frequency ω at position θ at time t. The evolution of ρ is then governed by the partial differential equation

$$\frac{\partial \rho}{\partial t} = -\frac{\partial}{\partial \theta}(\rho v), \tag{3.48}$$

which expresses conservation of the number of oscillators of frequency ω. This equation is called *the equation of continuity*. It is a well-known equation in continuum mechanics where it expresses conservation of mass, with ρ the mass density function. The vector field of (3.2) is translated to the PDE-setting by requiring

$$v(\theta, t, \omega) = \omega + Kr(t)\sin(\psi(t) - \theta), \tag{3.49}$$

with

$$r(t)e^{i\psi(t)} = \int_0^{2\pi}\int_{-\infty}^{\infty} e^{i\theta}\rho(\theta, t, \omega)g(\omega)\mathrm{d}\omega\mathrm{d}\theta. \tag{3.50}$$

Combining (3.49) and (3.50) yields a single equation for ρ in closed form:

$$\frac{\partial \rho}{\partial t} = -\frac{\partial}{\partial \theta}\Big[\rho \cdot \Big(\omega + K\int_0^{2\pi}\int_{-\infty}^{\infty}\sin(\theta' - \theta)\rho(\theta', t, \omega')g(\omega')\mathrm{d}\omega'\mathrm{d}\theta'\Big)\Big]. \tag{3.51}$$

Assume the density function ρ is constant in time. From (3.48) it follows that

$$\frac{\partial \rho}{\partial t} = 0 \Leftrightarrow \exists C : \mathbb{R}^2 \to \mathbb{R} : \rho(\theta, t, \omega)v(\theta, t, \omega) = C(\omega, t).$$

Then

$$\rho(\theta, t, \omega) = \frac{C(t, \omega)}{v(\theta, t, \omega)} = \frac{C(t, \omega)}{\omega + Kr(t)\sin(\psi(t) - \theta)}. \tag{3.52}$$

From (3.52) it follows that ρ is constant in time if and only if

$$\begin{cases} \exists C' : \mathbb{R} \to \mathbb{R} : C(t, \omega) = C'(\omega), & \forall \omega, t \in \mathbb{R}, \\ \exists r_\infty \in [0, 1] : r(t) = r_\infty, & \forall t \in \mathbb{R}, \\ \exists \psi_0 \in [0, 2\pi) : \psi(t) = \psi_0, & \forall t \in \mathbb{R}, \end{cases}$$

and

$$\rho(\theta, t, \omega) = \frac{C(\omega)}{\omega - Kr_\infty \sin(\psi_0 - \theta)},$$

which is equivalent to Kuramoto's assumption (3.42) on the drifting oscillators if $C(\omega) \neq 0$.

Furthermore, if for a given natural frequency $C(\omega) = 0$, then

$$\rho(\theta, t, \omega)v(\theta, t, \omega) = 0. \tag{3.53}$$

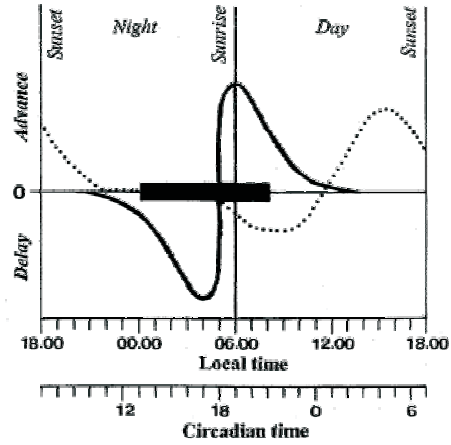

Figure 3.7: Schematic human phase response curve to light and melatonin (modified from [50, 61]).

Since

$$\begin{cases} v(\theta, t, \omega) = 0, & \theta = \arcsin(\omega / K r_\infty), \\ v(\theta, t, \omega) \neq 0, & \text{elsewhere}, \end{cases}$$

the density function ρ that satisfies (3.53) is given by $\rho(\theta, t, \omega) = \delta(\omega - Kr_\infty \sin(\psi_0 - \theta))$, where δ denotes the Dirac impulse distribution. This represents those oscillators of the phase locking oscillator group with natural frequency ω and satisfying (3.40) as found by Kuramoto.

3.4 The Kuramoto Model versus the Phase Resetting Curve

In experimental science, oscillators are classified and determined by their phase resetting curves (PRC, also called phase response curve). A phase resetting curve shows the response of an oscillator to an external stimulus. The oscillator's response is a phase shift, the size of which depends on the phase at which the stimulus is applied. A more complete picture of the oscillator is obtained when several PRCs are plotted with different durations of the applied stimulus.

An example of a phase response curve is presented in Figure 3.7. The vertical axis of the phase-response curve (PRC) shows the phase shift of the body temperature rhythm induced by light exposure (solid line) and the phase shift of the melatonin rhythm produced by melatonin administration (dotted line) at various times in the oscillator's cycle, shown on the hori-

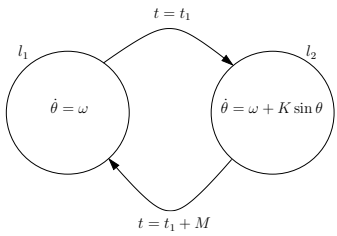

Figure 3.8: A hybrid system representation of the stimulation of an oscillator.

zontal axis as local or circadian times. The circadian time 18 corresponds roughly to the minimum of the body temperature (the temperature values themselves are not indicated on the figure!). The black bar indicates a typical time for sleep relative to the minimum of the body temperature when the circadian system is entrained to the 24-hour day. For orientation purposes, sunrise and sunset are drawn for the time of year when the night and day are of equal length. The PRC to light is about 12 hours out of phase with the PRC to melatonin.

In the remainder of this section the connection between the Kuramoto model and phase resetting curves is exposed. The most general form of the phase dynamics of an externally perturbed (or stimulated) oscillator is given by (3.19). Similar to Kuramoto's proposal to investigate the coupled dynamics (3.32) with $\Lambda = \sin$, the perturbation/stimulus is represented by a sinusoidal function, yielding a simplified stimulated oscillator dynamics [96]

$$\dot{\theta} = \omega + K \sin \theta, \tag{3.54}$$

where K is now interpreted as the strength of the stimulus. This equation is often called the Adler equation after Robert Adler, who investigated the forcing of electric oscillators in [2]. The effect of a stimulus on the phase of the oscillator is most clearly explained in the hybrid system setting of Figure 3.8. At first the system evolves according to $\dot{\theta} = \omega$ at location l_1. At the time instant t_1, the system switches to location l_2 where $\dot{\theta} = \omega + K \sin \theta$. This means the stimulus has been turned on. At time $t_1 + M$ the system switches back to l_1 and the state evolves again freely. It is assumed that trajectories of the hybrid system are continuous, i.e. the switchings do not cause a discontinuous jump in the phase θ. Let $\theta_s(t, \theta_0)$ denote the value of the phase at time t in this switching scenario, corresponding to the initial state θ_0. Similarly, let $\theta_u(t, \theta_0)$ denote the solution of $\dot{\theta} = \omega$, i.e. when no stimulus is applied, at time t with initial state θ_0. The phase shift resulting from the stimulus is

$$\Delta\theta(\theta_0) = \theta_s(t, \theta_0) - \theta_u(t, \theta_0), \quad t > t_1 + M. \tag{3.55}$$

The phase shift depends on the initial state, or equivalently, on the phase at time t_1, which is $\theta_0 + \omega t_1$.

The phase shift can be analytically determined for the dynamics (3.54) as follows. First rearrange (3.54) as

$$\frac{\mathrm{d}\theta}{\omega + K\sin\theta} = \mathrm{d}t.$$

With θ_1 the phase at the beginning of the stimulus, θ' the phase at the stimulus' end, and M the duration of the stimulus,

$$M = \int_0^M \mathrm{d}t = \int_{\theta_1}^{\theta'} \frac{\mathrm{d}\theta}{\omega + K\sin\theta}. \tag{3.56}$$

Computation of the integral shows that

$$\int \frac{\mathrm{d}\theta}{\omega + K\sin\theta} = \begin{cases} \frac{2}{\sqrt{\omega^2-K^2}} \arctan\left(\frac{\omega\tan(\frac{\theta}{2})+K}{\sqrt{\omega^2-K^2}}\right), & K < |\omega|, \\ \frac{-1}{\omega}\tan\left(\frac{\pi}{4}-\frac{\theta}{2}\right), & K = |\omega|, \\ \frac{1}{\sqrt{K^2-\omega^2}} \ln\left[\frac{\omega\tan(\frac{\theta}{2})+K-\sqrt{K^2-\omega^2}}{\omega\tan(\frac{\theta}{2})+K+\sqrt{K^2-\omega^2}}\right], & K > |\omega|. \end{cases}$$

Its computation is included for completeness. It suffices to notice that there exists a function f such that

$$M = f(\theta', \theta_1, K).$$

This can then be used to calculate the new phase θ' in terms of θ_1, M, and K. Once θ' is known, the phase shift caused by the stimulus can be computed via (3.55):

$$\Delta\theta = \theta' - (\theta_1 + M\omega).$$

Figure 3.9 depicts several numerically computed phase response curves be-

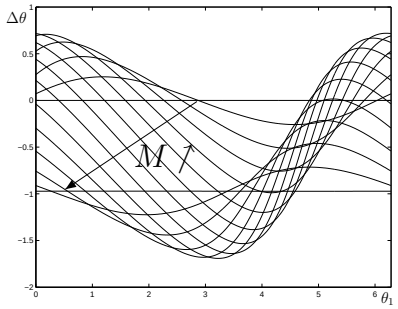

(a) $\omega = 1$, $K = 0.5$. The stimulus duration increases in steps of 0.518.

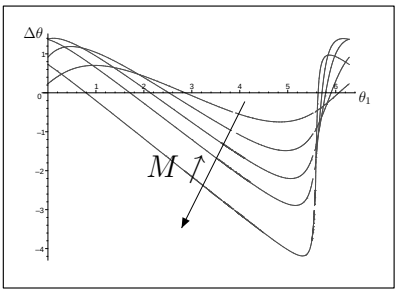

(b) $\omega = 1$, $K = 1.5$

Figure 3.9: Phase response curves belonging to system (3.54).

longing to the system equation (3.54). Two qualitatively different situations can be observed, namely $K < \omega$ and $K > \omega$, the vector fields of which have

already been discussed in Figure 3.5 and Figure 3.6, with $K = a$. The arrows in both figures indicate that the stimulus' duration increases between curves.

Consider first the situation when the stimulus strength is smaller than the natural frequency of the oscillator. The phase shift depends on the stimulus' duration as follows. Trivially, when $M = 0$ the phase shift is zero everywhere. When M is small there is an advance in phase for initial phases in $[0, \pi]$, and a delay for $\theta_1 \in [\pi, 2\pi]$. With increasing M the interval of initial phases yielding a phase advance moves clockwise on the circle and decreases in size until at about $M = 5.2$ the stimulus only causes phase delays. When $M = 7.257$ the phase delay is the same for all initial phases, which is explained as follows. Since for $K < \omega$ the vector field of (3.54) does not have equilibria, the phase moves periodically over the circle with a period depending on the stimulus strength. For $\omega = 1$, $K = .5$, as chosen in Figure 3.9 (a), the period of the stimulated oscillator is 7.257. If the stimulus duration equals this period (i.e. $M = 7.257$) then $\theta'(\theta_1) = \theta_1 + 2\pi$, $\forall \theta_1 \in S^1$, yielding a constant phase shift

$$\Delta\theta(\theta_1) = 2\pi - M\omega = -.974, \quad \forall \theta_1 \in S^1.$$

The constant phase shift is indicated on the figure as the horizontal line at $\Delta\theta = -.974$. When M increases further the above scenario repeats itself periodically with an additional offset of $-.974$ at each repetition.

Now, the situation $K > \omega$ is explained. The parameter values chosen are $\omega = 1$ and $K = 1.5$ The vector field of (3.54) possesses an asymptotically stable equilibrium at $\theta_s = 3.87$ and an unstable equilibrium at $\theta_u = 5.55$. When the stimulus is applied at an initial phase slightly larger than θ_u the phase increases towards the stable phase θ_s. When the initial phase is slightly smaller than θ_u the stimulus forces the phase to *decrease* and converge towards θ_s. This explains the large difference in phase shift near θ_u. With increasing M this difference becomes larger and happens more abruptly for increasing initial phases. For sufficiently large stimuli, θ' is close to θ_s. When the stimulus is turned off the oscillator moves freely again with a "new" initial phase $\theta \approx \theta_s$. It is said that the stimulus *resets* the oscillator.

This resetting phenomenon is observed in the human biological clock. The solid line in Figure 3.7 represents the phase response curve of the oscillator to exposure to bright light. The abrupt increase in phase shift at circadian time 18 indicates that the situation of Figure 3.9 (b) is manifested, which in turn implies the possibility to reset the oscillator via stimulation with light. The experimental results displayed in Figure 3.7 validate Kuramoto's model as suitable to produce the phase response curve of a real oscillator.

3.5 Conclusions

In this chapter we developed the Kuramoto model, based on [46]. We have introduced concepts from differential geometry into the development in order to make the mathematical reasoning more rigorous compared to [46]. The Kuramoto model is based on two simplifying assumptions proposed by Winfree:

- each oscillator is represented by its phase,
- interactions between oscillators are weak.

These assumptions allow for a simple model retaining all the characteristics of the original system. Each oscillator is described by a scalar dynamics on the unit circle, replacing the original M-dimensional nonlinear dynamics describing the oscillator in detail. The evolution of the oscillator can be visualized as a point moving on the unit circle. One revolution on the circle represents one oscillation.

The Kuramoto model allows for a mathematical analysis. We reviewed the analysis as performed by Kuramoto himself together with later refinements made by Mirollo and Strogatz [87]. The analysis treats populations of *infinitely* many oscillators. For small coupling strengths the oscillators act as if they were uncoupled and the population is said to behave incoherently. When the coupling strength exceeds a critical value K_C, the system starts to exhibit *partial synchronization*: one group of oscillators phase locks while the phase differences between the oscillators of the remaining group vary with time. The stronger the interactions between oscillators, the larger the phase locking group, until in the limit $K \to \infty$ all oscillators synchronize. The stability properties of partial synchronization are not obtained by Kuramoto. This was the starting point for our research. We decided to perform an analysis of *finite* populations of all-to-all coupled oscillators which made a full stability analysis possible. Our results on the finite case are presented in the next three chapters.

The present chapter is concluded by a description of the *phase resetting curve*. The phase resetting curve is a popular tool to characterize oscillators. It shows the response of an oscillator (i.e. a change in phase) to a stimulus. The oscillator response depends on the time the stimulus is applied in the oscillator's cycle and on the stimulus' duration. It is shown how starting from the Kuramoto model a realistic phase resetting curve is obtained.

Chapter 4

Networks of Linearly Coupled Agents

Before embarking on the analysis of finite coupled oscillator networks, we shortly examine networks of linearly coupled agents. We present novel results on *state locking* of these systems, i.e. all state differences $x_i - x_j$ are constant in time. We obtain a qualitative result which these linear networks have in common with their nonlinear counterparts (i.e. networks with the same interconnection topology but consisting of oscillators).

4.1 Mathematical Preliminaries

A *directed graph* or *digraph* (also simply called graph) is a pair $\mathcal{G} = (V, A)$ consisting of a nonempty finite set V and a multiset $A = (E, m)$ where $E \subset V \times V$ and $m : E \to \mathbb{N}$. The elements of V are referred to as *nodes* and an element (k, l) of E is called *an arc from k to l*. The mapping m assigns to each arc its multiplicity; m(k,l) is the number of (parallel) arcs from k to l. In the remainder of this section it is assumed that $(k, k) \notin E$ for all $k \in V$ and that $m(e) = 1$, $\forall e \in E$.

Let $\mathcal{N}_j$ denote the set of nodes k for which there is an arc from k to j: $\mathcal{N}_j := \{k \in V : (k, j) \in E\}$, and let *the in-degree* of j be defined as $v_j := \#(\mathcal{N}_j)$, where $\#(U)$ denotes the cardinality of a set U . Similarly, $\mathcal{M}_j := \{k \in V : (j, k) \in E\}$ and the *out-degree of j* is $u_j := \#(\mathcal{M}_j)$

A *path* in a graph is an ordered set of distinct nodes $\{k_1, \ldots, k_n\}$ such that $(k_i, k_{i+1}) \in E$, $i = 1, \ldots, n-1$. A node j is *globally forward reachable* if there is a path from each node i in the graph to j. Similarly a node is called *globally backward reachable* if there is a path from this node to every other node in the graph.

When the direction of all arcs of $\mathcal{G}$ is reversed, the *reverse graph* $-\mathcal{G}$ is obtained. Clearly $\mathcal{N}_j(\mathcal{G}) = \mathcal{M}_j(-\mathcal{G})$ and $v_j(\mathcal{G}) = u_j(-\mathcal{G})$.

The *adjacency matrix* of a graph $\mathcal{G}$, denoted $\mathcal{A}(\mathcal{G})$, is a square matrix with rows and columns indexed by the nodes of $\mathcal{G}$, such that the (i,j)-th entry is 1 if $(i,j) \in E$ and zero otherwise. The *degree matrix* $\mathcal{D}(\mathcal{G})$ is defined as $\text{diag}(u_1, \ldots, u_n)$, with n the number of nodes of the graph. The *Laplacian* of $\mathcal{G}$ is defined as $\mathcal{L}(\mathcal{G}) = \mathcal{D}(\mathcal{G}) - \mathcal{A}(\mathcal{G})$.

Lemma 1. *Zero is an eigenvalue of the Laplacian; all other eigenvalues belong to the closed right half plane.*

Proof. From the definition of $\mathcal{L}$ it follows that the elements of each row add up to zero, implying the Laplacian has a zero-eigenvalue with corresponding eigenvector $1_N := [1\ 1\ \cdots\ 1]^T$. The location of the remaining eigenvalues follows directly from the Gershgorin disc theorem (which can be found in Appendix A). □

Lemma 2. *A digraph $\mathcal{G}$ has a globally forward reachable node if and only if zero is a simple eigenvalue of $\mathcal{L}(\mathcal{G})$.*

Proof. For the proof the reader is referred to [53]. □

4.2 Agents with Linear Interaction

The content of this section belongs to the domain of consensus problems. In many applications involving multi-agent systems, groups of agents are desired to agree upon certain quantities. The flow of information between agents determines the overall behavior of the system. Areas of application of consensus problems include formation control [63] and flocking [92].

Consider a system of N interacting agents. To each agent i a real state variable $x_i \in \mathbb{R}$ is attributed. The interactions between the agents can be represented by a digraph $\mathcal{G} = (V, E)$, where V is the set of agents and E is the set of interconnections between the agents. There is an arc from node j to node i if agent i is directly affected by agent j. An agent j *affects* another agent i by attracting the state of agent i to its own state according to the differential equation $\dot{x}_i = x_j - x_i$. Notice that the state of agent j itself does not change by this interaction. Furthermore it is assumed that each agent i is subject to a constant drift according to some *natural velocity* ω_i.

The equations governing the network of agents, represented by the graph $\mathcal{G}$, are:

$$\dot{x}_i = \omega_i + \sum_{j \in \mathcal{N}_i} (x_j - x_i), \quad i \in \mathcal{N}, \tag{4.1}$$

or equivalently, $\dot{x} = Ax + \omega$ with $x = [x_1 \ \cdots \ x_N]^T$, $\omega = [\omega_1 \ \cdots \ \omega_N]^T$, and

$$\begin{cases} A_{ii} = -v_i, \\ A_{ij} = \begin{cases} 1, & (j,i) \in E, \\ 0, & (j,i) \notin E. \end{cases} \end{cases} \tag{4.2}$$

It is straightforward to prove that the system matrix (4.2) satisfies

$$A = -\mathcal{L}(-\mathcal{G}). \tag{4.3}$$

Theorem 11. *The system matrix of (4.1) has a simple zero-eigenvalue if and only if the corresponding graph has a globally backward reachable node.*

Proof. This follows directly from Lemma 2 and the observation (4.3). □

The presence of a simple zero-eigenvalue is a structural property of the interconnected systems investigated in this dissertation. The strength of each interconnection is proportional to some function of *state differences*. In the present chapter this function is the identity function, in the case of coupled oscillators it is some odd 2π-periodic function, e.g. sinusoidal. This dependence on *state differences only* induces a translational symmetry into the system of which the simple zero-eigenvalue is the direct consequence. The symmetry is made explicit as follows: the system equations are invariant under the change of coordinates $x_i' = x_i + a, a \in \mathbb{R}, \forall i \in \mathcal{N}$. In the subsequent chapters this symmetry will be considered in more detail.

4.2.1 Identical Agents

Consider the system with $\omega_i = \omega$, $\forall i \in \mathcal{N}$. The change of coordinates $\tilde{x}_i := x_i - \omega t$ yields system equations of the form (4.1) where all ω_i are set to zero. Then $\tilde{x} = \alpha 1_N, \forall \alpha \in \mathbb{R}$, are the equilibrium points of the system. Each equilibrium point can be interpreted as a *consensus solution* where all agents assume the same value α. In the original coordinates a consensus solution is to be interpreted as a linearly increasing value which all oscillators assume: $x_i(t) = \omega t + \alpha$, $\forall t \in \mathbb{R}$, $\forall i \in \mathcal{N}$.

If and only if A has exactly one zero-eigenvalue and the remaining eigenvalues have a real part strictly smaller than zero, each initial state converges to one of the equilibrium points and the system is called asymptotically stable [43].

Theorem 12. *Let $\omega = 0$. Every initial state of (4.1) converges to a consensus solution if and only if the graph corresponding to the system has a globally backward reachable node.*

Proof. This follows from Lemma 1, Theorem 11 and equation (4.3). □

In [67] a sufficient condition for the asymptotic stability of system (4.1) is obtained.

4.2.2 Nonidentical Agents

Now consider the case where not all ω_i are the same. The consensus solution is no longer a solution of the system equations. We define a solution type which satisfies weaker conditions:

Definition 22. *A solution of (4.1) is called* state locked *if* $\forall i, j \in \mathcal{N},\ \exists c_{ij} \in \mathbb{R} : (x_i - x_j)(t) = c_{ij},\ \forall t \in \mathbb{R}$.

Notice that the consensus solution is included in the above definition: the consensus solution can be regarded as a state locked solution with $c_{ij} = 0,\ \forall i, j, \in \mathcal{N}$. It follows directly from the system equations (4.1) that the state of each agent increases linearly in time when the system is state locked.

Theorem 13. *If the graph corresponding to the system has a globally backward reachable node, system (4.1) possesses state locked solutions.*

Proof. From Theorem 11, A has a simple zero-eigenvalue. Reduce the matrix A to its Jordan normal form. Since zero is a simple eigenvalue, the Jordan block belonging to zero is trivial. One easily verifies that this implies $\ker(A) \not\subset \mathrm{Im}(A)$.

Substitution of

$$x_i(t) = \omega_0 t + x_{i0}, \quad \omega_0, x_{i0} \in \mathbb{R}, \quad i \in \mathcal{N},$$

representing a state locked solution, into (4.1) yields

$$\omega_0 1_N - \omega = A x_0. \tag{4.4}$$

The system has a state locked solution if and only if $\exists \omega_0 \in \mathbb{R}$ such that $\omega_0 1_N - \omega \in \mathrm{Im}(A)$. Define the set $X := \{\gamma 1_N - \omega, \forall \gamma \in \mathbb{R}\}$. Since $1_N \notin \mathrm{Im}(A)$, $X \cap \mathrm{Im}(A) \neq \emptyset$ which concludes the proof. □

Since the system matrix describing the dynamics of deviations with respect to a state locked solution is identical to A, the following theorem is straightforward to prove.

Theorem 14. *Every initial state of (4.1) converges to a state locked solution if and only if the graph corresponding to the system has a globally backward reachable node.*

4.3 Conclusions

This chapter treated networks of linearly coupled agents. We found that the system matrix has a structural zero-eigenvalue. This is a manifestation of the translation symmetry of the system: if $t \mapsto x(t)$ is a solution of the system, then so is $t \mapsto x(t) + \alpha 1_N$, with $\alpha \in \mathbb{R}$ and $1_N = [1 \cdots 1]^T \in \mathbb{R}^N$. We will see in Chapter 6 that the Kuramoto model possesses the same translation symmetry, resulting in a structural zero-eigenvalue of the *linearization matrix* about a phase locking solution.

The main result of this chapter can be found in Theorem 14. Consider system (4.1). Then every initial state converges to a state locked solution if and only if the graph corresponding to the system has a globally backward reachable node. In Chapter 6 and Chapter 7 two types of networks of coupled (nonidentical) oscillators are investigated, both having a globally backward reachable node. It will be shown that for these oscillator networks having a globally backward reachable node is not sufficient for the stability of phase locking solutions.

Chapter 5

Finite Networks of All-to-All Coupled Identical Oscillators

The key idea in Kuramoto's analysis of (3.33) was to consider an infinite number of oscillators. However, the Kuramoto model is very well applicable to small networks of a finite number of oscillators and nowadays attention and interest are drawn to finite populations in particular [13, 87]. This chapter and the next address networks of a finite number of oscillators described by (3.33). Our main result comprises

- a proof of existence of phase locking,
- the determination of all phase locking solutions,
- a complete stability analysis of the system, showing that all phase locking solutions are unstable except for one,
- a description of partial entrainment, a behavior similar to partial synchronization in the infinite N case.

Before investigating the more complicated case of nonidentical oscillators, i.e. oscillators with different natural frequencies, in Chapter 6, we first treat finite networks of all-to-all coupled *identical* oscillators. As will be proven here, the Kuramoto model of a finite population with identical oscillators is a gradient system on the torus. Although the gradient structure of the Kuramoto system is well known in the literature [91], the detailed information on the equilibrium points obtained in Theorem 17 of this section has not been presented in the literature before.

5.1 Gradient Systems: Definitions and Properties

Before investigating the finite population of identical oscillators, the gradient structure of a system is defined (see also [37]). The definitions make use of geometrical concepts introduced in Section 3.2.1.

Definition 23. *Let V be a vector space over $\mathbb{R}$. The map $< \quad , \quad >: V \times V \to \mathbb{R}$ is a* bilinear form on V *if $\forall \alpha, \beta \in \mathbb{R}$, and $\forall v_1, v_2, w_1, w_2 \in V$,*

$$< \alpha v_1 + \beta v_2, w_1 > = \alpha < v_1, w_1 > + \beta < v_2, w_1 >,$$
$$< v_1, \alpha w_1 + \beta w_2 > = \alpha < v_1, w_1 > + \beta < v_1, w_2 > .$$

Definition 24. *A bilinear form $< \quad , \quad >: V \times V \to \mathbb{R}$ is called*

- symmetric *if $< v, w > = < w, v >$, $\forall v, w \in V$,*
- positive definite *if $< v, v > \leq 0$, $\forall v \in V$ and if equality holds if and only if $v = 0$.*

Definition 25. *A* field $< \quad , \quad >$ of $(C^\infty-)$bilinear forms on a manifold M *consists of a function assigning to each point $m \in M$ a bilinear form $< \quad , \quad >_m$ on T_mM, i.e. a bilinear mapping $< \quad , \quad >_m : T_mM \times T_mM \to \mathbb{R}$ such that for each chart (U, ϕ) the functions $\alpha_{ij} : \mathbb{R}^n \to \mathbb{R}; a \mapsto < E_i(\phi^{-1}(a)), E_j(\phi^{-1}(a)) >_m$ are of class C^∞.*

Definition 26. *A manifold M on which there is defined a field of symmetric, positive definite, bilinear forms $< \quad , \quad >$ is called a* Riemannian manifold *with* Riemannian metric $< \quad , \quad >$.

Denote by T_m^*M the dual vector space to T_mM. An element $\sigma_m \in T_m^*M$ is a linear mapping $\sigma_m : T_mM \to \mathbb{R}$. Define the *cotangent bundle* as

$$T^*M = \cup_{m \in M} T_m^*M.$$

Definition 27. *Let $f : M \to \mathbb{R}$ be a smooth function on the manifold M. The* differential of f at m, *denoted df_m, is defined as*

$$df_m : T_mM \to \mathbb{R}, \qquad X(m) \mapsto df_m(X(m)) := X(m)(f).$$

Definition 28. *The* gradient vector field *$grad f$ with respect to the Riemannian metric $< \quad , \quad >$ on M is the vector field uniquely characterized by the following two properties:*

$$grad f(m) \in T_mM, \qquad \forall m \in M, \tag{5.1}$$
$$df_m(X(m)) = < grad f(m), X(m) >_m, \qquad \forall X(m) \in T_mM. \tag{5.2}$$

To find an expression in local coordinates, (5.2) is evaluated with respect to the basis of coordinate frames E_j:

$$\begin{gathered}
\mathrm{d}f_m(X(m)) =< \mathrm{grad}f(m), X(m) >_m, \\
\Leftrightarrow \\
X(m)(f) =< \sum_{i=1}^{n} \mathrm{grad}f^i(m)E_i(m), \sum_{j=1}^{n} X^j(m)E_j(m) >_m, \\
\Leftrightarrow \\
\sum_{j=1}^{n} X^j(m)E_j(m)(f) = \sum_{i=1}^{n}\sum_{j=1}^{n} \mathrm{grad}f^i(m)X^j(m) < E_i(m), E_j(m) >_m, \\
\Leftrightarrow \\
\sum_{j=1}^{n} X^j(m)\frac{\partial f_\phi}{\partial x^j}(\phi(m)) = \sum_{i=1}^{n}\sum_{j=1}^{n} \mathrm{grad}f^i(m)X^j(m)\alpha_{ij}(m), \\
\Leftrightarrow \\
\frac{\partial f_\phi}{\partial x^j}(\phi(m)) = \sum_{i=1}^{n} \mathrm{grad}f^i(m)\alpha_{ij}(m),\ \forall j = 1, \ldots, n. \qquad (5.3)
\end{gathered}$$

Introduce the vectors $\nabla f(m) := [\frac{\partial f_\phi}{\partial x^1}(\phi(m)) \cdots \frac{\partial f_\phi}{\partial x^n}(\phi(m))]^T$ and $\mathrm{grad}f(x) := [\mathrm{grad}f^1(m) \ \cdots \ \mathrm{grad}f^n(m)]^T$, and the matrix $Q(m) := \Big(\alpha_{ij}(m)\Big)$. Equation (5.3) can be rewritten as

$$\begin{aligned}
& \nabla f(m)^T = \mathrm{grad}f(m)^T Q(m), \\
\Leftrightarrow \quad & \nabla f(m) = Q(m)^T \mathrm{grad}f(m), \\
\Leftrightarrow \quad & \nabla f(m) = Q(m)\mathrm{grad}f(m), \\
\Leftrightarrow \quad & \mathrm{grad}f(m) = Q(m)^{-1}\nabla f(m). \qquad (5.4)
\end{aligned}$$

Definition 29. *The system*

$$\dot{x} = -grad f(x) \qquad (5.5)$$

is called the gradient system *associated with the function f. Conversely, f is called the* gradient function *of system (5.5).*

For any solution x of this system

$$\begin{aligned}
\frac{\mathrm{d}}{\mathrm{d}t} f(x(t)) &= < \mathrm{grad}f(x(t)), \dot{x}(t) > \\
&= - \left\|\mathrm{grad}f(x(t))\right\|^2 \leq 0
\end{aligned}$$

and therefore $f(x(t))$ is non-increasing along solutions.

Definition 30. *A* critical point *of a smooth map $f : U \subset \mathbb{R}^n \to \mathbb{R}$ is a point $x_0 \in U$ where $\nabla f = 0$.*

From this definition, (5.4) and (5.5), it can be concluded that the critical points of the function f coincide with the equilibria of the associated gradient system.

Definition 31. *A* sublevel set *of a smooth function $f : M \to \mathbb{R}$ is the set $\{x \in M \mid f(x) \leq c, c \in \mathbb{R}\}$.*

Theorem 15 (LaSalle's theorem [43])**.** *Let Ω be a compact set with the property that every solution of $\dot{x} = f(x)$ which starts in Ω remains for all future time in Ω. Let $V : \Omega \to \mathbb{R}$ be a continuously differentiable function such that $\dot{V}(x) \leq 0$ in Ω. Let E be the set of all points in Ω where $\dot{V}(x) = 0$. Let M be the largest invariant set in E. Then every solution starting in Ω approaches M as $t \to \infty$.*

Theorem 16. *Let $f : M \to \mathbb{R}$ be a smooth function on a Riemannian manifold with compact sublevel sets. Then every solution $t \mapsto x(t) \in M$ of the gradient system (5.5) on M exists for all $t \geq 0$ and $x(t)$ converges to a connected component of the set of critical points of f as $t \to +\infty$.*

Proof. This follows directly from Theorem 15. Let the set Ω of Theorem 15 be one of the compact sublevel sets of the function f. Now,

$$\begin{aligned} \dot{f}(x(t)) = 0, \quad & \forall t \in \mathbb{R}, \\ \Leftrightarrow \|\mathrm{grad} f(x(t))\|^2 = 0, \quad & \forall t \in \mathbb{R}, \\ \Leftrightarrow \mathrm{grad} f(x(t)) = 0, \quad & \forall t \in \mathbb{R}, \\ \Leftrightarrow \dot{x}(t) = 0, \quad & \forall t \in \mathbb{R}. \end{aligned}$$

This proves that the set E of Theorem 15 is the set of all equilibrium points of (5.5). The largest invariant set in the set of equilibria is the set itself. Then every solution approaches an isolated equilibrium point or a connected component of equilibria as $t \to \infty$, concluding the proof. □

5.2 The Gradient Structure of Networks of Identical Oscillators

The governing equations of a network of globally coupled phase oscillators are (3.33):

$$\dot{\theta}_i = \omega_i + \frac{K}{N} \sum_{j=1}^{N} \sin(\theta_j - \theta_i), \qquad \forall i \in \mathcal{N}, \tag{5.6}$$

where $\theta_i \in S^1$, $\omega_i \in \mathbb{R}$, $\forall i \in \mathcal{N}$, $N \in \mathbb{N}$ and $K \in (0, +\infty)$. In this section the natural frequencies are assumed to be identical: $\exists \omega \in \mathbb{R} : \omega_i = \omega, \forall i \in \mathcal{N}$. By performing the change of coordinates $\theta \to \theta + \omega t$ the system equations become

$$\dot{\theta}_i = \frac{K}{N} \sum_{j=1}^{N} \sin(\theta_j - \theta_i), \qquad \forall i \in \mathcal{N}. \tag{5.7}$$

Recall Definition 20 of phase locking. In the case of *finite* identical oscillator networks the cooperative behavior of interest is phase locking of *all* the oscillators in the network. This type of solution can be regarded as the nonlinear equivalent of *state locking* of a finite network of linearly coupled agents as defined in Definition 22 of Chapter 4.

In the analysis of the system's properties the *complex order parameter* as defined by (3.34) in Section 3.3.1 is used to a great extent. First, from the definition it follows that

$$r(t) = 0,\ \forall t \in \mathbb{R} \Leftrightarrow \begin{cases} \sum_{j=1}^{N} \cos(\theta_j(t)) = 0,\ \forall t \in \mathbb{R}, \\ \sum_{j=1}^{N} \sin(\theta_j(t)) = 0,\ \forall t \in \mathbb{R}. \end{cases} \tag{5.8}$$

Second, r^2 in terms of θ_i is computed. The definition is rewritten as

$$r(\theta)e^{i\psi(\theta)} = \frac{1}{N}\left(\sum_{j=1}^{N} \cos\theta_j + i\sum_{j=1}^{N} \sin\theta_j\right).$$

Taking the squared modulus of both sides of the equality yields

$$r^2(\theta) = \frac{1}{N^2}\left(N + 2\sum_{\substack{i=1,j=1 \\ i<j}}^{N} \cos(\theta_i - \theta_j)\right), \tag{5.9}$$

$$= \frac{1}{N^2}\left(\sum_{i,j=1}^{N} \cos(\theta_i - \theta_j)\right). \tag{5.10}$$

Consider the function $V : T^N = \underbrace{S^1 \times \ldots \times S^1}_{N} \to \mathbb{R}$:

$$V(\theta) = \frac{KN}{2}(1 - r^2(\theta)). \tag{5.11}$$

This function V is a smooth function on the torus. System (5.7) can be regarded as a gradient system on the torus associated to the function V. The proof is straightforward and is hence omitted.

5.3 Equilibria of the System

Since the vector field of (5.7) consists only of sums of sines of differences of the state variables θ_i, solutions θ with

$$\theta = [\alpha + k_1\pi\ \alpha + k_2\pi\ \cdots\ \alpha + k_N\pi]^T \mod 2\pi,$$

with $k_1, \cdots, k_N \in \mathbb{Z}$ and for any $\alpha \in S^1$ are equilibria of (5.7). This class of equilibria is called the class of *elementary solutions* of the system. Terminology is derived from [8].

Theorem 17. *If and only if the state θ of system (5.7) is an equilibrium it belongs to the set of elementary solutions or to the set of states with $r = 0$.*

Proof. An simple calculation shows that

$$\dot{\theta}_i = \frac{K}{N}\Big(Q(\theta)\cos\theta_i - P(\theta)\sin\theta_i\Big), \quad \forall i \in \mathcal{N},$$

with

$$P(\theta) := \sum_{j=1}^{N} \cos\theta_j, \tag{5.12}$$

$$Q(\theta) := \sum_{j=1}^{N} \sin\theta_j. \tag{5.13}$$

An equilibrium of (5.7) satisfies the set of equations

$$\frac{K}{N}\Big(Q(\theta)\cos\theta_i - P(\theta)\sin\theta_i\Big) = 0, \quad \forall i \in \mathcal{N}. \tag{5.14}$$

Consider the case where the values of the phases of an equilibrium are such that $P(\theta) \neq 0$ and $Q(\theta) \neq 0$. Assume that for some (but not all, since this would yield $Q(\theta) = 0$) values of i, $\sin\theta_i = 0$. It follows from (5.14) that for these i-values $\cos\theta_i = 0$, which yields a contradiction, since $\sin\theta_i = 0$ and $\cos\theta_i = 0$ cannot be satisfied simultaneously. Similarly a contradiction is obtained if it is assumed that for some values of i, $\cos\theta_i = 0$. Hence, if $P(\theta) \neq 0 \wedge Q(\theta) \neq 0$, the equilibrium satisfies

$$P(\theta)\sin\theta_i = Q(\theta)\cos\theta_i \neq 0, \quad \forall i \in \mathcal{N},$$

or, equivalently,

$$\frac{Q(\theta)}{P(\theta)} = \tan\theta_i, \quad \forall i \in \mathcal{N}, \tag{5.15}$$

which implies that

$$\tan\theta_1 = \tan\theta_2 = \ldots = \tan\theta_N,$$

or

$$\exists \alpha \in S^1, \exists k_i \in \mathbb{Z} : \theta_i = \alpha + k_i\pi,\ \forall i \in \mathcal{N}.$$

This is precisely the set of elementary solutions.

If the values of θ_j are such that $P(\theta) = 0$ and $Q(\theta) \neq 0$, then, from (5.14), $\cos\theta_i = 0$, $\forall i \in \mathcal{N}$ which corresponds to elementary solutions of the form $\theta_i = \frac{\pi}{2} + k_i\pi$, $\forall i \in \mathcal{N}$, with $k_i \in \mathbb{Z}$.

For values of θ_j such that $P(\theta) \neq 0$ and $Q(\theta) = 0$, it follows from (5.14) that $\sin\theta_i = 0,\ \forall i \in \mathcal{N}$, which corresponds to elementary solutions of the form $\theta_i = k_i\pi,\ \forall i \in \mathcal{N}$, with $k_i \in \mathbb{Z}$.

Finally, consider the case $P(\theta) = 0$ and $Q(\theta) = 0$. As stated in equation (5.8),

$$P(\theta) = 0 \wedge Q(\theta) = 0 \Leftrightarrow r(\theta) = 0.$$

□

5.4 Stability Properties

In this section the gradient structure of the system is exploited to establish the stability of the equilibria of (5.7).

Theorem 18. *Every equilibrium point θ_{eq} of (5.7) for which $r(\theta_{eq}) = 0$, is unstable.*

Every equilibrium point θ_{eq} of (5.7) for which $r(\theta_{eq}) = 1$, is asymptotically stable.

Proof. Since V is a gradient function of (5.7), $V(x(t))$ is non-increasing along solutions x of (5.7). This implies that the critical points of V that are maxima correspond to unstable equilibria of (5.7). Similarly, minima of V correspond to asymptotically stable equilibria.

The range of V is the interval $[0, \frac{KN}{2}]$. States θ_0 for which $V(\theta_0) = 0$ are minima of V and hence asymptotically stable equilibria. Via (5.11), $V(\theta_0) = 0 \Leftrightarrow r^2(\theta_0) = 1 \Leftrightarrow r(\theta_0) = 1$. Similarly, states θ_0 for which $V(\theta_0) = \frac{KN}{2}$ are maxima of V and hence unstable equilibria with $r(\theta_0) = 0$. □

From (5.10) it follows that $r^2(\theta) = 1 \Leftrightarrow \theta_i = \theta_j,\ \forall i, j \in \mathcal{N}$. Hence, the synchronizing solution is asymptotically stable.

According to Theorem 17, the only equilibria that remain to be investigated are elementary solutions for which r is different from 0 and 1.

Theorem 19. *Every elementary solution θ_{el} of (5.7) with $r(\theta_{el}) \neq 0$ and $r(\theta_{el}) \neq 1$ is unstable.*

Proof. Let $\alpha \in S^1$. Consider the elementary solution

$$\theta_{\text{el}} := [\underbrace{\alpha\ \cdots\ \alpha}_{M}\ \underbrace{\alpha+\pi\ \cdots\ \alpha+\pi}_{N-M}]^T \mod 2\pi,$$

where $M \in \mathcal{N} \setminus \{\frac{N}{2}, N\}$ since $M = N$ corresponds to synchronization ($r(\theta_{\text{el}}) = 1$) and $M = \frac{N}{2}$ has $r(\theta_{\text{el}}) = 0$.

Define the vectors ϵ_1 and ϵ_2 as follows: for all $i \in \mathcal{N}$,

$$\begin{aligned} \epsilon_{1,i} &:= \epsilon\delta_{i,k}, \quad 0 < \epsilon \ll 1, \quad k \in \{1, \ldots, M\}, \\ \epsilon_{2,i} &:= \epsilon\delta_{i,l}, \quad 0 < \epsilon \ll 1, \quad l \in \{M+1, \ldots, N\}, \end{aligned} \tag{5.16}$$

with δ the Kronecker delta:

$$\delta_{i,k} := \begin{cases} 1 & i = k, \\ 0 & i \neq k. \end{cases}$$

A simple computation reveals that regardless the values of k and l in (5.16)

$$\begin{aligned} A_1 &:= V(\theta_{\text{el}} + \epsilon_1) - V(\theta_{\text{el}}) = \frac{K}{2N}(1 - \cos\epsilon)(2N - 4M - 2), \\ A_2 &:= V(\theta_{\text{el}} + \epsilon_2) - V(\theta_{\text{el}}) = -\frac{K}{2N}(1 - \cos\epsilon)(2N - 4M + 2). \end{aligned} \tag{5.17}$$

It can be easily proven that the expressions $2N-4M-2$ and $2N-4M+2$ possess the same sign if and only if $M \notin \{\frac{N-1}{2}, \frac{N}{2}, \frac{N+1}{2}\}$. It then follows that A_1 and A_2 have opposite signs, which via the definition of A_1 and A_2 directly implies that the equilibrium under consideration is a saddle point and hence unstable.

If $M = \frac{N-1}{2}$, then $A_1 = 0$ and $A_2 = -\frac{2K}{N}(1 - \cos\epsilon) < 0$. It follows that the corresponding equilibrium is either a saddle point or a maximum of V. This implies that the equilibrium is unstable.

Similarly, if $M = \frac{N+1}{2}$, then $A_2 = 0$ and $A_1 = -\frac{2K}{N}(1 - \cos\epsilon) < 0$. It follows that the corresponding equilibrium is either a saddle point or a maximum of V, implying that the equilibrium is unstable. □

From the above theorems it follows that synchronization is the only asymptotically stable solution. However, the synchronized solution is not *globally* asymptotically stable: every initial state located on the stable manifold of one of the equilibrium points corresponding to a saddle point of V, converges to that equilibrium point and not to an equilibrium point representing synchronization. The synchronized solution is called *asymptotically stable almost everywhere*.

5.5 Conclusions

This chapter treated finite populations of all-to-all coupled oscillators with identical natural frequencies. First we obtained a characterization of the phase locking solutions using the concept of the *complex order parameter*. Every phase locking solution belongs to the class of elementary solutions (i.e. the phase difference between each pair of oscillators assumes either the value zero or π), or the amplitude of the corresponding order parameter is zero. These two conditions are not mutually exclusive: some phase locking solutions satisfy both conditions.

In a second step, the stability of the system was established. This is done by taking advantage of the gradient structure of the system. We proved that

each initial state that is not situated on the stable manifold of one of the unstable equilibria converges to an equilibrium corresponding to synchronization. This implies that the synchronizing solution (all phase differences equal to zero) is asymptotically stable almost everywhere.

Chapter 6

Finite Networks of All-to-all Coupled Nonidentical Oscillators

6.1 Introduction

This chapter contains original results on the behavior of finite nonidentical oscillator populations. Again we start from the system equations (3.33). Contrary to Chapter 5 the natural frequencies are allowed to differ. First, as in the previous chapter, the questions about existence and stability of phase locking behavior are raised and answered. Contrary to the identical case where phase locking was a stable behavior for all non-zero coupling strengths, phase locking does not exist below a critical value K_T of the coupling strength.

For small coupling strengths we assert and define the existence of a finite-N behavior similar to partial synchronization and name it *partial entrainment*. The system exhibits partial entrainment if there exists a subgroup of oscillators with bounded mutual phase differences while the remaining oscillators are drifting. We are the first to mention this behavior in the literature. In the case of the three oscillator network we give an analysis determining the onset value K_P of partial entrainment.

The chapter is concluded by a comparison of the behavior of a finite population to the behavior of an infinite population as described in Section 3.3.

6.2 Existence of Phase Locking Solutions

6.2.1 The Consistency Condition on the Amplitude of the Order Parameter

As stated in Section 3.3.1, using the complex order parameter (3.34) the equations (3.33) can be rewritten as

$$\dot{\theta}_i = \omega_i + Kr\sin(\psi - \theta_i), \qquad \forall i \in \mathcal{N}. \tag{6.1}$$

Introduce the phase differences ϕ_j as

$$\phi_i := (\theta_i - \theta_1) \bmod 2\pi, \ \forall i \in \mathcal{N}. \tag{6.2}$$

Although $\phi_1 \equiv 0$, we prefer to leave it as such for notational reasons. In the new coordinates $(\theta_1, \phi_2, \ldots, \phi_N)$ the system equations are

$$\begin{cases} \dot{\theta}_1 &= \omega_1 + Kr\sin(\psi - \theta_1), \\ \dot{\phi}_i &= \omega_i - \omega_1 + Kr(\sin(\psi - \phi_i - \theta_1) - \sin(\psi - \theta_1)), \quad \forall i \in \mathcal{N} \setminus \{1\}. \end{cases} \tag{6.3}$$

Assuming the network allows for phase locking, the order parameter satisfies

$$r(t)e^{i\psi(t)} = \left(\frac{1}{N}\sum_{j=1}^{N} e^{i\phi_j}\right) e^{i\theta_1(t)}, \quad \forall t \in \mathbb{R}, \tag{6.4}$$

with all ϕ_j constant in time. Denoting $\frac{1}{N}\sum_{j=1}^{N} e^{i\phi_j}$ as $r_\infty e^{i\lambda}$ with $r_\infty \in [0,1]$ and $\lambda \in \mathbb{R} \mod 2\pi$, we obtain the following expression for the order parameter in the phase locking situation:

$$r(t)e^{i\psi(t)} = r_\infty e^{i(\lambda + \theta_1(t))}, \quad \forall t \in \mathbb{R}. \tag{6.5}$$

From (6.3) en (6.5), a phase locking solution must satisfy

$$\begin{cases} \dot{\theta}_1(t) &= \omega_1 + Kr_\infty \sin\lambda, \quad \forall t \in \mathbb{R}, \\ 0 &= \omega_i - \omega_1 + Kr_\infty \sin(\lambda - \phi_i) - Kr_\infty \sin\lambda, \quad \forall i \in \mathcal{N} \setminus \{1\}. \end{cases} \tag{6.6}$$

Adding the last $N-1$ equations in (6.6) yields

$$\omega_1 + Kr_\infty \sin\lambda = \frac{1}{N}\sum_{j=1}^{N}\omega_j + \frac{Kr_\infty}{N}\sum_{j=1}^{N}\sin(\lambda - \phi_j).$$

This yields

$$\dot{\theta}_1(t) = \frac{1}{N}\sum_{j=1}^{N}\omega_j + \frac{Kr_\infty}{N}\sum_{j=1}^{N}\sin(\lambda - \phi_j), \quad \forall t \in \mathbb{R}. \tag{6.7}$$

From (6.4) and (6.5) it follows that

$$\begin{cases} r_\infty = \dfrac{1}{N}\displaystyle\sum_{j=1}^{N} \cos(\phi_j - \lambda), \\ \\ 0 = \dfrac{1}{N}\displaystyle\sum_{j=1}^{N} \sin(\phi_j - \lambda). \end{cases} \tag{6.8}$$

Equation (6.7) then reduces to

$$\dot{\theta}_1(t) = \frac{1}{N}\sum_{j=1}^{N} \omega_j =: \omega_m, \quad \forall t \in \mathbb{R}, \tag{6.9}$$

with ω_m the *mean natural frequency*. We conclude that in case of phase locking the phase $\psi(t)$ of the complex order parameter is

$$\psi(t) = \theta_1(t) + \lambda = \omega_m t + \beta, \tag{6.10}$$

with $\beta := \lambda + \theta_1(0)$. In a phase locking solution all the phases of the oscillators move with a velocity equal to the mean natural frequency of the entire population.

Substituting (6.9) into (6.6) yields

$$0 = \omega_i - \omega_m + K r_\infty \sin(\lambda - \phi_i), \ \forall i \in \mathcal{N}. \tag{6.11}$$

Phase locking solutions satisfy, with $\omega_i' := \omega_i - \omega_m$,

$$\sin(\phi_i - \lambda) = \frac{\omega_i'}{K r_\infty}, \ \forall i \in \mathcal{N}, \tag{6.12}$$

The equations (6.12) yield a solution $(\lambda, \phi_2, \ldots, \phi_N)$ if and only if

$$K r_\infty \geq |\omega_i'|, \ \forall i \in \mathcal{N}. \tag{6.13}$$

Consider (6.8) and (6.12) and eliminate ϕ_i and λ, yielding *a set* of equations in r_∞:

$$r_\infty = \frac{1}{N}\sum_{j=1}^{N} \pm\sqrt{1 - \left(\frac{\omega_j'}{K r_\infty}\right)^2}. \tag{6.14}$$

In accordance with equation (3.47), expression (6.14) is called *the consistency condition on* r_∞ of the phase locking solution. It represents 2^N equations, each of which may possess multiple solutions r_∞ for some fixed value of K. Existence of such a solution $r_\infty(K)$ is equivalent to existence of a phase locking solution if and only if (6.13) is satisfied. The $\pm$-signs indicate that each term in the sum can have either a plus or a minus sign. These $\pm$-signs arise from the fact that $\cos(\arcsin(x)) = \pm\sqrt{1 - x^2}, x \in [-1, 1]$.

As explained in Section 3.3.1, the consistency condition (3.47) appearing in [46] and [87], is a condition for *partial synchronization*. It is obtained in a similar way as (6.14) is. However, it is only one scalar equation. This is because solutions corresponding to minus signs are not taken into consideration, implying that possibly not all partially synchronized solutions were obtained. For a complete discussion see Section 6.6.

When K and ω_i, $\forall i \in \mathcal{N}$, are known, equation (6.14) can be solved yielding values of r_∞. The values of λ and $\phi_i, \forall i \in \mathcal{N}$, of the existing phase locking solutions are then obtained from those values r_∞ for which (6.13) is satisfied, by using equation (6.12). The above results provide necessary conditions for phase locking. These conditions are summarized in the following theorem.

Theorem 20. *Phase locking exists if and only if there is a solution of which the constant amplitude r_∞ of the corresponding order parameter satisfies*

$$r_\infty \in [0,1] : \frac{|\omega_i'|}{K r_\infty} \leq 1, \ \forall i \in \mathcal{N}, \tag{6.15}$$

$$r_\infty = \frac{1}{N} \sum_{j=1}^{N} \pm \sqrt{1 - \left(\frac{\omega_j'}{K r_\infty} \right)^2}. \tag{6.16}$$

The sufficiency of the above conditions for phase locking is proven as follows:

Proof. If (6.15) holds, values $\theta_{i,\text{eq}}'$ can be found such that

$$\sin \theta_{i,\text{eq}}' = \frac{\omega_i'}{K r_\infty}, \quad \forall i \in \mathcal{N}. \tag{6.17}$$

It follows that $\theta_{\text{eq}}' := [\theta_{1,\text{eq}}' \ \cdots \ \theta_{N,\text{eq}}']^T$ is an equilibrium solution of

$$\dot{\theta}_i' = \omega_i' - K r_\infty \sin \theta_i', \quad \forall i \in \mathcal{N}, \tag{6.18}$$

or equivalently $t \mapsto \theta_s(t) := \theta_{\text{eq}}' + \omega_m t$ is a solution of

$$\dot{\theta}_i = \omega_i - K r_\infty \sin(\theta_i - \omega_m t), \quad \forall i \in \mathcal{N}, \tag{6.19}$$

where $\theta_i = \theta_i' + \omega_m t$. Remark that $\theta_s(t)$ is a phase locking solution since $\frac{\mathrm{d}\theta_{s,i}}{\mathrm{d}t}(t) = \omega_m$, $\forall i \in \mathcal{N}$.

From (6.17) it follows that

$$\sum_{i=1}^{N} \sin \theta_{i,\text{eq}}' = 0. \tag{6.20}$$

Assumption (6.16) together with (6.17) implies that ((6.20) is used to attain second line):

$$\begin{aligned} r_\infty &= \frac{1}{N}\sum_{l=1}^{N}\cos\theta'_{l,\mathrm{eq}}, \\ \Leftrightarrow r_\infty &= \frac{1}{N}\sum_{l=1}^{N}e^{i\theta'_{l,\mathrm{eq}}}, \\ \Leftrightarrow r_\infty e^{i\omega_m t} &= \frac{1}{N}\sum_{l=1}^{N}e^{i\theta_{s,l}(t)}, \quad \forall t\in\mathbb{R}, \\ \Leftrightarrow r_\infty e^{i\omega_m t - i\theta_{s,i}(t)} &= \frac{1}{N}\sum_{l=1}^{N}e^{i\theta_{s,l}(t)-i\theta_{s,i}(t)}, \quad \forall t\in\mathbb{R}. \end{aligned} \tag{6.21}$$

From (6.21) it follows that

$$-r_\infty\sin(\theta_{s,i}(t)-\omega_m t) = \frac{1}{N}\sum_{l=1}^{N}\sin(\theta_{s,l}(t)-\theta_{s,i}(t)). \tag{6.22}$$

Since $t\mapsto\theta_s(t)$ is a solution of (6.19),

$$\frac{\mathrm{d}\theta_{s,i}}{\mathrm{d}t}(t) = \omega_i - Kr_\infty\sin(\theta_{s,i}(t)-\omega_m t), \quad \forall i\in\mathcal{N}. \tag{6.23}$$

Using (6.22), (6.23) changes into

$$\frac{\mathrm{d}\theta_{s,i}}{\mathrm{d}t}(t) = \omega_i + \frac{K}{N}\sum_{l=1}^{N}\sin(\theta_{s,l}(t)-\theta_{s,i}(t)), \quad \forall i\in\mathcal{N}.$$

Hence, $t\mapsto\theta_s(t)$ is a phase locking solution of (6.1), which concludes the proof. □

Solutions (K, r_∞) of (6.14) for a typical case are depicted in Figure 6.1. The figure shows that phase locking is only possible for those values of the coupling strength that are larger than a threshold value. In the remainder of this dissertation this threshold value is called K_T.

Consider the consistency condition (6.14) containing only plus signs:

$$r_\infty = \frac{1}{N}\sum_{j=1}^{N}\sqrt{1-\left(\frac{\omega'_j}{Kr_\infty}\right)^2}. \tag{6.24}$$

In Section 6.3 it will be proven that one of the solutions to this equation is stable. If the phases θ_i of the stable solution are perturbed, they will converge back to that phase locking solution. This renders the stable solution the physically relevant one. Its existence is proven in the following theorem.

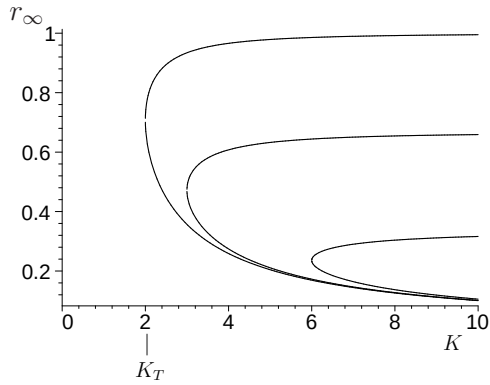

Figure 6.1: Representation of all phase locking solutions (6.14) of a population consisting of 6 oscillators with $\omega_i = -1$, $i = 1, 2, 3$ and $\omega_i = 1$, $i = 4, 5, 6$.

Theorem 21. *Let $|\omega'|_{max}$ denote the largest absolute value of the natural frequencies ω_i' of the population. Then for each coupling strength $K > 2|\omega'|_{max}$ there exist a phase locking solution with the property that $r_\infty \to 1$ for $K \to \infty$.*

Proof. Construct the surface f in (K, r)-space defined as

$$f(K, r) := r - \frac{1}{N} \sum_{j=1}^{N} \sqrt{1 - \left(\frac{\omega_j'}{Kr}\right)^2}. \tag{6.25}$$

In the points of the (K, r)-plane where $f(K, r) = 0$, condition (6.24) is satisfied.

Consider a fixed value $K_0 > 2|\omega'|_{max}$. Then $f(K_0, r) < r - \sqrt{1 - \frac{1}{4r^2}}$ and in particular $f(K_0, \frac{1}{\sqrt{2}}) < 0$. Also, from (6.25), $f(K_0, 1) \geq 0$.

For a fixed value K_0, the curve $f(K_0, r)$ is continuous in r for $r \in (1/2, \infty)$. This implies that

$$\forall K_0 \in (2|\omega'|_{max}, \infty), \ \exists r_0 \in (\frac{1}{\sqrt{2}}, 1) : \ f(K_0, r_0) = 0,$$

corresponding to a phase locking solution. From (6.24) it can be concluded that for this solution $r_\infty \to 1$ for $K \to \infty$. □

The plus signs in (6.14) arise if $\phi_i - \lambda \in (-\pi/2, \pi/2)$, $\forall i \in \mathcal{N}$. The values of all ϕ_i are situated in an interval of length π. There exists a permutation σ of $(1, 2, \ldots, N)$ such that

$$\omega'_{\sigma(1)} \geq \omega'_{\sigma(2)} \geq \ldots \geq \omega'_{\sigma(N)}.$$

The sine-function is monotonically increasing in the interval $(-\pi/2, \pi/2)$. By (6.12), this implies that

$$\omega'_{\sigma(1)} \geq \omega'_{\sigma(2)} \geq \ldots \geq \omega'_{\sigma(N)} \Leftrightarrow \phi_{\sigma(1)} \geq \phi_{\sigma(2)} \geq \ldots \geq \phi_{\sigma(N)}.$$

The larger the natural frequency, the larger the phase difference with respect to the reference oscillator 1.

In [25] a *chain* of $N+1$ coupled oscillators is investigated and 2^N phase locking solutions are obtained. At first sight this is a remarkable correspondence to the number of equations in (6.14). We will show that this correspondence is a coincidence.

The system equations of the chain are

$$\begin{cases} \dot{\theta}_1 = \omega_1 + K\sin(\theta_2 - \theta_1), \\ \dot{\theta}_i = \omega_i + K\sin(\theta_{i-1} - \theta_i) + K\sin(\theta_{i+1} - \theta_i), \quad i = 2, \ldots, N, \\ \dot{\theta}_{N+1} = \omega_{N+1} + K\sin(\theta_N - \theta_{N+1}). \end{cases} \tag{6.26}$$

Defining the phase differences $\phi_i := \theta_{i+1} - \theta_i, i = 1, \ldots, N-1$, (notice the difference with the definition (6.2)), (6.26) can be written as

$$\dot{\phi} = \omega + HF(\phi), \tag{6.27}$$

where $F(\phi) = [\sin\phi_1 \ \cdots \ \sin\phi_N]^T$, $\omega = [\omega_2 - \omega_1 \ \omega_3 - \omega_2 \ \cdots \ \omega_{N+1} - \omega_N]^T$, $\phi = [\phi_1 \cdots \phi_N]^T$, and H is a tridiagonal matrix with $H_{ii} = -2K$ and $H_{i+1,i} = H_{i,i+1} = K$. Since the matrix H is invertible, equilibrium solutions of (6.27) satisfy

$$F(\phi) = -H^{-1}\omega. \tag{6.28}$$

This is a system of *decoupled* equations. For each i, the i-th equation can be solved separately, yielding 2 solutions ϕ_i for large enough coupling strength K; there are 2^N solutions of (6.26).

In the present chapter an all-to-all coupled network of N oscillators is investigated described by (3.33). The phase dynamics can be replaced by equivalent dynamics of the phase differences (6.3). The phase differences of a phase locking solution satisfy (6.6). Unlike the case of [25] described by (6.28), expression (6.6) is a set of *coupled* equations: they are coupled through r_∞ and λ, by means of the definition $r_\infty e^{i\lambda} = \frac{1}{N}\sum_{j=1}^{N} e^{i\phi_j}$. The set of equations (6.6) cannot be solved for the phase differences directly. After introducing the order parameter (3.34), its amplitude, which is a constant (denoted r_∞) for phase locking solutions, can be used as auxiliary variable. The phase locking solutions of (6.6) are obtained by solving 2^N equations in the variable r_∞, represented by expression (6.14). The phase differences corresponding to a solution r_∞ are given by (6.12).

Two more observations indicating that the similarity between the results in [25] and our results is a coincidence, are:

- The 2^N equations (6.14) correspond to N all-to-all coupled oscillators, whereas the 2^N solutions in [25] correspond to $N+1$ coupled oscillators.
- The 2^N equations do not necessarily yield 2^N solutions. First, some of the equations (6.14) do not yield any solution r_∞ for any value of K; consider for example (6.14) with only minus signs: the right hand side of the expression assumes a negative value regardless of r_∞ and K, whereas the left hand side r_∞ is defined to be positive. Second, some of the equations belonging to (6.14) possess multiple solutions r_∞ at certain fixed values of K. Hence, it is not a priori known how many phase locking solutions the all-to-all coupled network possesses, whereas in [25] 2^N distinct solutions are obtained.

6.2.2 Application of the Consistency Condition to Some Special Cases

Identical Oscillators

Let us consider the case with all oscillators having the same frequency ω_0. It follows that $\omega_j' = 0, \forall j \in \mathcal{N}$. Let us consider $r_\infty > 0$. The solutions r_∞ of the consistency condition (6.14) are then given by

$$\begin{aligned} r_\infty &\in \{\frac{k}{N} \ : k = 2, 4, 6, \ldots, N\}, \quad \text{if } N \text{ is even,} \\ r_\infty &\in \{\frac{k}{N} \ : k = 1, 3, 5, \ldots, N\}, \quad \text{if } N \text{ is odd.} \end{aligned} \tag{6.29}$$

Now consider the case $r_\infty = 0$. Is it a solution of (6.14) with $\omega_j' = 0, \forall j \in \mathcal{N}$? Nothing can be concluded from the consistency condition since we end up with $0/0$, which is not determined. However, if the initial states of the N oscillators are distributed around the circle in such a way that $r_\infty = 0$, the system equations reduce to $\dot{\theta}_i(t) = \omega_0, \ \forall i \in \mathcal{N}$. Since all oscillators move on the circle with the same velocity the initial phase differences are maintained and a phase locking solution is obtained.

The above results are consistent with those obtained in Section 5.3. The solution of (6.29) with $k = N$ is the synchronized solution; the remaining solutions of (6.29) are all elementary solutions. Although we did not obtain the phase locking solutions with $r_\infty = 0$ by means of the consistency condition, we easily proved that they do exist.

Two Natural Frequencies

In this section a population with the following properties is considered. There are only two natural frequencies ω_a and ω_b present in the population

and the number of oscillators possessing the natural frequency ω_a is equal to the number of oscillators with natural frequency ω_b. In this and the next section we do not consider the consistency condition with minus signs, since this yields only unstable solutions, as will be proven in Section 6.3. Equation (6.24) becomes

$$r_\infty = \sqrt{1 - \left(\frac{\omega_x}{K r_\infty}\right)^2},$$

where

$$\omega_x := \left|\frac{\omega_b - \omega_a}{2}\right|.$$

This yields the following equation to solve:

$$r_\infty^4 - r_\infty^2 + \left(\frac{\omega_x}{K}\right)^2 = 0. \tag{6.30}$$

The 4 solutions are

$$r_\infty = \pm\sqrt{\frac{1}{2} \pm \sqrt{\frac{1}{4} - \left(\frac{\omega_x}{K}\right)^2}}.$$

In this expression we can drop the first minus sign since r_∞ is defined to be positive. There exist only real solutions, if and only if

$$\frac{1}{4} - \left(\frac{\omega_x}{K}\right)^2 \geq 0$$

or equivalently if and only if

$$K \geq |\omega_b - \omega_a|.$$

Hence the smallest value of K that allows phase locking to take place is $K_T = |\omega_b - \omega_a|$. The corresponding value of r_∞ is $\frac{\sqrt{2}}{2}$. Oscillators with equal natural frequencies possess the same phase. The population splits into two groups on the phase circle and for $K = K_T$ the phase difference between the two groups of oscillators is $\pi/2$. The solutions of (6.30) are plotted in Figure 6.2. Two distinct branches of solutions $r_\infty(K)$ different from zero are found that correspond to phase locking. In Section 6.3 it is proven that the upper branch is stable while the lower branch is unstable.

A Special Case with Three Natural Frequencies

Consider a population with 3 natural frequencies ω_1, ω_2 and $\omega_3 \in \mathbb{R}$, where the number of oscillators is the same for each natural frequency. Assume that $\omega_1 < \omega_2 < \omega_3$ and $\omega_3 - \omega_2 = \omega_2 - \omega_1 =: \omega_x$. Then r_∞ satisfies (6.24) if and only if

$$r_\infty = \frac{1}{3}\left(1 + 2\sqrt{1 - \left(\frac{\omega_x}{K r_\infty}\right)^2}\right).$$

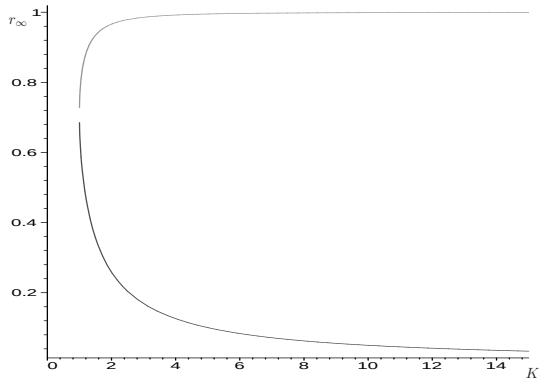

Figure 6.2: The phase locking solution satisfying (6.24) of a population with two natural frequencies

Thus, r_∞ is the solution of

$$9r_\infty^4 - 6r_\infty^3 - 3r_\infty^2 + 4\left(\frac{\omega_x}{K}\right)^2 = 0.$$

If and only if $4\left(\frac{\omega_x}{K}\right)^2 \leq 1.3769$ this equation possesses real solutions. Hence $K_T = 1.7044\omega_x$. This is in correspondence with simulations and with the numerical value computed by the algorithm presented in Section 6.4.

6.3 Stability Properties of the Phase Locking Solutions

Consider a set of oscillators described by (3.33). Substituting $\theta_i(t)$ by $\theta_i'(t) + \omega_m t$ yields

$$\dot{\theta}_i' = f_i(\theta') = \omega_i' + \frac{K}{N}\sum_{j=1}^{N}\sin(\theta_j' - \theta_i'),\ \forall i \in \mathcal{N}, \tag{6.31}$$

with $\omega_i' = \omega_i - \omega_m$and $\theta' := [\theta_1' \ \cdots \ \theta_N']^T$. Recall that for a phase locking solution, $\dot{\theta}_i(t) = \omega_m,\ \forall i \in \mathcal{N}$, or in the new coordinates $\dot{\theta}_i'(t) = 0,\ \forall i \in \mathcal{N}$.

6.3.1 Curves of Equilibrium Points

Similar to the linear systems of Chapter 4, the system equations (6.31) are invariant under translations

$$\theta' \to \theta' + \alpha\begin{bmatrix}1\\ \vdots \\ 1\end{bmatrix}, \quad \forall \alpha \in \mathbb{R}. \tag{6.32}$$

This means that each equilibrium point of (6.31) belongs to a curve of equilibrium points, all representing the same phase locking solution in the sense that their phase differences are identical.

Definition 32. *A phase locking solution is defined* locally asymptotically stable *if and only if*

- *all solutions of (6.31) with initial conditions in the neighborhood of the curve corresponding to this phase locking solution, converge to one of the equilibria on the curve,*
- *every equilibrium on the curve is locally stable.*

For each phase locking solution of (6.31), the curve of the corresponding equilibrium points is a center manifold of the system dynamics at the equilibrium point under study [43]. The reduced system on this center manifold is stable, since the manifold consists only of equilibria. As a consequence the linearization around each equilibrium point will contain at least one zero-eigenvalue (cfr. Lemma 3).

If the linearization at an equilibrium point of (6.31) has at least one positive eigenvalue, this equilibrium point is locally unstable. Because of the invariance of the system under (6.32), all the equilibrium points on the corresponding curve of equilibrium points are then locally unstable. This is the case for phase locking solutions with r_∞ satisfying (6.14) with minus signs in the expression as will be shown in Theorem 23.

On the other hand, if the linearization contains one zero-eigenvalue and all the other eigenvalues are negative, the equilibrium point is locally stable [17]. Local asymptotic stability of the corresponding phase locking solution follows.

6.3.2 Linearization about an Equilibrium Point

Phase locking solutions (or, equivalently, equilibrium points of (6.31)) are determined by (6.10), (6.12) and (6.14). The equations (6.31) can be rewritten as

$$\dot{\theta}'_i = \omega'_i + \frac{K}{N}\sum_{j=1}^{N}\sin((\theta'_j - \theta'_1 - \lambda) - (\theta'_i - \theta'_1 - \lambda)),\ \forall i \in \mathcal{N}.$$

Theorem 22. *The Jacobian matrix of (6.31) about an equilibrium point is of the form:*

$$J = \frac{K}{N}(A + bb^T + cc^T), \tag{6.33}$$

with

$$A = -diag(a_1, \ldots, a_N), \quad a_i := \pm N r_\infty \sqrt{1 - \Big(\frac{\omega_i'}{K r_\infty}\Big)^2},$$
$$b = \begin{bmatrix} \pm\sqrt{1 - \Big(\frac{\omega_1'}{K r_\infty}\Big)^2} \\ \vdots \\ \pm\sqrt{1 - \Big(\frac{\omega_N'}{K r_\infty}\Big)^2} \end{bmatrix} \in \mathbb{R}^N, \qquad c = \begin{bmatrix} \frac{\omega_1'}{K r_\infty} \\ \vdots \\ \frac{\omega_N'}{K r_\infty} \end{bmatrix} \in \mathbb{R}^N. \tag{6.34}$$

Proof. The linearization about a phase locking solution is obtained as follows. The off-diagonal elements of the Jacobian matrix are $(i \neq l)$

$$\frac{\partial f_i}{\partial \theta_l'}\bigg|_{\text{eq}} = \frac{K}{N} \cos((\theta_l' - \theta_1' - \lambda) - (\theta_i' - \theta_1' - \lambda))\bigg|_{\text{eq}},$$
$$= \frac{K}{N}\Big(\cos(\theta_l' - \theta_1' - \lambda)\cos(\theta_i' - \theta_1' - \lambda) + \sin(\theta_l' - \theta_1' - \lambda)\sin(\theta_i' - \theta_1' - \lambda)\Big)\bigg|_{\text{eq}}.$$

With $\theta_i' - \theta_1' \equiv \theta_i - \theta_1 = \phi_i$ and the use of (6.12),

$$\frac{\partial f_i}{\partial \theta_l'}\bigg|_{\text{eq}} = \frac{K}{N}\left[\left(\pm \sqrt{1 - \Big(\frac{\omega_l'}{K r_\infty}\Big)^2}\right)\left(\pm \sqrt{1 - \Big(\frac{\omega_i'}{K r_\infty}\Big)^2}\right) + \frac{\omega_i' \omega_l'}{K^2 r_\infty^2}\right].$$

The diagonal elements of the Jacobian matrix are computed as follows:

$$\frac{\partial f_i}{\partial \theta_i'}\bigg|_{\text{eq}} = \frac{K}{N} \sum_{\substack{j=1 \\ j\neq i}}^{N} -\cos((\theta_j' - \theta_1' - \lambda) - (\theta_i' - \theta_1' - \lambda))\bigg|_{\text{eq}},$$
$$= -\frac{K}{N}\left[\left(\pm \sqrt{1 - \Big(\frac{\omega_i'}{K r_\infty}\Big)^2}\right)\left(\sum_{\substack{j=1 \\ j\neq i}}^{N} \pm \sqrt{1 - \Big(\frac{\omega_j'}{K r_\infty}\Big)^2}\right) + \frac{\omega_i' \sum_{\substack{j=1 \\ j\neq i}}^{N} \omega_j'}{K^2 r_\infty^2}\right].$$

From (6.14) it follows that

$$N r_\infty - \left(\pm \sqrt{1 - \Big(\frac{\omega_i'}{K r_\infty}\Big)^2}\right) = \sum_{\substack{j=1 \\ j\neq i}}^{N} \pm \sqrt{1 - \Big(\frac{\omega_j'}{K r_\infty}\Big)^2},$$

from which

$$\left.\frac{\partial f_i}{\partial \theta_i'}\right|_{\text{eq}} = \frac{K}{N}\left[\sqrt{1-(\frac{\omega_i'}{Kr_\infty})^2}\sqrt{1-\left(\frac{\omega_i'}{Kr_\infty}\right)^2}\right.$$
$$\left. - Nr_\infty\left(\pm\sqrt{1-\left(\frac{\omega_i'}{Kr_\infty}\right)^2}\right) + \frac{(\omega_i')^2}{K^2r_\infty^2}\right]. \quad (6.35)$$

□

Lemma 3. *The matrix J has an eigenvalue zero with corresponding eigenvector $[1 \cdots 1]^T$.*

Proof. With v equal to $[1 \cdots 1]^T$, the i-th component of Jv is

$$\frac{K}{N}\left[\left(\pm\sqrt{1-\left(\frac{\omega_i'}{Kr_\infty}\right)^2}\right)\left(\sum_{l=1}^{N}\pm\sqrt{1-\left(\frac{\omega_l'}{Kr_\infty}\right)^2}\right)\right.$$
$$\left. - Nr_\infty\left(\pm\sqrt{1-\left(\frac{\omega_i'}{Kr_\infty}\right)^2}\right) + \left(\frac{\omega_i'}{Kr_\infty}\right)\left(\sum_{l=1}^{N}\frac{\omega_l'}{Kr_\infty}\right)\right].$$

Since the sum in the first term is equal to Nr_∞, the first and second term add up to zero. Furthermore the sum in the third term is equal to zero implying $Jv = 0$. □

6.3.3 Stability Results

From now on, we restrict to phase locking solutions with

$$\frac{|\omega_i'|}{Kr_\infty} < 1, \quad \forall i \in \mathcal{N}. \quad (6.36)$$

This implies that all eigenvalues of A are different from zero and that $b_i \neq 0, \forall i \in \mathcal{N}$, which simplifies the stability analysis.

Theorem 23. *Suppose that the equilibrium point under consideration corresponds to a phase locking solution that satisfies (6.14) containing at least one minus sign. Then J possesses at least one positive eigenvalue and the corresponding phase locking solution is locally unstable.*

Proof. The matrices bb^T and cc^T are positive semidefinite. Applying Theorem 48 with $\tilde{A} = A + bb^T$ and $\tilde{B} = cc^T$ shows that

$$\lambda_k(J) \geq \lambda_k(\frac{K}{N}(A + bb^T)), \quad k \in \mathcal{N}.$$

Similarly,

$$\lambda_k(A + bb^T) \geq \lambda_k(A), \quad k \in \mathcal{N}.$$

Therefore

$$\lambda_k(J) \geq \lambda_k(\frac{K}{N}A), \quad k \in \mathcal{N}. \tag{6.37}$$

If the equilibrium point under consideration corresponds to a phase locking solution satisfying (6.14) with at least one minus sign, at least one eigenvalue of A is positive and, by (6.37), J possesses at least one positive eigenvalue. □

The only phase locking solutions left to be examined with respect to their stability properties, are those satisfying (6.24). The Jacobian corresponding to these phase locking solutions is given by (6.33) and (6.34), with the restriction that A is negative definite:

$$a_i = -Nr_\infty\sqrt{1 - \left(\frac{\omega_i'}{Kr_\infty}\right)^2}, \quad \forall i \in \mathcal{N}. \tag{6.38}$$

Lemma 4. *The matrix J restricted to (6.38) has at least $(N-2)$ negative eigenvalues.*

Proof. The matrix A is negative definite. The matrices bb^T and cc^T each have one strictly positive eigenvalue; their remaining eigenvalues are zero. This implies that the sum $bb^T + cc^T$ has at most two non-zero, strictly positive eigenvalues. Applying Theorem 48 with $\tilde{A} = \frac{K}{N}(-bb^T - cc^T)$ and $\tilde{B} = -\frac{K}{N}A$, it follows that $\lambda_k(-J) > \lambda_k(\frac{K}{N}(-bb^T - cc^T))$. Hence the matrix J has at least $N-2$ negative eigenvalues. □

Lemma 5 (Schur's lemma)**.** *With $A \in \mathbb{R}^{n\times n}$ symmetric and $b, c \in \mathbb{R}^n$ it holds that*

$$\det(A + bb^T + cc^T) = \det(A)\left(\left(1 + b^TA^{-1}b\right)\left(1 + c^TA^{-1}c\right) - \left(c^TA^{-1}b\right)^2\right).$$

Proof. Consider the matrix

$$M := \begin{bmatrix} 1 & -b^T & 0 \\ b & A & -c \\ 0 & c^T & 1 \end{bmatrix}.$$

Performing elementary row and column operations on M to turn it into a lower triangular matrix yields two different matrices M_1, M_2, depending on the row and column operations:

$$M_1 = \begin{bmatrix} 1 & 0 & 0 \\ b & A + bb^T + cc^T & 0 \\ 0 & c^T & 1 \end{bmatrix},$$

and

$$M_2 = \begin{bmatrix} 1 + b^T A^{-1} b & 0 & 0 \\ b & A & 0 \\ 0 & c^T & 1 - c^T A^{-1} \left(\frac{b b^T A^{-1} c}{1 + b^T A^{-1} b} - c \right) \end{bmatrix}.$$

Now $\det(M_1) = \det(M_2)$, leading to

$$\det(A + bb^T + cc^T) = \det(A) \left(\left(1 + b^T A^{-1} b\right) \left(1 + c^T A^{-1} c\right) - \left(c^T A^{-1} b\right)^2 \right).$$

□

Theorem 24. *The phase locking solution corresponding to r_∞ satisfying (6.24), is locally asymptotically stable if and only if*

$$\sum_{j=1}^{N} \frac{1 - 2(\frac{\omega_j'}{K r_\infty})^2}{\sqrt{1 - (\frac{\omega_j'}{K r_\infty})^2}} > 0. \tag{6.39}$$

Proof. The eigenvalues of J are the roots of $\det(A - \lambda I + bb^T + cc^T)$. Define $A' := A - \lambda I$. From Lemma 5 it follows that

$$\det(A' + bb^T + cc^T) = \det(A') \left(\left(1 + b^T A'^{-1} b\right) \left(1 + c^T A'^{-1} c\right) - \left(c^T A'^{-1} b\right)^2 \right). \tag{6.40}$$

The determinant $\det(A - \lambda I + bb^T + cc^T)$ is a polynomial in λ and, since J possesses a zero-eigenvalue, the coefficient belonging to the zero-th order term is zero and the one belonging to the first order term is the product of all non-zero eigenvalues. Denote the zero- eigenvalue of J by λ_N. For small values of λ,

$$\det(A - \lambda I + bb^T + cc^T) = -(\lambda_1 \lambda_2 \ldots \lambda_{N-1})\lambda + O(\lambda^2). \tag{6.41}$$

Using the definitions of A, b and c, the right hand side of (6.40) can be rewritten. This involves a Taylor series expansion in λ:

$$A'^{-1} = A^{-1} + O(\lambda).$$

We obtain

$$\begin{aligned} c^T A'^{-1} b &= c^T A^{-1} b + O(\lambda), \\ &= \frac{1}{K N r_\infty^2} \sum_{i=1}^{N} \omega_i' + O(\lambda), \\ &= O(\lambda). \end{aligned}$$

Also,

$$1 + c^T A'^{-1} c = 1 + c^T A^{-1} c + O(\lambda),$$

and

$$1 + b^T A'^{-1} b = 1 + \sum_{i=1}^{N} \frac{1 - \left(\frac{\omega_i'}{Kr_\infty}\right)^2}{-Nr_\infty \sqrt{1 - \left(\frac{\omega_i'}{Kr_\infty}\right)^2} - \lambda},$$
$$= \frac{1}{Nr_\infty^2}\lambda + O(\lambda^2).$$

Furthermore

$$\det(A') = \det(A) + O(\lambda).$$

This changes the right hand side of (6.40) into

$$(\det(A) + O(\lambda)) \left((\frac{1}{Nr_\infty^2}\lambda + O(\lambda^2)) \left(1 + c^T A^{-1} c + O(\lambda)\right) - O(\lambda^2) \right),$$

which can be written as

$$(1 + c^T A^{-1} c) \frac{\det(A)}{Nr_\infty^2}\lambda + O(\lambda^2). \tag{6.42}$$

Since (6.41) is equal to (6.42),

$$-(\lambda_1 \lambda_2 \dots \lambda_{N-1}) = (1 + c^T A^{-1} c) \frac{\det(A)}{Nr_\infty^2}. \tag{6.43}$$

The matrix J possesses $N-2$ negative eigenvalues. Denote these eigenvalues by $\lambda_2, \dots, \lambda_{N-1}$. The sign of the product of these eigenvalues is equal to the sign of $(-1)^{N-2}$. From (6.38), the sign of $\det(A)$ is equal to the sign of $(-1)^N$. From (6.43),

$$\text{sgn}((-1)^{N-1}\lambda_1) = \text{sgn}((-1)^N (1 + c^T A^{-1} c))$$

implying

$$\text{sgn}(\lambda_1) = -\text{sgn}((1 + c^T A^{-1} c)) \tag{6.44}$$

Now,

$$1 + c^T A^{-1} c = 1 - \sum_{i=1}^{N} \frac{\left(\frac{\omega_i'}{Kr_\infty}\right)^2}{Nr_\infty \sqrt{1 - \left(\frac{\omega_i'}{Kr_\infty}\right)^2}}, \tag{6.45}$$
$$= \sum_{j=1}^{N} \frac{1 - 2(\frac{\omega_j'}{Kr_\infty})^2}{\sqrt{1 - (\frac{\omega_j'}{Kr_\infty})^2}}. \tag{6.46}$$

The phase locking solution is locally asymptotically stable if and only if $\lambda_1 < 0$, or equivalently (from (6.44)), if and only if expression (6.46) is strictly positive. □

Remark 1**:**

Inequality (6.39) has a nice geometric interpretation. Assume that the explicit expression of a phase locking solution has the form $r_\infty = \phi(K)$. This can be written implicitly as $f(K, r_\infty) = 0$. Then

$$\frac{\mathrm{d}r_\infty}{\mathrm{d}K} = -\frac{\partial f(K, \phi(K))/\partial K}{\partial f(K, \phi(K))/\partial r_\infty}.$$

The value of this derivative gets infinitely large if the denominator $\partial f(K, \phi(K))/\partial r_\infty$ is equal to zero. The denominator is equal to the expression (6.46). The phase locking solution $r_\infty = \phi(K)$ intersects the locus of points satisfying

$$\partial f(K, \phi(K))/\partial r_\infty = 0,$$

with an infinitely large derivative $\mathrm{d}\phi(K)/\mathrm{d}K$. At the K-value of the intersection of (6.46) with the curve representing phase locking, a bifurcation is present, as can be seen in Figure 6.3. For coupling strengths smaller than this value phase locking is not a possible behavior. For K larger than this threshold value, two phase locking solutions arise.

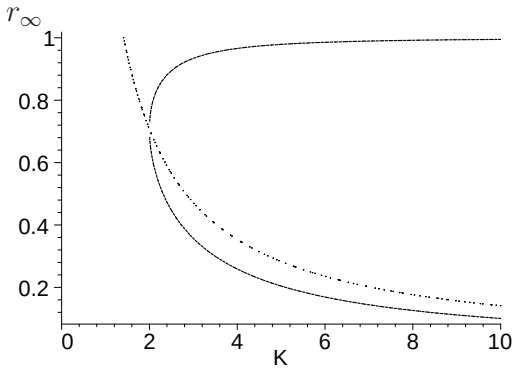

Figure 6.3: The phase locking solutions (6.24) of the population in Figure 6.1, together with the curve of points where (6.46) is zero. The upper branch is locally asymptotically stable.

Remark 2**:**

An easily interpretable sufficient condition for locally asymptotically stable phase locking follows from noticing that condition (6.39) is satisfied if all the numerators in the summation are positive, i.e.

$$\frac{|\omega_i'|}{K r_\infty} < \frac{1}{\sqrt{2}}, \ \forall i \in \mathcal{N}. \tag{6.47}$$

This is equivalent with $0 < \sin(\phi_j - \lambda) < \frac{\sqrt{2}}{2}$ and

$$0 < \sin(\theta_j - \psi) < \frac{\sqrt{2}}{2}. \tag{6.48}$$

As stated before, the phase differences satisfying (6.24) fulfill $\phi_i - \lambda \in (-\frac{\pi}{2}, \frac{\pi}{2})$, or equivalently

$$\theta_j - \psi \in (-\frac{\pi}{2}, \frac{\pi}{2}). \tag{6.49}$$

Combining (6.48) and (6.49) yields $\theta_j - \psi \in (0, \frac{\pi}{4})$. Requiring that the difference between each phase and the mean phase be smaller than $\frac{\pi}{4}$ is equivalent to requiring that the phase difference between each pair of oscillators be smaller than $\frac{\pi}{2}$. This yields the following theorem.

Theorem 25. *If the phase locking solution is such that its phase differences between each pair of oscillators are smaller than $\frac{\pi}{2}$, it is locally asymptotically stable.*

6.4 Phase Locking and Bifurcation Theory

The value K_T bears a great importance, since it indicates the onset of phase locking. This section presents an algorithm enabling the computation of the value of K_T, provided the values of the natural frequencies are known. In principle, this algorithm is applicable to all-to-all coupled networks with an arbitrary number of oscillators, but the calculations become involved for large numbers of oscillators. The algorithm was developed by Byrnes in a totally different context: in [8–10] the N-node electric power grid is investigated. Each node of the power system is represented by a complex voltage with amplitude V_i and phase δ_i. The phases are typically expressed with respect to some reference frequency ω:

$$\delta_i(t) = \omega t + \theta_i(t),$$

where θ_i is called the *voltage angle* of the i-th node. The dynamic operation of an N-node power system is described by the so-called *swing equations*:

$$\begin{cases} M_i\ddot{\theta}_i + D_i\dot{\theta}_i = P_i - \sum_{j=1}^{N} B_{ij}\sin(\theta_i - \theta_j), & i = 1, \ldots, g, \\ 0 = P_i - \sum_{j=1}^{N} B_{ij}\sin(\theta_i - \theta_j), & i = g+1, \ldots, N. \end{cases}$$

where M_i is the moment of inertia, D_i is the damping constant and P_i is the mechanical input torque to the generator or minus the real electrical load, and $g < N \in \mathcal{N}$. The first g equations represent the generator nodes of the

network, the last $N - g$ nodes represent loads. One is typically interested in solutions with $\dot{\theta}_i = 0$ and $\ddot{\theta}_i = 0$, for all i, i.e.

$$0 = P_i - \sum_{j=1}^{N} B_{ij} \sin(\theta_i - \theta_j), \quad \forall i \in \mathcal{N}. \tag{6.50}$$

Furthermore θ_N is taken to be a reference angle (i.e. $\theta_N \equiv 0$), reducing (6.50) to

$$P_i = B_{iN} \sin \theta_i + \sum_{j=1}^{N} B_{ij} \sin(\theta_i - \theta_j), \quad \forall i \in \mathcal{N}. \tag{6.51}$$

These equations are called the *load flow equations* and have been the subject of extensive research. Ideally, all *load flow solutions*, with values for θ_i satisfying (6.51) are now obtained. In practice, however, this is hardly ever feasible since the problem consists of solving a set of N coupled nonlinear equations. A second best result would be the knowledge of the *number of load flow solutions* when the values of the parameters P_i are given. This knowledge yields the opportunity to inspect when solutions arise or disappear as the parameter values are varied. An algorithm to obtain the number of solutions of (6.51) is described in [10] and is based on Bifurcation Analysis. Roughly speaking, a *bifurcation* is said to take place when the qualitative dynamics of a system change as the parameters of the system are varied. A more precise definition goes as follows:

Definition 33. *Consider a system described by $\dot{x} = f(x, \lambda)$, with x the system variables and $\lambda \in \mathbb{R}$ a parameter. A* bifurcation point *is a solution (x_0, λ_0) of $f(x, \lambda) = 0$ where the number of solutions changes when λ passes λ_0.*

The bifurcation points are computed as follows. For a general system $\dot{x} = f(x)$ the Jacobian matrix $\frac{\partial f}{\partial x}$ of the system is constructed and its eigenvalues are determined. The points in the state space of interest are those with one or more eigenvalues equal to zero. At these points a bifurcation occurs [79], depending on the parameter values.

Definition 34. *The set of all equilibrium solutions (x_0, λ_0) for which $det(\frac{\partial f}{\partial x}) = 0$ is called the* bifurcation surface*.*

The bifurcation surface of (6.51) is constructed using the trigonometric substitutions [10]:

$$\begin{aligned} x_i = \sin \theta_i \quad , \qquad & y_i = \cos \theta_i, \\ x_i^2 + y_i^2 = 1. & \end{aligned}$$

These substitutions turn the goniometric equations into algebraic equations. Eliminating all x_i, y_i variables yields a surface in parameter space

$(P_1, \ldots, P_{n-1})$. This surface is the bifurcation surface of the system. It divides the parameter space in areas with a different number of solutions of (6.51). When the parameters are varied a curve in parameter space is traversed. At points where this curve intersects the bifurcation surface the number of load flow solutions changes.

Let us now return to the setting of coupled oscillators. The phase equations (3.33) can be transformed into system equations describing $N-1$ independent phase differences $\phi_i = \theta_i - \theta_1,\ i \in \{2, \ldots, N\}$:

$$\dot{\phi}_i = \Omega_i - \frac{K}{N}\left[\sum_{k=2}^{N} \sin\phi_k + \sum_{l=1}^{N} \sin(\phi_i - \phi_l)\right], \quad i \in \{2, \ldots, N\}, \tag{6.52}$$

where $\Omega_i := \omega_i - \omega_1$. Phase locking solutions of (3.33) correspond to equilibrium points of (6.52). In other words, the phase differences ϕ_i of a phase locking solution satisfy

$$\Omega_i = \frac{K}{N}\sum_{k=2}^{N} \sin\phi_k + \frac{K}{N}\sum_{l=1}^{N} \sin(\phi_i - \phi_l), \quad i \in \{2, \ldots, N\}. \tag{6.53}$$

Notice the structural similarity between (6.51) and (6.53) (the difference between both expression being the summation over $\sin\phi_k$ in (6.53)). This leads us to assume that an algorithm solving (6.51) is also applicable to (6.53).

In the oscillator network the natural frequencies, and consequently Ω_i, are considered given constants. The parameter set λ in Definition 33 applied to the oscillator network is $\{K\}$, with K the coupling strength. When an increasing coupling strength K crosses the K_T-value, the phase portrait of the system changes its topological structure and the dynamics change qualitatively: for values smaller than $K = K_T$ there are no equilibria present; when $K > K_T$ at least two equilibria exist. The system undergoes a bifurcation at $K = K_T$.

As an example, the algorithm to construct the bifurcation surface for the load flow equations is now applied to the three oscillator network described by

$$\begin{cases} \dot{\phi}_2 &= \Omega_2 - \frac{K}{3}\Big(2\sin\phi_2 + \sin\phi_3 + \sin(\phi_2 - \phi_3)\Big), \\ \dot{\phi}_3 &= \Omega_3 - \frac{K}{3}\Big(\sin\phi_2 + 2\sin\phi_3 - \sin(\phi_2 - \phi_3)\Big), \end{cases} \tag{6.54}$$

with $\phi_i = \theta_1 - \theta_i$ and $\Omega_i = \omega_1 - \omega_i$. Define

$$\begin{cases} P_1 = \dfrac{2}{3}\Omega_2 - \dfrac{1}{3}\Omega_3, \\ P_2 = -\dfrac{1}{3}\Omega_2 + \dfrac{2}{3}\Omega_3. \end{cases} \tag{6.55}$$

Equilibria of (6.54) satisfy

$$\begin{aligned} P_1 &= K\sin\phi_2 + K\sin(\phi_2 - \phi_3) \\ P_2 &= K\sin\phi_3 - K\sin(\phi_2 - \phi_3). \end{aligned} \tag{6.56}$$

The following goniometric substitutions

$$\begin{aligned} \sin(\phi_2-\phi_3) &= x_2, & \sin\phi_2 &= x_1,\\ \cos(\phi_2-\phi_3) &= y_2, & \cos\phi_2 &= y_1, \end{aligned}$$

render (6.56) of the form

$$\begin{cases} P_1/K = x_1 + x_2,\\ P_2/K = (x_2y_1 - y_2x_1) - x_1,\\ \quad 1 = x_1^2 + y_1^2,\\ \quad 1 = x_2^2 + y_2^2. \end{cases} \tag{6.57}$$

The condition $\det(\frac{\partial f}{\partial \phi}) = 0$ yields

$$K^2y_1y_2 + K^2(y_1+y_2)(y_1y_2 + x_1x_2) = 0. \tag{6.58}$$

This system of equations (6.57), (6.58) was explicitly considered in [10] and the corresponding bifurcation surface is stated in its appendix. Written as a function of Ω_2/K and Ω_3/K this surface assumes the expression

$$\begin{gathered} -27 - 204006(\Omega_2/K)^6(\Omega_3/K)^2 + 672960(\Omega_2/K)^5(\Omega_3/K)^3 - \\ 907437(\Omega_2/K)^4(\Omega_3/K)^4 + 672960(\Omega_2/K)^3(\Omega_3/K)^5 - 204006(\Omega_2/K)^2(\Omega_3/K)^6 - \\ 17412(\Omega_2/K)(\Omega_3/K)^7 + 153516(\Omega_2/K)^4(\Omega_3/K)^2 - 309872(\Omega_2/K)^3(\Omega_3/K)^3 + \\ 153516(\Omega_2/K)^2(\Omega_3/K)^4 + 1704(\Omega_2/K)(\Omega_3/K)^5 - 20682(\Omega_2/K)^2(\Omega_3/K)^2 + \\ 13788(\Omega_2/K)(\Omega_3/K)^3 - 864(\Omega_2/K)(\Omega_3/K) + 13788(\Omega_2/K)^3(\Omega_3/K) + \\ 1704(\Omega_2/K)^5(\Omega_3/K) - 10080(\Omega_2/K)^9(\Omega_3/K) + 121608(\Omega_2/K)^8(\Omega_3/K)^2 - \\ 425952(\Omega_2/K)^7(\Omega_3/K)^3 + 821664(\Omega_2/K)^6(\Omega_3/K)^4 - 1016496(\Omega_2/K)^5(\Omega_3/K)^5 + \\ 821664(\Omega_2/K)^4(\Omega_3/K)^6 - 425952(\Omega_2/K)^3(\Omega_3/K)^7 + 121608(\Omega_2/K)^2(\Omega_3/K)^8 - \\ 10080(\Omega_2/K)(\Omega_3/K)^9 - 17412(\Omega_2/K)^7(\Omega_3/K) - 1536(\Omega_2/K)^{11}(\Omega_3/K) + \\ 1920(\Omega_2/K)^{10}(\Omega_3/K)^2 + 4480(\Omega_2/K)^9(\Omega_3/K)^3 - 10224(\Omega_2/K)^8\Omega_3/K)^4 + \\ 4480(\Omega_3/K)^9(\Omega_2/K)^3 + 1920(\Omega_3/K)^{10}(\Omega_2/K)^2 - 1536(\Omega_3/K)^{11}(\Omega_2/K) - \\ 10224(\Omega_3/K)^8(\Omega_2/K)^4 - 2880(\Omega_2/K)^7(\Omega_3/K)^5 + 16224(\Omega_2/K)^6(\Omega_3/K)^6 - \\ 2880(\Omega_2/K)^5(\Omega_3/K)^7 + 2016(\Omega_2/K)^{10} + 2016(\Omega_3/K)^{10} + 4353(\Omega_2/K)^8 + \\ 4353(\Omega_3/K)^8 - 568(\Omega_2/K)^6 - 568(\Omega_3/K)^6 - 6894(\Omega_3/K)^4 - 6894(\Omega_2/K)^4 + \\ 864(\Omega_2/K)^2 + 864(\Omega_3/K)^2 + 256(\Omega_3/K)^{12} + 256(\Omega_2/K)^{12} = 0, \end{gathered} \tag{6.59}$$

which is plotted in figure 6.4. This figure can be considered an adaptation of the bifurcation surface for the three node power system, obtained by Távora and Smith [89].

We are interested in bifurcations connected to the change of the parameter K with the values of the natural frequencies Ω_2, Ω_3 fixed. The values of

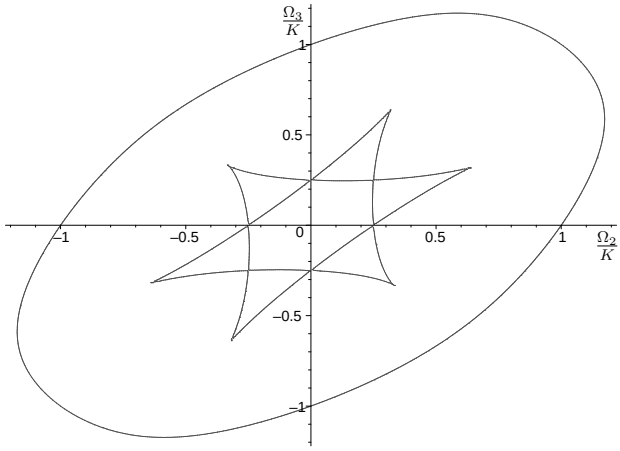

Figure 6.4: Bifurcation surface for the three oscillator network. The number of phase locking solutions are: 6 for parameter values inside the hexagon, 4 inside the triangular shaped regions, 2 inside the ellipse and no phase locking solutions outside the ellipse.

Ω_2, Ω_3 and K fix a point in the $(\frac{\Omega_2}{K}, \frac{\Omega_3}{K})$-space and the position of this point with respect to the bifurcation surface determines how many equilibrium points the system possesses. The values of the natural frequencies are assumed given, e.g. $\Omega_2 = \alpha$, $\Omega_3 = \beta$. The locus of all points in $(\frac{\Omega_2}{K}, \frac{\Omega_3}{K})$-space with these natural frequencies and with $K \in (0, \infty)$ is the half line starting in the origin with direction vector (α, β). For a sufficiently small value of K the corresponding point lies outside of the ellipse in Figure 6.4 and the system has no phase locking solutions. By increasing the K-value, the point is being shifted towards the origin and at the K-value equal to K_T it crosses the ellipse. This is the bifurcation point indicating onset of phase locking and in the case of the three oscillator network it can be proven that at this bifurcation point two equilibria originate, one of which is locally asymptotically stable [8]. Figure 6.4 shows that generically there are 3 bifurcation points for $K \in (0, \infty)$ in the case of the three oscillator network. When $\Omega_2 = \Omega_3$, $\Omega_2 = 0$ or $\Omega_3 = 0$ there are only 2 bifurcation points.

Using mathematics software it is possible to calculate the numerical value of K_T for the three oscillator network. Substituting the given values of the natural frequencies in equation (6.59), one obtains a polynomial in $1/K$ of which the roots are the bifurcation values of K. In the case of three oscillators a 12-th degree polynomial in the variable $1/K$ has to be solved. Generically this polynomial has got 3 positive real roots. The smallest one of these roots is the bifurcation value K_T, which is plotted for several values of Ω in Figure 6.5. The figure shows that the larger the mutual natural frequency

differences are, the larger the coupling strength has to be in order to obtain phase locking.

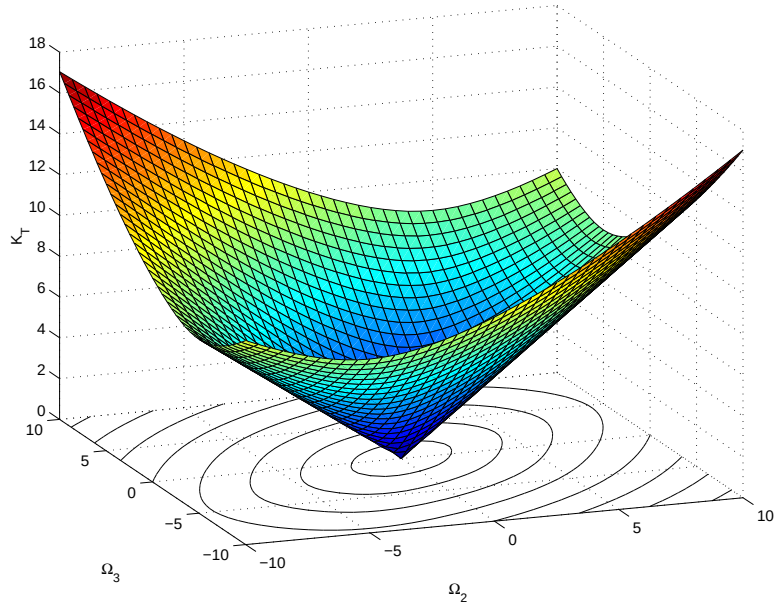

Figure 6.5: The three oscillator network: dependence of the value of K_T on the natural frequency differences. The curves displayed in the (Ω_2, Ω_3)-plane are equilevelsets of the surface.

6.5 Partial Entrainment

6.5.1 Definition

Let us now have a look at the behavior of a finite population of all-to-all coupled oscillators when the coupling strength is smaller than K_T. Simulations show that there exists a second critical value of the coupling strength, called K_P. Below K_P the oscillators act as if they were uncoupled; for $K_P < K < K_T$ the system exhibits *partial entrainment*: there exist one or more subgroups of oscillators with bounded mutual phase differences while the remaining oscillators are drifting. A mathematical definition of this behavior goes as follows:

Definition 35. *A finite number all-to-all coupled network is said to exhibit* partial entrainment *if there exist at least two oscillators θ_i and θ_j with different natural*

frequencies such that

$$\exists A_{ij}, B_{ij} \in \mathbb{R},\ 0 \leq A_{ij} \leq B_{ij} < 2\pi : A_{ij} \leq |\theta_i(t) - \theta_j(t)| \leq B_{ij}, \forall t \in \mathbb{R}.$$

This definition includes phase locking as a special case with $A_{ij} = B_{ij}, \forall i, j \in \mathcal{N}$. If K exceeds the threshold value K_P, two or more oscillators start to entrain each other, i.e. their phase difference remains bounded. With

$$W := \{\omega_{ij} \ :\ \omega_{ij} = |\omega_i - \omega_j|,\ i \neq j\}, \tag{6.60}$$

the oscillators that start entraining are those for which ω_{ij} assumes the minimal value in W. For K increasing between K_P and K_T, discrete values of K can be found at which drifting oscillators start to be entrained. Finally, at the value K_T, all oscillators become phase locked, as proven. (Simulations show that entrainment of *all* oscillators implies that $A_{ij} = B_{ij},\ \forall i, j \in \mathcal{N}$.) In other words, the entraining subgroup grows in discrete steps with increasing K. This behavior can be compared to the behavior in the Kuramoto model. There for $K > K_C$ the phase locked subgroup grows *continuously* with the value of the coupling strength.

One more important remark concerning the definition of partial entrainment has to be made. Simulations indicate that oscillators with the same natural frequency possess the same phase at each time instant for every nonzero coupling, implying they are mutually phase locking. This motivates the exclusive consideration of pairs of oscillators with different values of the natural frequency: without this restriction, partial entrainment cannot indicate the difference in behavior between systems with $K < K_P$ and systems with $K > K_P$. If there are at least two identical oscillators in the population, partial entrainment is trivially satisfied if the above restriction is not included in the definition.

In the remainder of this section only networks consisting of three oscillators are considered. The above phase locking property is proven for the three oscillator network:

Theorem 26. *Consider the three oscillator network. If the natural frequencies are such that $\omega_1 = \omega_2$, then there exist solutions with $(\theta_2 - \theta_1)(t) = 0,\ \forall t \in \mathbb{R}$ and these solutions are locally stable.*

Proof. The dynamics of the three oscillator network is described by

$$\begin{aligned}
\dot{\phi}_2 &= -2\frac{K}{3}\sin\phi_2 - \frac{K}{3}\sin\phi_3 - \frac{K}{3}\sin(\phi_2 - \phi_3),\\
\dot{\phi}_3 &= \omega_3 - \omega_1 - 2\frac{K}{3}\sin\phi_3 - \frac{K}{3}\sin\phi_2 + \frac{K}{3}\sin(\phi_2 - \phi_3),
\end{aligned} \tag{6.61}$$

with $\phi_2 := \theta_2 - \theta_1$ and $\phi_3 := \theta_3 - \theta_1$.

If a solution $t \mapsto (\phi_2(t), \phi_3(t))$ of these equations is such that $\exists t_0 \in \mathbb{R} : \phi_2(t_0) = 0$, then $\phi_2(t) = 0,\ \forall t > t_0$ for this solution. This can be easily

derived from the system equations (6.61): setting $\phi_2 = 0$ in the first equation yields $\dot{\phi}_2 = 0$.

Now, local stability properties of this class of solutions are investigated. Consider a solution $\Phi = (\phi_2(t), \phi_3(t))$:

$$\phi_2(t) = 0,$$
$$\phi_3(t) = f(t) \text{ such that } \frac{\mathrm{d}f}{\mathrm{d}t}(t) = \omega_3 - \omega_1 - K \sin f(t).$$

Linearizing (6.61) about this solution yields the Jacobian

$$\frac{K}{3}\begin{bmatrix} -2 - \cos f(t) & 0 \\ \cos f(t) - 1 & -3\cos f(t) \end{bmatrix}.$$

In a neighborhood of Φ, the dynamics of ϕ_2 are

$$\dot{\phi}_2 = \frac{K}{3}(-2 - \cos f(t))\phi_2.$$

Each solution with an initial condition in the neighborhood of Φ, converges to Φ, since $-2 - \cos f(t) < 0, \forall t \in \mathbb{R}$, which proves the local stability. □

Partial entrainment of a three oscillator network is illustrated in Figure 6.6. This figure shows trajectories in (ϕ_2, ϕ_3)-space, with $\phi_i := \theta_1 - \theta_i$. Along the trajectories, ϕ_2 increases whereas for sufficiently large time the value of ϕ_3 is confined inside some closed interval modulo 2π, with length much smaller than 2π. Oscillators 1 and 3 entrain each other.

To visualize the relation between partial entrainment and phase locking, we show the phase portrait of the three oscillator network for K slightly larger than K_T in Figure 6.7. Comparing it with the phase portrait of Figure 6.6, where $K_P < K < K_T$, the following can be concluded. When the coupling strength exceeds K_T the unstable limit cycle persists; on the stable limit cycle a saddle-node pair arises and phase locking comes into existence.

6.5.2 Estimating the Onset of Partial Entrainment

In this section two particular frequency distributions are analyzed. The first distribution possesses an infinitely large value of ω_3. In order to analyze this configuration the Riemann-Lebesgue lemma turns out to be useful.

Lemma 6 (Riemann-Lebesgue lemma [6]). *Let $\alpha \in \mathbb{R}$. If $f \in L^1([a, b])$, then*

$$\lim_{\alpha \to \infty} \int_a^b f(t) \sin(\alpha t) dt = 0.$$

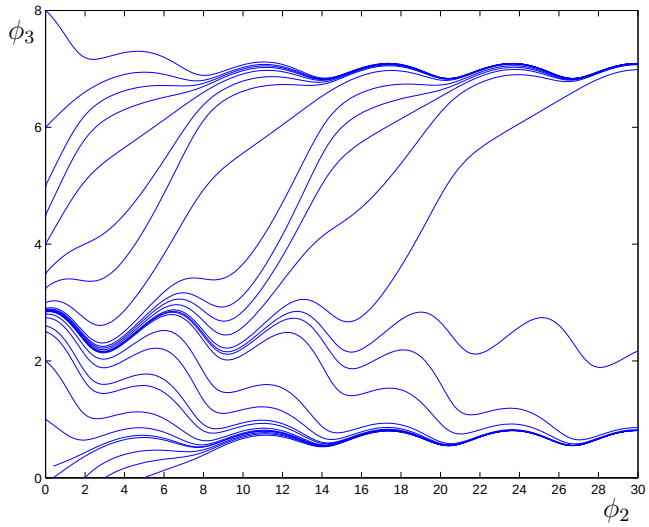

Figure 6.6: Partial entrainment in the three oscillator network. Along trajectories the state variable ϕ_2 increases monotonically. The figure shows the existence of an unstable limit cycle (in the middle of the figure) and two stable limit cycles that can be identified with each other, since the system is considered on the torus. The coupling strength K is bigger than K_P, but smaller than K_T.

Theorem 27. *Consider the three-oscillator network with $\omega_1 < \omega_2 < \omega_3$ and $\omega_2 - \omega_1 = \min(W)$, where W is defined as in (6.60). Assume $\omega_3 \to \infty$. If and only if $K \geq 1.5|\omega_2 - \omega_1|$ partial entrainment exists.*

Proof. The dynamics of the phase difference $\phi := \theta_2 - \theta_1$ is

$$\dot{\phi} = (\omega_2 - \omega_1) - \frac{2K}{3}\sin\phi - \frac{2K}{3}\sin(\theta_3 - \theta_1) + \frac{2K}{3}\sin(\theta_3 - \theta_2). \qquad (6.62)$$

If oscillators 1 and 2 entrain each other and oscillator 3 drifts around on the circle, then

$$\theta_3(t) - \theta_i(t) = \omega_3 t + f_i(t), \quad i = 1, 2,$$

where $f_i(t)$ is a function with bounded derivative. The phase difference ϕ then satisfies

$$\phi(t) = \phi(t_0) + \int_{t_0}^{t} (\omega_2 - \omega_1)\mathrm{d}s + \frac{K}{3}\int_{t_0}^{t} [-2\sin\phi(s) - \sin(\omega_3 s + f_1(s)) + \sin(\omega_3 s + f_2(s))]\,\mathrm{d}s.$$

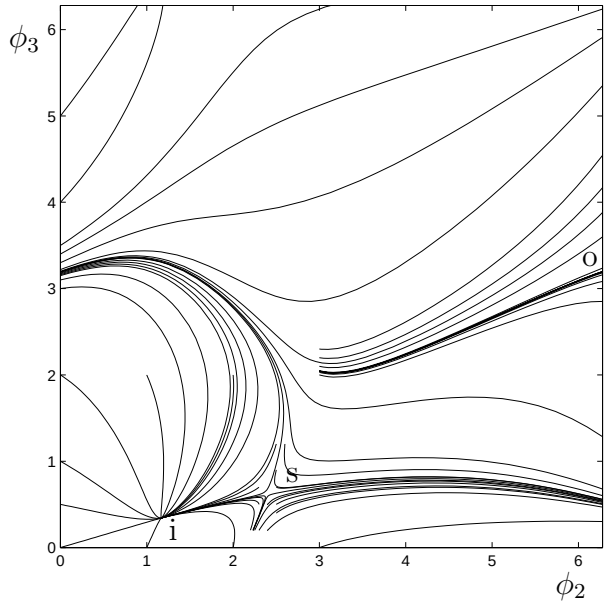

Figure 6.7: Phase portrait on the torus of the three oscillator network with the coupling strength slightly larger than K_T. One can clearly discern a sink (i) , a saddle (s) and an unstable limit cycle (o).

Letting $\omega_3 \to \infty$, and applying Lemma 6, this changes into

$$\phi(t) = \phi(t_0) + \int_{t_0}^{t} \left[(\omega_2 - \omega_1) - 2\frac{K}{3} \sin \phi(s) \right] \mathrm{d}s,$$

and consequently $\phi(t)$ is a solution of

$$\dot{\phi} = (\omega_2 - \omega_1) - 2\frac{K}{3} \sin \phi.$$

This equation has equilibria if and only if $K \geq K_P = 1.5|\omega_2 - \omega_1|$. If $K \geq K_P$ a partially entraining solution exists with $A_{12} = B_{12}$. If $K < K_P$, then $\phi(t)$ is unbounded and the network behaves incoherently. □

Theorem 28. *Consider the three-oscillator network with* $\omega_3 - \omega_2 = \omega_2 - \omega_1 =: \omega_x$. *If and only if* $K > 1.7044\omega_x$ *partial entrainment exists.*

Proof. If $\omega_3 - \omega_2 = \omega_2 - \omega_1 =: \omega_x$, then $K_P = K_T$. It is possible to calculate K_T explicitly: the consistency condition (6.14) corresponding to this network is

$$r_\infty = \frac{1}{3}\left(1 + 2\sqrt{1 - \left(\frac{\omega_x}{K r_\infty}\right)^2}\right).$$

As shown in Section 6.2.2, $K_T = 1.7044\omega_x$. □

Via Theorem 27 and Theorem 28 we have obtained the value of K_P for the configurations $\omega_1 < \omega_2 < \omega_3$ with $\omega_3 - \omega_2 = \omega_2 - \omega_1$ and $\omega_1 < \omega_2$, $\omega_3 \to \infty$. Simulations show that if the value of ω_3 increases while ω_1 and ω_2 remain constant, the value of K_P decreases monotonically. Hence, we have determined a lower and upper bound for K_P of a three oscillator network, namely

$$K_P \in (1.5\Delta\omega, 1.7044\Delta\omega],$$

with $\Delta\omega = \min(W)$.

6.5.3 Proof of Existence of Partial Entrainment

In the previous section an estimate was given of K_P partially based on calculations and partially based on observations from simulations. This means that the estimation is not valid as a proof of the existence of the partially entraining behavior. In this section it is proven that for $\omega_2 - \omega_1$ sufficiently small and for K sufficiently large, partial entrainment exists.

Theorem 29. *Consider the three-oscillator network with $\omega_1 < \omega_2 < \omega_3$ and $|\omega_2 - \omega_1| = \min W$. If $K > 4.065(\omega_2 - \omega_1)$ then $\theta_2 - \theta_1$ is bounded.*

Proof. The dynamics of the phase difference $\theta_2 - \theta_1$ is (6.62), which is equivalent to

$$\dot{\theta}_2 - \dot{\theta}_1 = (\omega_2 - \omega_1) - \frac{2K}{3}\sin(\frac{\theta_2 - \theta_1}{2})\left(2\cos(\frac{\theta_2 - \theta_1}{2}) - \cos(\theta_3 - \frac{\theta_1 + \theta_2}{2})\right).$$

Suppose $\theta_2 - \theta_1 \in [0, \pi/2]$. Then $\sin(\frac{\theta_2 - \theta_1}{2}) \geq 0$. Because $\cos(\theta_3 - \frac{\theta_1 + \theta_2}{2}) \leq 1$,

$$\dot{\theta}_2 - \dot{\theta}_1 \leq (\omega_2 - \omega_1) - \frac{2K}{3}\sin(\frac{\theta_2 - \theta_1}{2})\left(2\cos(\frac{\theta_2 - \theta_1}{2}) - 1\right).$$

Let $\theta_2 - \theta_1$ assume the value $\gamma \in [0, \pi/2]$. If K is such that

$$K > \frac{\omega_2 - \omega_1}{\frac{2}{3}\sin\frac{\gamma}{2}\left(2\cos\frac{\gamma}{2} - 1\right)}, \tag{6.63}$$

then $\dot{\theta}_2 - \dot{\theta}_1 < 0$ for this state $\theta_2 - \theta_1 = \gamma$.

Similarly, suppose $\theta_2 - \theta_1 \in [-\pi/2, 0]$. Then

$$\dot{\theta}_2 - \dot{\theta}_1 \geq (\omega_2 - \omega_1) - \frac{2K}{3}\sin(\frac{\theta_2 - \theta_1}{2})\left(2\cos(\frac{\theta_2 - \theta_1}{2}) - 1\right).$$

If

$$K > \frac{\omega_1 - \omega_2}{\frac{2}{3}\sin\frac{\gamma}{2}\left(2\cos\frac{\gamma}{2} - 1\right)}, \tag{6.64}$$

then $\dot{\theta}_2 - \dot{\theta}_1 > 0$ for $\theta_2 - \theta_1 = -\gamma$. Since $K > 0$ and the right hand side of (6.64) is always smaller than zero, condition (6.64) is always satisfied.

This way an interval $[-\gamma, \gamma]$ is obtained for which the following holds if (6.63) is satisfied:

$$\exists t_0 \in \mathbb{R} : (\theta_2 - \theta_1)(t_0) \in [-\gamma, \gamma] \Rightarrow (\theta_2 - \theta_1)(t) \in [-\gamma, \gamma], \forall t > t_0.$$

If $\gamma = 1.135$, the right hand side of (6.63) is minimal, namely $4.065(\omega_2 - \omega_1)$,. In other words, the interval $[-\gamma, \gamma]$ is at most $[-1.135, 1.135]$, corresponding to the condition $K > 4.065(\omega_2 - \omega_1)$. □

This theorem does not exclude the possibility that $K_T < 4.065(\omega_2 - \omega_1)$, since phase locking also implies boundedness of $\theta_2 - \theta_1$. However, if ω_3 is taken sufficiently large with respect to ω_1 and ω_2, then, according to (6.15), $K_T > 4.065(\omega_2 - \omega_1)$ and partial entrainment is proven to exist.

6.6 Comparison to Infinite Populations

6.6.1 Infinite Networks

The original Kuramoto model [46] studies all-to-all coupled networks of infinitely many oscillators, while the present chapter investigates finite populations. A comparison of both results is quite delicate.

The results in the present chapter on a finite number of oscillators do not extend to the Kuramoto case by letting the number of oscillators tend to infinity: this limit process leads to a countable number of oscillators, while results in the Kuramoto model strongly depend on the presence of a continuum (cardinality of $\mathbb{R}$) of oscillators. Indeed, the Kuramoto results on partial synchronization depend on

1. a (unimodal and even) probability density function $g : \mathbb{R} \to \mathbb{R}$ from which the natural frequencies of the oscillators are drawn,
2. a number density $\rho_\omega : S^1 \times \mathbb{R} \to \mathbb{R}; (\theta, t) \mapsto \rho_\omega(\theta, t)$ of oscillators on the circle corresponding to the natural frequency ω.

For reference we recall that partial synchronization is defined as the behavior with

- a subgroup of mutually phase locking oscillators,
- a subgroup of drifting oscillators,
- a constant amplitude of the order parameter $r(t)e^{i\psi(t)}$ which is defined as

$$r(t)e^{i\psi(t)} := \int_{-\pi/2}^{3\pi/2} e^{i\theta(t)} n(\theta, t) \mathrm{d}\theta,$$

where $n(\theta, t)$ denotes the number density of oscillators with phase between θ and $\theta + \mathrm{d}\theta$ at time t.

Furthermore the Kuramoto results do not persist in the case of a finite number of oscillators. In the present chapter we defined the behavior "partial entrainment" as the behavior with

- one or more subgroups of mutually entraining oscillators defined by the set of oscillators with different natural frequencies and with phases satisfying

  $$\exists A_{ij}, B_{ij} \in \mathbb{R},\ 0 \leq A_{ij} \leq B_{ij} < 2\pi : A_{ij} \leq |\theta_i(t) - \theta_j(t)| \leq B_{ij}, \forall t \in \mathbb{R},$$

- a subgroup of drifting oscillators.

Partial synchronization is a particular case of partial entrainment, by requiring $A_{ij} = B_{ij}$. Notice also that the definition of partial entrainment does not require a constant amplitude of the order parameter. In the finite case, the more general case of partial entrainment was observed, not the more restrictive partial synchronization behavior. One could suspect that for the system of [46] with weaker restrictions on the continuum of oscillators $n(\theta, t)$ and the probability density function g than those of Section 6.6.1, partial entrainment –not partial synchronization– may be observed, as in the finite case.

6.6.2 Existence of Partially Synchronizing Solutions

References [46, 87] investigate partial synchronization while the present chapter treats phase locking. However, some parallels between both analyses can be observed. In this section we focus on the phase locking subgroup of a partially synchronizing solution.

On page 7 of [87] the phase locking subgroup is examined in detail. We recalled the analysis in Section 3.3.1 of Chapter 3. From (3.44) it followed that the amplitude of the order parameter had to satisfy

$$r_\infty = \int_{-\pi}^{\pi} (\tilde{n}_{pl}(\theta, t) + \tilde{n}_d(\theta, t)) e^{i\theta} \mathrm{d}\theta, \tag{6.65}$$

$$= \int_{-\pi}^{\pi} \tilde{n}_{pl}(\theta, t) e^{i\theta} \mathrm{d}\theta, \tag{6.66}$$

with

$$\tilde{n}_{pl}(\theta, t) = \tilde{g}(\omega) \left| \frac{\mathrm{d}\omega}{\mathrm{d}\theta} \right| = K r_\infty \cos\theta \tilde{g}(K r_\infty \sin\theta).$$

This led to (3.45):

$$r_\infty = K r_\infty \int_{-\pi/2}^{\pi/2} \cos^2\theta \tilde{g}(K r_\infty \sin\theta) \mathrm{d}\theta. \tag{6.67}$$

From this, the solutions $r_\infty(K)$ were calculated, yielding partially synchronizing solutions.

A short discussion of (6.67) now follows. The integral of (6.66) takes all oscillators satisfying $\sin\theta = \omega/(Kr_\infty)$ into account. The phase of such an oscillator can be one of two distinct values on the circle, namely $\arcsin\left(\frac{\omega}{Kr_\infty}\right) \in [-\pi/2, \pi/2]$ or $\pi - \arcsin\left(\frac{\omega}{Kr_\infty}\right) \in (\pi/2, 3\pi/2)$. The integral of (6.67) integrates the phase over the interval $[-\pi/2, \pi/2]$. Hence it is tacitly assumed that the phase of each oscillator of the phase locking subgroup satisfies $\theta = \arcsin\left(\frac{\omega}{Kr_\infty}\right)$. This clearly shows that solutions with $\theta = \pi - \arcsin\left(\frac{\omega}{Kr_\infty}\right)$ for some oscillators have been discarded altogether.

Our analysis, presented in Section 6.2, takes *all* possibilities into account, yielding a consistency condition (6.14) representing 2^N equations, from which *all* phase locking solutions can be computed. The similarity between the analysis of phase locking in the finite case and the analysis of the phase locking subgroup in the infinite case leads to suggest that removing the restriction to an integration interval $(\frac{-\pi}{2}, \frac{\pi}{2})$ in (6.67) leads to a (uncountable) set of consistency conditions, with each condition yielding partially synchronizing solutions.

6.6.3 Stability of Partially Synchronizing Solutions

The phase locking subgroup

In the previous section similarities concerning the *existence* of solutions between the finite and the Kuramoto case were described. In this section *stability properties* of the solutions are compared and a possible justification for discarding the solutions as explained in Section 6.6.2 is proposed.

It is not a priori known that the discarded solutions in [46, 87] are unstable. If $r(t)$ is assumed constant and if $\psi(t) = \omega_m(t)$, then the system equations of the infinite case can be regarded as decoupled:

$$\dot{\theta}_i = \omega_i - Kr_\infty \sin\theta_i, \quad \forall i \in \mathcal{N}.$$

A solution with $\theta_i = \pi - \arcsin\left(\frac{\omega_i}{Kr_\infty}\right)$ for at least one oscillator i belonging to the phase locking subgroup, is then indeed unstable. However, when investigating the full dynamics of the system, denoted by

$$\dot{\theta}_i = \omega_i - Kr(\theta_1, \ldots, \theta_N)\sin(\psi(\theta_1, \ldots, \theta_N) - \theta_i), \forall i \in \mathcal{N},$$

it is not clear if the instability of the above solution persists.

On the other hand, we have been shown in the present chapter that all the solutions of (6.14) containing minus signs, i.e. those with some phases

satisfying $\theta = \pi - \arcsin\left(\frac{\omega}{Kr_\infty}\right)$ are unstable. This would support the idea that the partially synchronizing solutions discarded in [87] are unstable, justifying discarding them.

The drifting subgroup

Up to this point, only stability of the phase locking subgroup was inspected. However, partial synchronization consists of both a phase locking subgroup and a drifting subgroup. In order to determine the stability of partial synchronization, the stability of the drifting subgroup has to be taken into account, too. When a partially synchronizing solution possesses a locally stable phase locking subgroup, the drifting subgroup, which is described by stationary densities $\rho(\theta, \omega)$, $\forall \omega : |\omega| > Kr_\infty$, can be unstable, leading to instability of the partially synchronizing solution. The stability of this drifting subgroup remains an open problem.

In the finite case either *all* or *no* oscillators mutually phase lock. The above situation (phase locking with the presence of a drifting subgroup) does not occur, rendering our stability analysis complete.

6.7 Conclusions

In this chapter our results on finite networks of all-to-all interconnected phase oscillators modelled by the Kuramoto model are presented. Here, the natural frequencies of the oscillators are assumed to be nonidentical. Contrary to the identical case where phase locking was a stable behavior for all non-zero coupling strengths, phase locking does not exist below a critical value K_T of the coupling strength. In Section 6.4 an algorithm is presented to compute the value of K_T. The algorithm reveals an unexpected link between the theory of coupled oscillators and the theory of power systems. A necessary and sufficient condition for phase locking is obtained in Theorem 20.

The main result of this chapter is the establishment of stability of *each* phase locking solution for general frequency distributions:

- If the amplitude r_∞ of the complex order parameter satisfies the consistency condition (6.14) containing minus signs, the corresponding phase locking solution is *unstable* in the variables $\theta_i,\ i \in \mathcal{N}$,

- The phase locking solution of which the amplitude r_∞ satisfies the consistency condition (6.14) containing only plus signs, is *locally asymptot-*

ically stable if and only if

$$\sum_{i=1}^{N} \frac{1 - 2(\frac{\omega_j - \omega_m}{Kr_\infty})^2}{\sqrt{1 - (\frac{\omega_j - \omega_m}{Kr_\infty})^2}} > 0. \tag{6.68}$$

When the coupling strength is larger than K_T there is a unique locally stable phase locking solution present. For $K \to \infty$ the phase differences of the stable phase locking solution tend to zero and synchronization arises.

If the coupling strength assumes values smaller than K_T, but larger than a threshold value K_P, all-to-all coupled networks still exhibit a behavior with a certain degree of coherence, called *partial entrainment*. The system is partially entraining if there exists a subgroup of oscillators with bounded mutual phase differences while the remaining oscillators are drifting.

The following results about partial entrainment are obtained for the three oscillator network:

- The onset of partial entrainment K_P of a three oscillator network satisfies $K_P \in (1.5\Delta\omega, 1.7044\Delta\omega]$, with $\Delta\omega = \min\{\omega_{ij} : \omega_{ij} = |\omega_i - \omega_j|, i \neq j\}$.
- Consider the three-oscillator network with $\omega_1 < \omega_2 < \omega_3$ and $|\omega_2 - \omega_1| = \min W$. If $K > 4.065(\omega_2 - \omega_1)$ then $\theta_2 - \theta_1$ is bounded.
- If the natural frequencies are such that $\omega_1 = \omega_2$, then there exist solutions with $(\theta_2 - \theta_1)(t) = 0$, $\forall t \in \mathbb{R}$ and these solutions are locally stable.

Chapter 7

Phase Locking in a Ring of Unidirectionally Coupled Oscillators

7.1 Introduction

Oscillating systems coupled into a ring formation serve as a model for a wide array of applications: gaits of n-legged animals [32], twining of plants [54], rings of semiconductor lasers [81], and circular antenna arrays [21, 23].

Several mathematical models have been proposed and studied in the literature. In [24] and [48], each oscillator is modelled as a nonlinear system with an attracting limit cycle and the coupling is *bidirectional* and of the nearest neighbor type. In [24] the existence and necessary conditions for the stability of phase locking behavior of the network is established. In [48] a ring of *identical* oscillators is considered and a Hopf bifurcation of the network is investigated to obtain different types of stable oscillation. In [33] more general networks of identical oscillators are considered: the symmetries of the network are exploited in order to obtain different types of phase locking behavior. In [97], initial conditions and distributions on the natural frequencies of the oscillators are determined that correspond to a given type of rational frequency ratio.

In this chapter we consider a ring structure of N oscillators with *unidirectional* coupling: the i-th oscillator is influenced by the $(i+1)$-th oscillator for $i = 1, \ldots, N-1$, and the N-th oscillator is influenced by the first. Rings of unidirectionally coupled oscillators are typically encountered in the modelling of animal locomotion [16, 20, 22, 55]. These structures are candidates for rhythmic pattern-generating networks of mutually coupled neurons in

the central nervous system. They are called *central pattern generators* (CPG) and control the motion of the limbs of an n-legged animal. In a simplified model, each neuron in the network corresponds to one leg of the animal. We obtain the full picture of this type of networks when modelled by the Kuramoto equations, by developing both an algorithm to determine all phase locking solutions of the system and an algorithm to determine the stability of these phase locking solutions. Moreover, these results are extended to couplings more general than sinusoidal coupling. Notice also that we allow for oscillators with distinct natural frequencies of oscillation. Different configurations of natural frequencies lead to different sets of phase locking solutions. In this way it is possible to influence the dynamic behavior of the system by adjusting the natural frequencies. The algorithm on stability is applied to a practical case of antenna arrays in Section 8.4.2.

In a different context of cyclic pursuit problems, patterns remarkably similar to the phase locking solutions obtained in the present chapter emerge. In the case of N mobile robots moving in two-dimensional space, where the i-th robot follows the $i+1$-th and the N-th follows the first, it is shown by [57,58] that the robots end up moving in a circle at the same velocity. There exist several qualitatively different stable formations of this kind, mutually distinguishable by the relative positions of the robots on the circle. The connection with the stable phase locking solutions of the unidirectional oscillator ring is established in Section 7.5

As stated in Section 3.2, each oscillator is regarded as a dynamical system with a unique, stable, isolated limit cycle when not coupled to other oscillators, i.e. each oscillator exhibits a periodic behavior when uncoupled. As explained before, this behavior can be captured by a model where the state of the oscillator is one scalar variable θ, called the phase of the oscillator. The system equations of N ($N \in \mathbb{N}$) oscillators unidirectionally coupled in a ring are

$$\dot{\theta}_i = \omega_i + K \sin(\theta_{i+1} - \theta_i), \quad i \in \mathcal{N}, \tag{7.1}$$

with $\theta_{N+1} \equiv \theta_1$ and $K > 0$. For the moment, the interaction is implemented by a sine function. See Section 7.4 for an extension.

7.2 Existence of Phase Locking Solutions

7.2.1 Identical Oscillators

All oscillators have the same natural frequency ω. After substitution $\theta_i \rightarrow \theta_i + \omega t$, the system equations are

$$\dot{\theta}_i = K \sin(\theta_{i+1} - \theta_i), \quad i \in \mathcal{N}. \tag{7.2}$$

Define the phase differences $\phi_i \in S^1 : \phi_i := (\theta_i - \theta_{i-1}) \bmod 2\pi$, $i = 2, \ldots, N$ and $\phi_1 := (\theta_1 - \theta_N) \bmod 2\pi$.

Theorem 30. *Consider all couples* $(\alpha, m),\ \alpha \in S^1,\ m \in \mathcal{N}$*, satisfying*

$$m\alpha + (N-m)(\pi - \alpha) = 2\pi k, \quad k \in T,$$

with $T := \{0, \ldots, N-1\}$*. Assign to each such couple* (α, m) *the vector*

$$[\underbrace{\alpha \ \cdots \ \alpha}_{m} \ \underbrace{\pi - \alpha \ \cdots \ \pi - \alpha}_{N-m}]^T. \tag{7.3}$$

Every vector $\phi = [\phi_1 \ \cdots \ \phi_N]^T$ *that is a permutation of such a vector (7.3), corresponds to a phase locking solution of (7.2).*

Proof. The phase differences $\phi_1, \ldots, \phi_N$ are solutions of the system equations

$$\dot{\phi}_i = K(\sin\phi_{i+1} - \sin\phi_i), \quad i \in \mathcal{N}, \tag{7.4}$$

with $\phi_{N+1} \equiv \phi_1$. The phase locking solutions of (7.2) are the equilibrium points of (7.4), hence each phase locking solution satisfies the set of equations

$$(\phi_i - \phi_{i+1})(\phi_i - \pi + \phi_{i+1}) = 0, \quad \forall i \in \mathcal{N}. \tag{7.5}$$

Every combination of either the first factor or the second factor equal to zero in each of these equations corresponds to a phase locking solution. Suppose that one of the phase differences assumes the value $\alpha \in S^1$. From (7.5) it follows that the other phase differences assume the values α or $\pi - \alpha$. Assume there are m phase differences equal to α present. In a phase locking solution the phase differences ϕ_i have to add up to an integer multiple of 2π:

$$\sum_{j=1}^{N} \phi_j = 2\pi k, \quad k \in T, \tag{7.6}$$

with $T = \{0, \ldots, N-1\}$. It follows that

$$m\alpha + (N-m)(\pi - \alpha) = 2\pi k, \quad k \in T.$$

□

A solution (7.3) with $\alpha = 0$ and $m \neq N$ is called *an elementary solution*. The solution $\phi = [0 \ \cdots \ 0]^T$ is called the *synchronized solution*. The solutions

$$\phi = [\frac{2\pi k}{N} \ \cdots \ \frac{2\pi k}{N}]^T, \quad k \in \{1, \ldots, N-1\}, \tag{7.7}$$

are the so-called *travelling wave solutions*.

Because of (7.2), constant phase differences for all i imply the constancy of the phase velocities, $\dot{\theta}_i = \Omega_i$. But on the other hand, $\theta_{i+1} - \theta_i = a_i = const$ implies also $\dot{\theta}_i = \dot{\theta}_{i+1}$, and therefore $\dot{\theta}_i = \Omega,\ \forall i \in \mathcal{N}$. The constant Ω is called *the group velocity* of the phase locking solution.

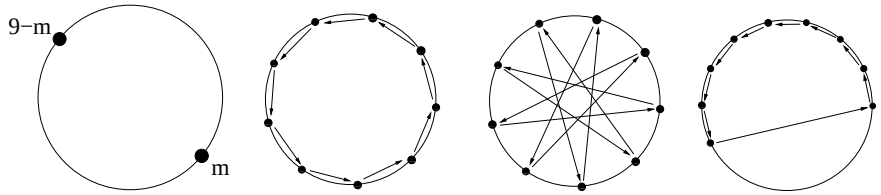

(a) Elementary solution (b) Travelling wave solutions (c) Other type of solution

Figure 7.1: Different types of phase locking solutions for a ring of 9 identical oscillators.

From (7.2), the group velocity at which a phase locked travelling wave group moves is $\Omega = K\sin((2\pi k)/N)$. Stronger coupled oscillators results in a faster motion, in case of a travelling wave. If the oscillators synchronize, the group velocity Ω is zero. This behavior is completely different from the case in which the oscillators are bidirectionally coupled, since in the bidirectional case Ω is independent of K for all phase locking solutions. Remark that in the original coordinates, i.e. before the substitution $\theta_i \to \theta_i + \omega t$ at the beginning of this section, the group velocity is $\Omega + \omega$.

Figure 7.1 shows different types of possible phase locking solutions in a ring of 9 identical oscillators. Each figure is a snapshot taken of the population moving along the circle at the group velocity Ω. The figure on the left hand side shows all elementary solutions $(m = 1, \ldots, 8)$. In this figure it is indicated how many oscillators are represented by each dot on the circle. The middle figure shows two travelling wave solutions. Each dot corresponds to one oscillator. The arrows represent the interconnections between the oscillators. Figure 7.1 (c) is an example of a solution not belonging to the previous two classes.

7.2.2 Nonidentical Oscillators

In this section the dynamics described by (7.1) is investigated. It turns out that in this case there exist phase locking solutions as well. Assume that $\dot{\theta}_i = \Omega$, $\forall i \in \mathcal{N}$. The phase differences $\phi_i := \theta_i - \theta_{i-1}$ have to satisfy

$$\omega_i + K\sin\phi_{i+1} = \Omega, \quad i \in \mathcal{N}, \tag{7.8}$$

or equivalently,

$$\phi_{i+1} = g_i\left(\frac{\Omega - \omega_i}{K}\right), \quad i \in \mathcal{N}, \tag{7.9}$$

where each function g_i is one of the functions f_0 and f_1, defined as

$$\begin{aligned} &f_0 : [-1,1] \to [-\pi/2, \pi/2] : t \mapsto \arcsin(t), \\ &f_1 : (-1,1) \to (\pi/2, 3\pi/2) : t \mapsto \pi - \arcsin(t). \end{aligned} \tag{7.10}$$

Since the phase differences ϕ_i have to add up to an integer multiple of 2π in a phase locking solution, it holds that

$$g_1\left(\frac{\Omega-\omega_1}{K}\right)+g_2\left(\frac{\Omega-\omega_2}{K}\right)+\ldots+g_N\left(\frac{\Omega-\omega_N}{K}\right)=2\pi k,\quad k\in\mathbb{Z}. \tag{7.11}$$

with every g_i, $i\in\mathcal{N}$, replaced by f_0 or f_1, leading in general to 2^N equations for a fixed value of k. (If there are ω_i present for which $(\Omega-\omega_i)/K=1$, then $g_i=f_0$ for these frequencies. The total number of equations corresponding to this configuration is less than 2^N.) Expression (7.11) is called *the consistency condition on the group velocity*. Each phase locking solution $[\phi_1\ \cdots\ \phi_N]^T$ satisfies exactly one of these equations, since the images of f_0 and f_1 are disjunct. Each equation of (7.11) *separately* yields a number of solutions of the group velocity Ω. However, how many solutions correspond to each equation is not known. It is also possible that an equation does not possess any solution at all.

Computing all phase locking solutions is done by investigating the consistency condition. Let the coupling strength assume some value K_1 and let $k=0$. Then (7.11) is a set of 2^N equations with Ω the remaining unknown. For each equation separately the corresponding solutions Ω are determined. The solutions Ω computed in this way are the group velocities of those phase locking solutions with phase differences adding up to zero (since $k=0$) and corresponding with a coupling strength K_1. Once a value of Ω is obtained from (7.11), the values of the corresponding phase differences can be determined via (7.9). This procedure is then repeated for all $k\in\mathbb{Z}$, resulting in all solutions of Ω corresponding to the coupling strength K_1. Performing the above procedure for every K results in a diagram as shown in Figure 7.2 (b).

Notice that the set of k-values for which the computation has to be done can be reduced to a subset of $\mathbb{Z}$. Each phase difference ϕ_i assumes a value in $[-\pi/2,3\pi/2)$, according to (7.10). The left hand side of (7.11) then assumes a value in $[-\pi N/2,3\pi N/2)$. Hence, equations of (7.11) with k not belonging to $\{l\in\mathbb{Z}:(-\pi N)/2\leq 2\pi l<(3\pi N)/2\}$ do not yield phase locking solutions.

In Fig. 7.2, $\Omega(K)$ is plotted for two ring configurations. On the left hand side the group velocity of a ring with three identical oscillators with $\omega=0$ is displayed. The group velocity is calculated using (7.11) and the resulting branches are $\Omega(K)=0$, $\Omega(K)=K\sin(\pi/3)$ and $\Omega(K)=-K\sin(\pi/3)$. The six corresponding solutions are displayed in Figure 7.3 and Figure 7.4. The phase differences ϕ_i of each of these solutions are independent of the coupling strength.

In Figure 7.2 (b) the case of a ring of 3 oscillators with $\omega_1=0.1$, $\omega_2=0.2$, and $\omega_3=-0.3$ is shown. The shaded area in this picture is the set of points (K,Ω) that do not satisfy $K\geq|\Omega-\omega_i|,\forall i\in\mathcal{N}$. For these points,

$$\exists i\in\mathcal{N}:|\sin\phi_{i+1}|=\frac{|\Omega-\omega_i|}{K}>1,$$

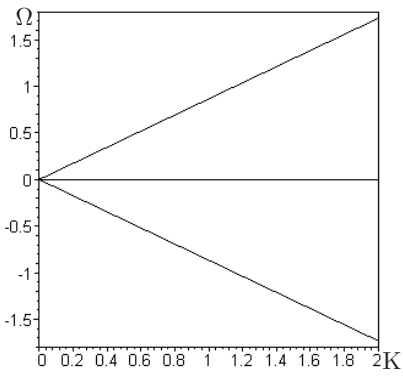

(a) The group velocity $\Omega(K)$ of all phase locking solutions of the ring of three identical oscillators with $\omega = 0$.

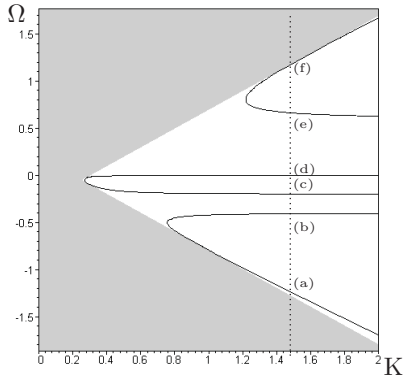

(b) The group velocity $\Omega(K)$ of all phase locking solutions of the ring of three oscillators with $\omega_1 = 0.1, \omega_2 = 0.2, \omega_3 = -0.3$.

Figure 7.2: The group velocity $\Omega(K)$ of 2 ring configurations of 3 oscillators. (The symbols $(a) - (f)$ in figure (b) refer to Figure 7.5).

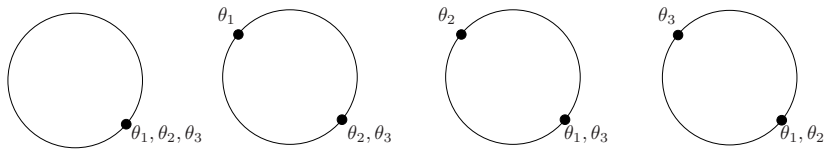

Figure 7.3: All phase locking solutions corresponding to the central branch (with group velocity zero) of Figure 7.2 (a).

yielding a contradiction. Hence the shaded area is the area where no phase locking solutions are possible. The oscillator configuration of Figure 7.2 (b) has the following properties. For small K no phase locking solutions exist. When the coupling strength exceeds some threshold value K_T, phase locking solutions arise. For sufficiently large K, six solutions $\Omega(K)$ exist. Computation of the corresponding phase locking solutions via (7.9) reveals that there corresponds only one phase locking solution to each solution $\Omega(K)$. Three of the solutions $\Omega(K)$, corresponding to branches (a), (d) and (f), converge in the limit $K \to \infty$ to the solutions of Figure 7.2 (a). The remaining three branches are solutions of the following three equations of (7.11):

$$\begin{aligned}
\arcsin((\Omega-\omega_1)/K) - \arcsin((\Omega-\omega_2)/K) - \arcsin((\Omega-\omega_3)/K) &= 0,\\
-\arcsin((\Omega-\omega_1)/K) + \arcsin((\Omega-\omega_2)/K) - \arcsin((\Omega-\omega_3)/K) &= 0,\\
-\arcsin((\Omega-\omega_1)/K) - \arcsin((\Omega-\omega_2)/K) + \arcsin((\Omega-\omega_3)/K) &= 0.
\end{aligned} \tag{7.12}$$

The limit value of these branches for $K \to \infty$ is analytically determined as

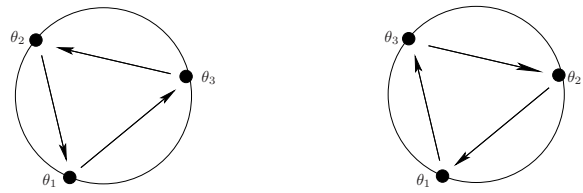

Figure 7.4: On the left: the phase locking solution corresponding to the branch $\Omega(K) = -K\sin(\pi/3)$ of Figure 7.2 (a). On the right: the phase locking solution corresponding to the branch $\Omega(K) = K\sin(\pi/3)$.

follows. Assume that the solution Ω is bounded. Then for $K \to \infty$, the arcsine-function can be approximated by its argument and (7.12) changes into

$$\begin{aligned}(\Omega-\omega_1)/K - (\Omega-\omega_2)/K - (\Omega-\omega_3)/K &= 0,\\ -(\Omega-\omega_1)/K + (\Omega-\omega_2)/K - (\Omega-\omega_3)/K &= 0,\\ -(\Omega-\omega_1)/K - (\Omega-\omega_2)/K + (\Omega-\omega_3)/K &= 0,\end{aligned}$$

resulting in three limit values for Ω: $-\omega_1+\omega_2+\omega_3$, $-\omega_1-\omega_2+\omega_3$ and $\omega_1+\omega_2-\omega_3$, which can be observed in Figure 7.2.

For $K = 1.5$ the six phase locking solutions corresponding to Figure 7.2 (b) are depicted in Figure 7.5. The solutions are ordered by increasing group velocity Ω.

To conclude this section we give a proof of the existence of phase locking in the unidirectional ring of nonidentical oscillator. Consider the consistency conditions

$$\sum_{j=1}^{N} \arcsin\left(\frac{\Omega-\omega_j}{K}\right) = 2\pi l, \quad l \in \{0,\dots,\lfloor N/4\rfloor\}, \tag{7.13}$$

where $\lfloor . \rfloor : \mathbb{R} \to \mathbb{Z}$ maps a real number r to the largest integer number smaller than r.

It will now be proven that for sufficiently large values of the coupling strength each of the above equations yields a phase locking solution represented by $\Omega(K)$.

Theorem 31. *Let ω_{max} and ω_{min} denote the maximum and the minimum of the set $\{\omega_1,\dots,\omega_N\}$, respectively. If*

$$K > \frac{\omega_{max}-\omega_{min}}{1-\sin(\frac{2\pi l}{N})}, \quad l = 0,\dots,\lfloor N/4\rfloor, \tag{7.14}$$

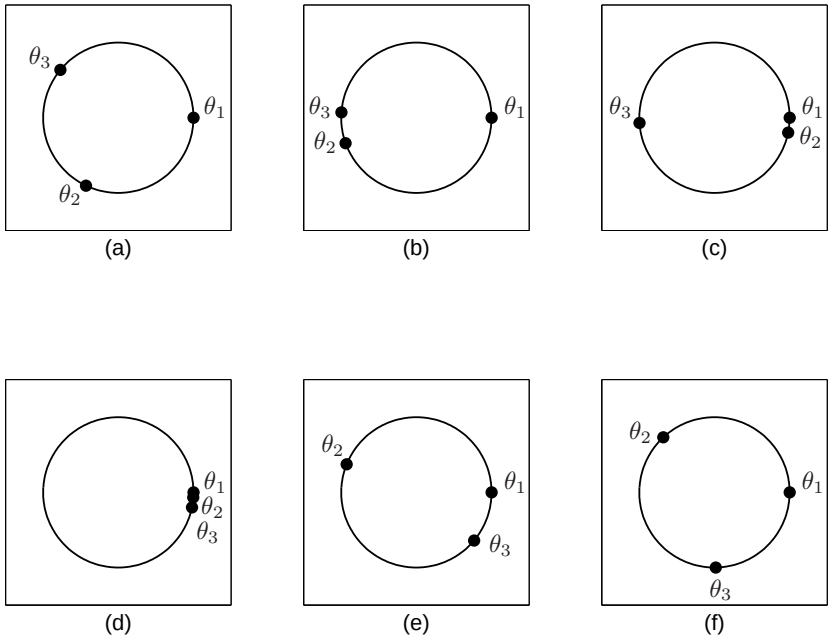

Figure 7.5: All phase locking solutions of the ring configuration of Figure 7.2 (b) with coupling strength $K = 1.5$, ordered by increasing group velocity Ω.

then the corresponding consistency condition

$$\sum_{j=1}^{N} \arcsin\left(\frac{\Omega-\omega_j}{K}\right) = 2\pi l, \tag{7.15}$$

yields a solution $\Omega(K) \in \mathbb{R}$.

Proof. Define the functions

$$F_j : \mathbb{R} \to \mathbb{R} : \Omega \mapsto \arcsin\left(\frac{\Omega-\omega_j}{K}\right),\ j \in \mathcal{N}, \tag{7.16}$$

with K considered as a parameter. Define $F_{\max}$ and $F_{\min}$ as those functions F_j for which ω_j is equal to $\omega_{\max}$ and $\omega_{\min}$ respectively.

Since $\mathrm{dom}(\sum_{j=1}^{N} F_j) = \cap_{j=1}^{N} \mathrm{dom}(F_j)$ and $\mathrm{dom}(F_j) = [\omega_j - K, \omega_j + K]$, it holds that

$$\mathrm{dom}(\sum_{j=1}^{N} F_j) = [\omega_{\max} - K, \omega_{\min} + K] \Leftrightarrow K \geq \frac{\omega_{\max} - \omega_{\min}}{2}.$$

The function $\sum_{j=1}^{N} F_j$ is increasing on its domain because each F_j is increasing. If K satisfies (7.14), then

$$\omega_{\min} + K > \omega_{\max} + K\sin(\frac{2\pi l}{N}),$$

implying

$$\omega_j + K > \omega_{\max} + K\sin(\frac{2\pi l}{N}), \quad \forall j \in \mathcal{N}. \tag{7.17}$$

Similarly,

$$\omega_{\max} - K < \omega_{\min} - K\sin(\frac{2\pi l}{N}),$$

implying

$$\omega_j - K < \omega_{\min} - K\sin(\frac{2\pi l}{N}), \quad \forall j \in \mathcal{N}. \tag{7.18}$$

From the definition (7.16),

$$F_j(\Omega) \geq F_{\max}(\Omega), \quad \forall \Omega \in [\omega_{\max} - K, \omega_j + K], \tag{7.19}$$
$$F_j(\Omega) \leq F_{\min}(\Omega), \quad \forall \Omega \in [\omega_j - K, \omega_{\min} + K]. \tag{7.20}$$

Equation (7.19) combined with (7.17) yields

$$F_j(\Omega) > F_j\left(\omega_{\max} + K\sin(\frac{2\pi l}{N})\right) \geq F_{\max}\left(\omega_{\max} + K\sin(\frac{2\pi l}{N})\right) = \frac{2\pi l}{N}, \tag{7.21}$$

for all $\Omega \in (\omega_{\max} + K\sin(\frac{2\pi l}{N}), \omega_{\min} + K]$, resulting in

$$\sum_{j=1}^{N} F_j(\Omega) > 2\pi l, \forall \Omega \in (\omega_{\max} + K\sin(\frac{2\pi l}{N}), \omega_{\min} + K]. \tag{7.22}$$

Similarly, (7.20) combined with (7.18) yields

$$\sum_{j=1}^{N} F_j(\Omega) < -2\pi l, \quad \forall \Omega \in [\omega_{\max} - K, \omega_{\min} - K\sin(\frac{2\pi l}{N})). \tag{7.23}$$

Because of (7.22) and (7.23) and since $\sum_{j=1}^{N} F_j$ is continuous and increasing, there exists exactly one value of Ω belonging to $(\omega_{\min} - K\sin(\frac{2\pi l}{N}), \omega_{\max} + K\sin(\frac{2\pi l}{N}))$ such that $\sum_{j=1}^{N} F_j(\Omega) = 2\pi l$. This concludes the proof. □

7.3 Stability Properties

7.3.1 Linearization

As explained in Section 6.3.1, every phase locking solution of (7.1) can be transformed into a curve of equilibrium points by applying the appropriate change of coordinates: if the group velocity of the phase locking solution under consideration is Ω, then the new coordinates $\tilde{\theta}$ are defined by $\tilde{\theta}_i := \theta_i - \Omega t$. Since only phase differences govern the dynamics, solutions are unique up to a uniform phase shift. As a consequence, the linearization around each equilibrium point will contain at least one zero-eigenvalue. This zero eigenvalue has no influence on the stability properties. However, when the linearization matrix possesses multiple zero-eigenvalues, and no eigenvalues with positive real part are present, nothing can be concluded about the local stability of the equilibrium under consideration.

The linearization about a phase locking solution is the matrix $J \in \mathbb{R}^{N\times N}$, with the phase differences ϕ_i assuming values corresponding to that phase locking solution:

$$J = K\begin{bmatrix} -\cos\phi_2 & \cos\phi_2 & 0 & \cdots & 0 \\ 0 & -\cos\phi_3 & \cos\phi_3 & 0 & 0 \\ \vdots & \ddots & \ddots & \ddots & \vdots \\ 0 & & 0 & -\cos\phi_N & \cos\phi_N \\ \cos\phi_1 & 0 & \cdots & 0 & -\cos\phi_1 \end{bmatrix}. \tag{7.24}$$

The characteristic polynomial of the linearization is

$$\prod_{j=1}^{N}(\lambda + \cos\phi_j) - \prod_{j=1}^{N}\cos\phi_j, \tag{7.25}$$

which clearly is invariant under permutations of the phase differences.

Stability of the phase locking solutions is determined by applying a novel extension of Gershgorin's theorem. This extension together with the original theorem can be found in Appendix A. Calculation of the Gershgorin disks reveals that each disk lies in a closed half plane and contains the origin. The centers of these disks are located on the real axis and given by the diagonal elements of J.

Phase locking solutions with phase differences equal to $\pi/2$ or $3\pi/2$ are not considered in this and the next section, so that all cosine-elements in the linearization matrix are different from zero.

7.3.2 Several Theorems on Stability

Theorem 32. *A phase locking solution defined by phase differences ϕ_i belonging to $(-\pi/2, \pi/2)$ is asymptotically stable.*

Proof. If all $\phi_j \in (-\pi/2, \pi/2)$, i.e. if all diagonal elements of J are smaller than zero, all Gershgorin disks lie in the closed left half plane, implying that all eigenvalues of J lie in the closed left half plane as well.

The zero order term of the characteristic polynomial (7.25) is zero, implying that at least one eigenvalue is zero. The coefficient corresponding to the first order term is

$$\sum_{j=1}^{N} \prod_{k=1,\, k\neq j}^{N} \cos\phi_k. \tag{7.26}$$

If $\phi_j \in (-\pi/2, \pi/2)$, $\forall j \in \mathcal{N}$, this coefficient is *strictly* positive. This implies that exactly one eigenvalue is zero and the remaining eigenvalues are located in the open left half plane. Local asymptotic stability of the corresponding phase locking solution follows. □

Theorem 33. *A phase locking solution with two or more phase differences ϕ_i inside $(\pi/2, 3\pi/2)$ is unstable if $\sum_{j=1}^{N} \prod_{k=1,\, k\neq j}^{N} \cos\phi_k \neq 0$.*

Proof. If there exist two or more phase differences belonging to $(\pi/2, 3\pi/2)$ then two or more Gershgorin disks lie in the closed right half plane. Because of Theorem 51, two or more eigenvalues are located in the closed right half plane. If $\sum_{j=1}^{N} \prod_{k=1,\, k\neq j}^{N} \cos\phi_k \neq 0$, then exactly one eigenvalue is zero, which implies that one or more eigenvalues have a strictly positive real part. The corresponding phase locking solution is locally unstable. □

Theorem 34. *If the ring consists of identical oscillators, a phase locking solution with two or more phase differences ϕ_i inside $(\pi/2, 3\pi/2)$ is unstable.*

Proof. In the identical oscillator case a phase locking solution is of the form

$$\phi = [\underbrace{\alpha \ \cdots \ \alpha}_{m} \ \underbrace{\pi - \alpha \ \cdots \ \pi - \alpha}_{N-m}]^T,$$

or a permutation thereof, with

$$m\alpha + (N-m)(\pi - \alpha) = 2\pi k, \ k \in T, \ m \in \mathcal{N}. \tag{7.27}$$

If $m \neq N/2$, it is easy to derive that $\sum_{j=1}^{N} 1/\cos\phi_j \neq 0$. Since

$$\left(\prod_{i=1}^{N} \cos\phi_j\right)\left(\sum_{j=1}^{N} \frac{1}{\cos\phi_j}\right) = \sum_{j=1}^{N} \prod_{k=1,\, k\neq j}^{N} \cos\phi_k,$$

Theorem 33 is applicable, yielding instability.

If $m = N/2$, then $\sum_{j=1}^{N} 1/\cos\phi_j = 0$. The linearization possesses at least two zero-eigenvalues. Since $m = N/2$, it is possible to perform a permutation of the phase differences such that the linearization matrix J transforms into $-J$. It has been shown in Section 7.3 that the eigenvalues of the linearization are invariant under such a permutation, implying that the set of eigenvalues of J is equal to the set of eigenvalues of $-J$. Hence, if λ is an eigenvalue of J, then so is $-\lambda$. The matrix J has some non-zero eigenvalues, since it is different from the null matrix. Gershgorin's theorem shows that these non-zero eigenvalues are not located on the imaginary axis. From this it can be concluded that at least one of the eigenvalues of J has a strictly positive real part. This proves the instability of the corresponding phase locking solution. □

Theorem 35. *If $\sum_{j=1}^{N} \prod_{k=1,\, k\neq j}^{N} \cos\phi_k < 0$, the phase locking solution with exactly one phase difference ϕ_i belonging to $(\pi/2, 3\pi/2)$ is locally unstable.*
If $\sum_{j=1}^{N} \prod_{k=1,\, k\neq j}^{N} \cos\phi_k > 0$, such a solution is stable.

Proof. If a phase locking solution possesses exactly one phase difference ϕ_i belonging to $(\pi/2, 3\pi/2)$, exactly one Gershgorin disk lies in the closed right half plane. At most one eigenvalue is positive. It can be shown that the coefficient (7.26) belonging to the first order term of the characteristic polynomial is equal to

$$(-1)^{N-1} \prod_{i=1}^{N-1} \lambda_i,$$

where λ_i are the eigenvalues of J from which one zero-eigenvalue, indicated by λ_N, is excluded. Now, with $\mathcal{M} := \mathcal{N} \setminus \{N\}$,

$$\Re e(\lambda_i) < 0, \ \forall i \in \mathcal{M} \Rightarrow (-1)^{N-1} \prod_{i=1}^{N-1} \lambda_i > 0,$$

$$\Re e(\lambda_i) \neq 0,\ \forall i \in \mathcal{M} \text{ and } \exists! \lambda_i\ \in \mathcal{M}\ :\ \Re e(\lambda_i) > 0 \Rightarrow (-1)^{N-1} \prod_{i=1}^{N-1} \lambda_i < 0.$$

Hence, the linearization is unstable if

$$\sum_{j=1}^{N} \prod_{k=1,\, k\neq j}^{N} \cos\phi_k < 0,$$

and stable if

$$\sum_{j=1}^{N} \prod_{k=1,\, k\neq j}^{N} \cos\phi_k > 0.$$

□

Theorem 36. *If all oscillators are identical then each phase locking solution with one phase difference ϕ_i belonging to $(\pi/2, 3\pi/2)$ is locally unstable.*

Proof. From Theorem 30 it follows that phase locking solutions with the above property are determined by a permutation of $\phi = [\alpha\ \cdots\ \alpha\ \ (\pi - \alpha)]^T$, with $\alpha \in (-\pi/2, \pi/2)$ satisfying (7.3). The coefficient of the first order term of the characteristic polynomial (7.26) then is $(2 - N)\cos^{N-1}\alpha$. For $N > 2$ this is strictly negative since $\cos\alpha > 0$. According to Theorem 35 the corresponding phase locking solution is unstable. □

Simulations show that for some, but not all, configurations of natural frequencies, there exist *stable* phase locking solutions belonging to the class treated in Theorem 35. This is surprising, because it implies a qualitative difference between the identical and the nonidentical oscillator case. Figure 7.6 shows a simulation of all stable phase locking solutions of a unidirectionally coupled ring consisting of seven oscillators. The natural frequencies of the oscillators are all zero, except $\omega_7 = -50$, and the coupling strength is 39.5. The solution on the left hand side belongs to the class investigated in Theorem 32, whereas the (stable) solution on the right hand side is considered in Theorem 35. To which of the two solutions the state of the system converges, depends on the initial conditions.

More information on the class of stable solutions of Theorem 35 is given in Figure 7.7, which is a close-up near the onset of phase locking of the right hand side figure of Figure 7.2. The figure displays a saddle-node bifurcation of a three-oscillator network with the coupling strength as parameter. At $K = 0.2617$ phase locking solutions come into existence. The upper branch is stable; the lower branch is unstable. The curve on the figure is split into three parts according to the location of the phase differences on the unit circle. Part (2) has all phase differences situated in $(-\frac{\pi}{2}, \frac{\pi}{2})$; its stability follows from Theorem 32. Part (3) has 2 phase differences in $(\frac{\pi}{2}, \frac{3\pi}{2})$ which implies its instability via Theorem 33. The interesting part of the curve is part (1).

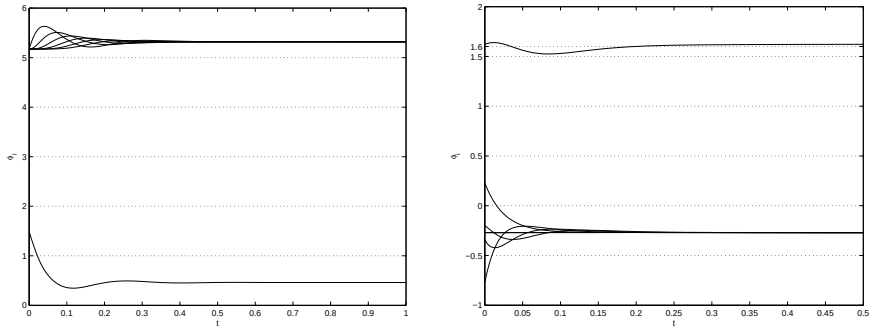

(a) no phase differences $\in (\pi/2, 3\pi/2)$ (b) one phase difference $\in (\pi/2, 3\pi/2)$

Figure 7.6: The evolution in time of the 7 phase differences $\phi_i := \theta_i - \theta_{i-1}$, $i = 1, \ldots 7$, of the ring consisting of 7 oscillators with the following properties: the coupling strength is $K = 39.5$ and the vector of natural frequencies is $[0\,0\,0\,0\,0\,0\,-50]^T$.

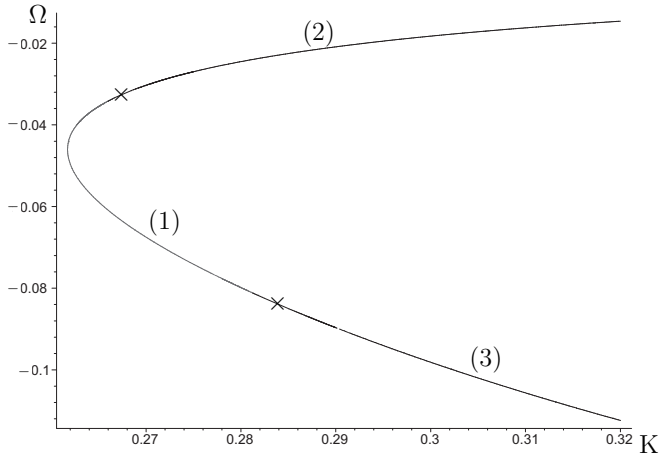

Figure 7.7: Detail from Figure 7.2 (b) at the onset of phase locking.

The phase locking solutions which this part represents belong to the class with exactly one phase difference in $(\frac{\pi}{2}, \frac{3\pi}{2})$. From bifurcation theory we know that the upper branch of (1) is stable and its lower branch unstable. This confirms our result that stability cannot be determined from the location of the phase differences with respect to $\frac{\pi}{2}$ and $\frac{3\pi}{2}$ alone. Computations confirm that the upper branch of (1) satisfies $\sum_{j=1}^{N} \prod_{k=1,\, k\neq j}^{N} \cos\phi_k > 0$, and similarly, that the lower branch satisfies $\sum_{j=1}^{N} \prod_{k=1,\, k\neq j}^{N} \cos\phi_k < 0$.

The above stability theorems are summarized in Table 7.1.

Table 7.1: Summary of the stability theorems.

Phase locking solution with	Stability
no phase differences $\in [\pi/2, 3\pi/2]$	stable
one phase difference $\in (\pi/2, 3\pi/2)$ and $\sum_{j=1}^{N} \prod_{k=1,\, k\neq j}^{N} \cos\phi_k > 0$	stable
one phase difference $\in (\pi/2, 3\pi/2)$ and $\sum_{j=1}^{N} \prod_{k=1,\, k\neq j}^{N} \cos\phi_k < 0$	unstable
two or more phase differences $\in (\pi/2, 3\pi/2)$; $\sum_{j=1}^{N} \prod_{k=1,\, k\neq j}^{N} \cos\phi_k \neq 0$	unstable
one or more phase differences $\in (\pi/2, 3\pi/2)$ and identical oscillators	unstable

Some remarks:

1. From Theorem 32, Theorem 34 and Theorem 36 it follows that a travelling wave solution $[\frac{2\pi k}{N} \ \cdots \ \frac{2\pi k}{N}]^T$ is stable if and only if $k < \frac{N}{4}$.

2. The above stability analysis is applicable in the more general case of non-uniform coupling:

$$\dot{\theta}_i = \omega_i + K_i \sin(\theta_{i+1} - \theta_i),$$

   with $K_i > 0$. The consistency condition (7.11) changes into

$$\sum_{j=1}^{N} g_j \left(\frac{\Omega - \omega_j}{K_j} \right) = 2\pi k,$$

   but the stability criteria remain unaltered.

3. The approach to the stability analysis by investigation of the linearization prohibits the study of a number of phase locking solutions. If the phase differences of a phase locking solution satisfy $\sum_{j=1}^{N} \prod_{k=1,\, k\neq j}^{N} \cos\phi_k = 0$, the linearization possesses multiple zero-eigenvalues. In most cases the presence of positive eigenvalues cannot be concluded. Local stability cannot be analyzed in this way.

   Furthermore, we assumed that the phase locking solutions do not possess phase differences equal to $\pi/2$ or $3\pi/2$. This assumption excludes all phase locking solutions of which the rank of the linearization is smaller than $N - 1$. These solutions have multiple zero-eigenvalues,

too. For instance, the linearization of the travelling wave solution $\phi = [\frac{\pi}{2}\ \frac{\pi}{2}\ \frac{\pi}{2}\ \frac{\pi}{2}]^T$ of the identical four-oscillator ring is a matrix with exclusively zero-entries, yielding no information whatsoever about stability. This results from the specific form of the coupling, namely sine-coupling. Instead of pursuing the stability of those remaining solutions, we generalize the coupling function in the next section; as a bonus we are able to deal with solutions of the type $\phi = [\frac{\pi}{2}\ \frac{\pi}{2}\ \frac{\pi}{2}\ \frac{\pi}{2}]^T$.

7.4 Generalized Coupling

For the unidirectionally coupled ring it is possible to generalize the study from sine-coupling to a broader class of coupling functions. The properties of the coupling functions $H : \mathbb{R} \to \mathbb{R};\ \phi \mapsto H(\phi)$ we consider are the following. The function H is continuous, 2π-periodic and odd, and has exactly one maximum belonging to $(0, \pi)$. An example is shown in Fig. 7.8. Phase

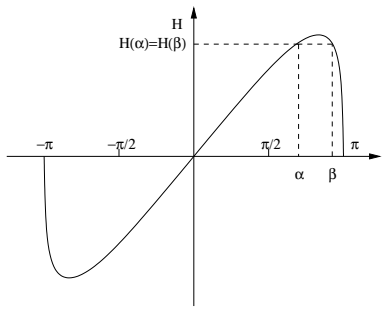

Figure 7.8: Generalized coupling function

locking solutions are obtained in a similar way as described in Section 7.2.1. Consider a network with identical oscillators:

$$\dot{\theta}_i = KH(\theta_{i+1} - \theta_i), \quad i \in \mathcal{N}. \tag{7.28}$$

Theorem 37. *Consider all triples* $(\alpha, \beta, m),\ m \in \mathcal{N}, \alpha, \beta \in S^1,\ (\alpha \neq \beta)$*, satisfying*

$$\begin{aligned} m\alpha + (N-m)\beta &= 2\pi k,\ k \in T, \\ H(\alpha) &= H(\beta). \end{aligned}$$

Assign to each such triple (α, β, m) *the vector*

$$[\underbrace{\alpha\ \cdots\ \alpha}_{m}\ \underbrace{\beta\ \cdots\ \beta}_{N-m}]^T,$$

Every vector $\phi = [\phi_1\ \cdots\ \phi_N]^T$ *that is a permutation of such a vector corresponds to a phase locking solution of (7.28).*

For $m = N$ the travelling wave solutions are retrieved, identical to the travelling wave solutions of (7.2). Their stability properties, however, may differ from the case with sine-coupling, as follows from the theorems below. With $K > 0$ and $\gamma \in (0, \pi) : \frac{\mathrm{d}H}{\mathrm{d}\phi}(\gamma) = 0$, the results in Table 7.2 can easily be proven. The proofs are similar to those of Theorem 32 to Theorem 35. In Table 7.2 we introduced the notation $H'(\phi) := \frac{\mathrm{d}H}{\mathrm{d}\phi}(\phi)$.

Table 7.2: Stability results for generalized coupling.

Phase locking solution with	Stability
all phase differences $\in (-\gamma, \gamma)$	stable
one phase difference $\in (\gamma, 2\pi - \gamma)$ and $\sum_{j=1}^{N} \prod_{k=1,\, k\neq j}^{N} H'(\phi_k) > 0$,	stable
one phase difference $\in (\gamma, 2\pi - \gamma)$ and $\sum_{j=1}^{N} \prod_{k=1,\, k\neq j}^{N} H'(\phi_k) < 0$,	unstable
two or more phase differences $\in (\gamma, 2\pi - \gamma)$; $\sum_{j=1}^{N} \prod_{k=1,\, k\neq j}^{N} H'(\phi_k) \neq 0$	unstable

7.5 N Robots in Cyclic Pursuit

In [57] cyclic pursuit of mobile robots in the plane is analyzed. Each agent is represented as a kinematic unicycle with nonlinear dynamics. The control strategy is such that agent i tries to reduce its distance with agent $i + 1$ to zero. This is done by a proportional feedback of the difference in heading, i.e. orientation, of both vehicles:

$$\begin{bmatrix} \dot{x}_i \\ \dot{y}_i \\ \dot{\theta}_i \end{bmatrix} = \begin{bmatrix} \cos\theta_i & 0 \\ \sin\theta_i & 0 \\ 0 & 1 \end{bmatrix} \begin{bmatrix} s \\ k(\theta_{i+1} - \theta_i) \end{bmatrix},$$

where (x_i, y_i) is the position of the i-th robot in the plane, θ_i is its heading, and s and k are positive real constants. In the resulting equilibrium motion all agents traverse the same circle in one direction. The motion in the physical plane clearly reflects the unidirectional interconnection structure. At each time instant the robots are located on the vertices of a regular polygon. The polygons are characterized by a parameter d as follows.

Definition 36. *Let N and d be positive integers so that $p := \frac{N}{d} > 1$ is a rational number. Let R be the positive rotation in the plane, about the origin, through an angle $\frac{2\pi}{p}$ and let $z_1 \neq 0$ be a point in the plane. Then the points $z_{i+1} = Rz_i$, $\forall i \in \mathcal{N} \setminus \{1\}$ and edges $e_i = z_{i+1} - z_i$, $\forall i \in \mathcal{N}$ define a generalized regular polygon, denoted $\{p\}$.*

The equilibrium formations are polygons $\{N/d\}$ with radius $\rho = \frac{sN}{k\pi d}$. The regular polygons can be identified with the travelling wave solutions of the identical oscillator ring described in the present chapter. Since the phase differences $\theta_{i+1} - \theta_i$ of a travelling wave solution are identical, the

phases of the oscillators form a polygon inscribed in the unit circle (see Figure 7.1 (b)). We have proven that a travelling wave solution $[\frac{2\pi k}{N} \ \cdots \ \frac{2\pi k}{N}]^T$ is locally asymptotically stable if and only if $k < \frac{N}{4}$. The question arises if the generalized regular polygons representing equilibrium formations of the interacting mobile robots satisfy a similar stability property. The answer is formulated in Theorem 7 of [57]:

Theorem 38. *A given N/d equilibrium polygon is locally asymptotically stable if and only if $0 < d \leq \frac{N}{2}$ and*

$$\cos(2\pi\frac{d-1}{N}) > \frac{2\tan(\frac{\pi d}{N})}{\frac{\pi d}{N}[1+\frac{\pi d}{N}\tan(\frac{\pi d}{N})]} - 1. \tag{7.29}$$

The integer parameter d of the polygons plays the same role as the parameter k of the travelling wave solutions in the ring of oscillators. Both parameters possess the same qualitative property that above some critical value the corresponding equilibrium solution is unstable. In the case of cyclic pursuit of agents the critical value is $\frac{N}{2}$ while in the case of oscillator rings it is $\frac{N}{4}$. The phase difference between the $i+1$-th and the i-th oscillator in a stable travelling wave solutions is at most $\frac{\pi}{2}$; the angle between the $i+1$-th and the i-th robot in a stable polygon formation is at most π. Both bounds are obtained by analyzing the location of the eigenvalues of the linearization around equilibrium.

In the case of the oscillator ring, $k < \frac{N}{4}$ is sufficient for a travelling wave solution to be stable whereas $d < \frac{N}{2}$ does not guarantee stability of the polygon in the cyclic pursuit strategy: the extra condition (7.29) is added. This condition does not allow for a direct interpretation on the level of the geometry of the equilibrium formation. It only guarantees that with $d < \frac{N}{2}$ all eigenvalues of the linearization have negative real part. We conclude that although the equilibrium solutions of both systems are similar, their stability properties are fundamentally different.

7.6 Conclusions

In this chapter we abandoned the all-to-all coupling of the Kuramoto model and replaced it by a unidirectional ring coupling. In Section 7.2.1 we have determined all phase locking solutions of a ring of identical oscillators explicitly. Phase locking solutions of nonidentical oscillators are determined implicitly. Similar to Chapter 6 rings of nonidentical oscillators have phase locking solutions for coupling strengths above a critical value, again denoted by K_T. We have determined all phase locking solutions. Contrary to the previous chapter they were not obtained through a consistency condition on the amplitude of the order parameter. We obtained a consistency condition on the velocity Ω of the phase locking solution, by using the trivial restriction

on the phase differences (7.6). Once the value of Ω was obtained, the corresponding phase differences could be readily calculated.

We performed a stability analysis such that all phase locking solutions were classified into classes, each with its own stability properties. The stability properties were obtained by means of a novel extension of Gershgorin's theorem. One class of stable solutions had the property that all phase differences between neighboring cells are contained in $(\frac{-\pi}{2}, \frac{\pi}{2})$. Contrary to intuition, a second class of stable solutions was established with exactly one of the phase differences contained in $(\frac{\pi}{2}, \frac{3\pi}{2})$. The stability analysis showed that several locally stable phase locking solutions can coexist in the state space of the system, in the case of identical as well as nonidentical oscillators. Recall that in the all-to-all coupled case there existed only one stable phase locking solution for $K > K_T$. For a ring of identical oscillators this coexistence was made explicit by proving the existence and stability of all travelling wave solutions (7.7) with $k < \frac{N}{4}$ together with the existence of the stable synchronized solution for all non-zero coupling strengths.

The chapter is concluded with a comparison of the oscillator ring to a cyclic pursuit strategy of mobile robots. The interconnection topologies of both systems are identical. The resulting formations of the interacting robots can be identified with the travelling wave solutions of the ring. Their stability properties, however, display qualitative differences.

Chapter 8

Antenna Arrays

8.1 Introduction

In this chapter we present an application of the unidirectional ring of oscillators analyzed in the previous chapter. The application consists of a group of interconnected antennas. Each antenna is driven by an electric oscillator. The antennas are interconnected on the level of the oscillators.

First the mathematical concept of an antenna is introduced. Then the dynamics of the interconnected oscillators steering an antenna array are constructed. Finally two applications are presented; the first illustrates how antenna arrays are used for beam scanning, the second shows how the unidirectional ring coupling can be used in antenna arrays.

8.2 Mathematical Description of Antenna Arrays

Consider a charge distribution $\rho(x, y, z, t) \in \mathbb{R}$ and a current density distribution $\mathbf{J}(x, y, z, t) \in \mathbb{R}^3$, $\forall t \in \mathbb{R}$, confined to a bounded region in $\mathbb{R}^3$. Using Maxwell's equations the corresponding electric field distribution $\mathbf{E}(x, y, z, t) \in \mathbb{R}^3$ and magnetic field distribution $\mathbf{B}(x, y, z, t) \in \mathbb{R}^3$ can be calculated for $[x\ y\ z\ t]^T \in \mathbb{R}^4$.

Definition 37. *The collection of sources $\rho(x, y, z, t)$ and $\mathbf{J}(x, y, z, t)$ is called a (transmitting) antenna.*

The goal of the antenna designer is to construct a charge and/or current density distribution (i.e. antenna) that produces a desired electric field distribution. In practice the desired electric field is strong in only one particular direction in order to meet the demands of long distance communications. Designing antennas with such articulated direction characteristics is possi-

ble in two ways: either the size of the antenna is very large, with a geometric structure adapted to the directivity demands, or an *array* of smaller antennas is constructed. Our focus is on the second option. Consider Figure 8.1 (a) depicting a linear antenna array: each black dot on the z-axis represents an antenna. The antennas are assumed to have rotational symmetry about the z-axis, rendering the entire system invariant with respect to φ. The figure shows a typical radiation pattern of the antenna array. A radiation pattern is a graphical depiction of the normalized magnitude of the electric field $\mathbf{E}(r, \theta, \varphi)$ on a sphere with fixed radius $r = R$, where it is assumed that R is much larger than the size of the antenna. Not to overload the pictures, the plots of the radiation patterns in Figure 8.1 are restricted to the (y, z)-plane. The *main beam* of a radiation pattern is the segment of the pattern with maximal field strength. The time variation of the charge and current density distribution of each antenna is taken harmonic:

$$\rho_i(x, y, z, t) = \Re e[\rho_i^0(x, y, z)e^{j(\omega_i t+\phi_i)}],$$
$$\mathbf{J}_i(x, y, z, t) = \Re e[\mathbf{J}_i^0(x, y, z)e^{j(\omega_i t+\phi_i)}],$$

with $i \in \mathcal{N}$. Each antenna is given the same frequency and amplitude: $\omega_i = \omega$, $\rho_i^0 \equiv \rho^0$, $\mathbf{J}_i^0 \equiv \mathbf{J}^0$, $\forall i \in \mathcal{N}$. The time variation is created by connecting each antenna to a *forced van der Pol oscillator* with resonance frequency ω (cfr. Section 8.3.1).

One of the main advantages of antenna arrays is that by changing the phases ϕ_i the radiation pattern can be adjusted in a suitable way, without any mechanical movement of the antenna. This is illustrated in Figure 8.1. In Figure 8.1 (a) the antennas are in phase (i.e. $\phi_i = \phi$, $\forall i \in \mathcal{N}$). the main beam of the radiation pattern is located at $\theta = \pi/2$. In Figure 8.1 (b) the constant phase difference between neighboring antennas is ϕ_0, resulting in a main beam at an angle θ_0 determined by

$$\theta_0 = \arccos\left(\frac{\phi_0\, c}{\omega\, d}\right),$$

with c the speed of light and d the distance between two neighboring antennas. In applications it is often desired to steer the direction of the main beam. This is called *beam steering* or *beam scanning*. Thus ϕ_0 can be used as a control parameter to steer the main beam. Varying ϕ_0 continuously in time results in a *scanning* beam.

A first way to control the phase difference ϕ_0 is by inserting a phase shifter between each antenna and the corresponding oscillator as illustrated in Figure 8.2 (a). A phase shifter is a device, the output of which is a phase shifted version of the input. The value of the phase shift that the device generates can be controlled by varying some parameter of the device.

A second method for controlling the phase difference ϕ_0 is based on the self-organizational properties of coupled oscillators (see Figure 8.2 (b)). The

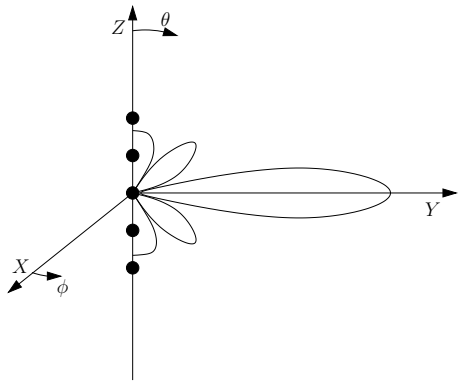

(a) Antenna array without phase shift ($\phi_0 = 0$)

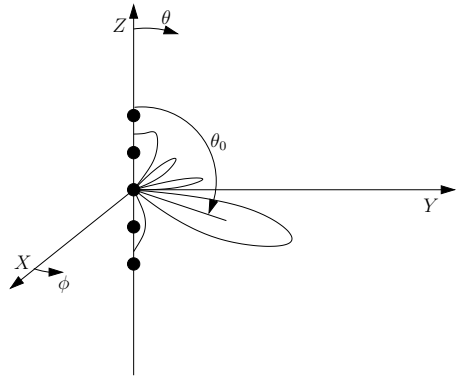

(b) Antenna array with phase shift ($\phi_0 \neq 0$ and $\theta_0 = \arccos\left(\frac{\phi_0\, c}{\omega\, d}\right)$)

Figure 8.1: Radiation patterns depend on the phase shift between the individual antennas.

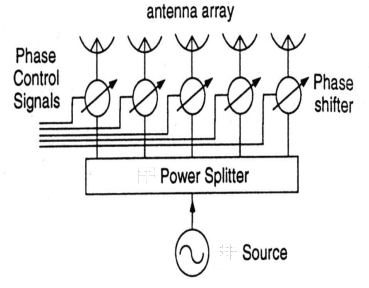

(a) Beam steering using phase shifters

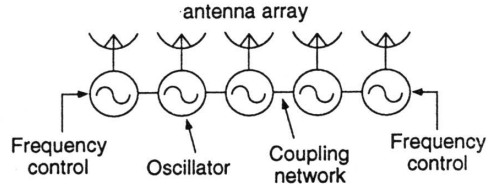

(b) Beam steering using coupled oscillators

Figure 8.2: Beam steering techniques (adopted from [51]).

van der Pol oscillators driving the antennas are interconnected electrically according to some network topology. If the oscillators had distinct frequencies ω_i when uncoupled, they now oscillate at a common frequency. The phase differences between the oscillators are constant and depend on the uncoupled frequencies ω_i and the strength of the coupling. The system dynamics governing this system are derived in the next section. In Section 8.4.1 the above beam scanning problem with coupled oscillators is revisited.

8.3 Systems Dynamics

In this section the system equations describing an ensemble of interinjection-locked oscillators are constructed. The approach of [84] is followed. Alternative approaches are described in [19, 47, 100, 101].

8.3.1 Modelling a Voltage Controlled Oscillator

A widely accepted circuit model for a microwave oscillator is given by an active device, modelled as a negative resistance (resp. conductance), which is embedded in a series (resp. parallel) resonant circuit. Such a circuit model is displayed in Figure 8.3 where the active device is represented as a negative conductance $-G_D(A) \in \mathbb{R}$, where A represents the amplitude of the voltage across the active device. When $i = 0$, the voltage v of the oscillator has

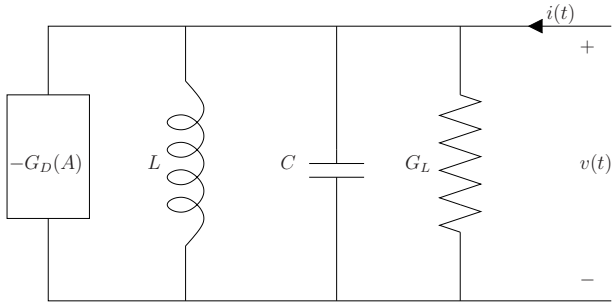

Figure 8.3: Canonical oscillator circuit.

a frequency $\omega_0 = 1/\sqrt{LC}$, which is called the *free-running frequency of the oscillator*. Now assume the oscillator circuit is driven by an external voltage with frequency ω_{in}:

$$v(t) = A(t)\cos(\omega_{in}t + \phi(t)), \forall t \in \mathbb{R}.$$

The corresponding current in the circuit i can then be expressed as

$$i(t) = I_c(t)\cos(\omega_{in}t + \phi(t)) + I_s(t)\sin(\omega_{in}t + \phi(t)). \tag{8.1}$$

According to [19], the assumption of a sinusoidal oscillation in the free-running state is fulfilled if the active device $-G_D(A)$, is described by

$$1 - G_D(A)/G_L = -\mu_p(1 - A^2/\alpha^2), \tag{8.2}$$

where $\alpha \in \mathbb{R}$ is the constant free-running amplitude of the oscillator and $\mu_p \in \mathbb{R}$ is a dimensionless nonlinear parameter. Assume that the amplitude A and phase ϕ vary slowly with respect to the frequency ω_{in} and that the frequency of the injected voltage is close to the free-running frequency: $\Delta\omega/\omega_{in} << 1$, with $\Delta\omega := \omega_{in} - \omega_0$. In [85] it is shown that under these conditions an approximating dynamics for A and ϕ can be obtained:

$$\begin{cases} \dot{\phi} = -\Delta\omega - \dfrac{I_s}{2CA}, \\ \dot{A} = \dfrac{A}{2C}(G_D - G_L) + \dfrac{I_c}{2C}. \end{cases} \tag{8.3}$$

8.3.2 Interconnections of Voltage Controlled Oscillators

Next a network of N oscillators, each separately described by (8.3) is considered. The oscillators, which differ in free-running frequency, are coupled through a general N-port network which is assumed passive and characterized by a frequency-dependent admittance matrix $Y = (Y_{ij}) \in \mathbb{C}^{N\times N}$. The current injected into the i-th oscillator is

$$i_i(t) = -\Re e\left[\sum_{k\in S_i} Y_{ik}(\omega_k(t))A_k(t)e^{j(\omega_{in}t+\phi_k(t))}\right], \quad \forall t \in \mathbb{R},\ i \in \mathcal{N}, \tag{8.4}$$

where S_i is the set of oscillators coupled to the i-th element via the interconnection network, and

$$\omega_j(t) = \omega_{in} + \frac{\mathrm{d}\phi_j}{\mathrm{d}t}(t), \quad \forall t \in \mathbb{R}.$$

Equating (8.4) to (8.1) for the i-th oscillator yields

$$\begin{aligned} I_{ci}(t)\cos(\omega_{in}t + \phi_i(t)) + I_{si}(t)\sin(\omega_{in}t + \phi_i(t)) = \\ - \Re e\left[e^{j(\omega_{in}t+\phi_i(t))}\left(\sum_{k\in S_i} Y_{ik}(\omega_k(t))A_k(t)e^{j(\phi_k(t)-\phi_i(t))}\right)\right]. \end{aligned}$$

Equating coefficients of $\cos(\omega_{in}t + \phi_i(t))$ and $\sin(\omega_{in}t + \phi_i(t))$ leads to expressions for $I_{ci}(t)$ and $I_{si}(t)$, $\forall i \in \mathcal{N}$, which are then substituted into (8.3) to yield a set of $2N$ differential equations. With $Y_{ik} = G_{ik} + jB_{ik}$, the behav-

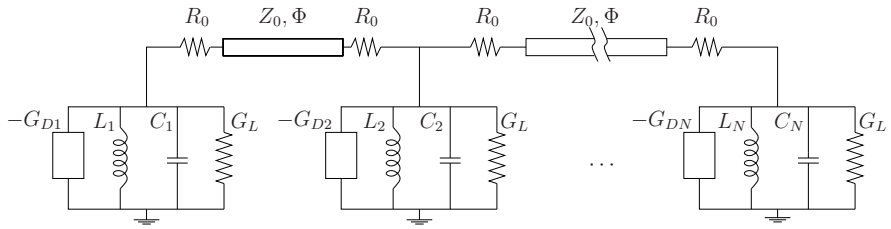

Figure 8.4: Schematic diagram of N oscillators coupled in a linear array.

ior of the i-th oscillator is given by

$$\begin{aligned}\dot{\phi}_i &= -\Delta\omega_i - \frac{1}{2CA_i}\left(\sum_{k\in S_i} A_k[B_{ik}\cos(\phi_k-\phi_i) + G_{ik}\sin(\phi_k-\phi_i)]\right),\\ \dot{A}_i &= \frac{A_i}{2C}(G_D - G_L) - \frac{1}{2C}\left(\sum_{k\in S_i} A_k[G_{ik}\cos(\phi_k-\phi_i) - B_{ik}\sin(\phi_k-\phi_i)]\right).\end{aligned} \tag{8.5}$$

8.3.3 Linear Arrays of Voltage Controlled Oscillators

Consider the nearest-neighbor coupling network of Figure 8.4. This circuit has desirable properties for the case $Z_0 = R_0$, for which the admittance matrix becomes [100]

$$Y_{ij} = \begin{cases} \frac{\eta_i}{2Z_0}, & i = j,\\ \frac{-e^{j\Phi}}{2Z_0}, & |i-j| = 1,\\ 0, & \text{otherwise,}\end{cases} \tag{8.6}$$

where Φ is the electrical length of the transmission line connecting neighboring oscillators and where $\eta_i = (2 - \delta_{i,1} - \delta_{i,N})$, with $\delta_{i,j}$ the Kronecker delta. Using (8.2) and (8.6), the system equations (8.5) are rewritten as

$$\begin{aligned}\dot{\phi}_i =& -\Delta\omega_i + \\ & \frac{1}{4CZ_0}\left(\frac{A_{i-1}}{A_i}\sin(\phi_{i-1}-\phi_i+\Phi) + \frac{A_{i+1}}{A_i}\sin(\phi_{i+1}-\phi_i+\Phi)\right),\\ \dot{A}_i =& \left(\frac{G_L\mu_p}{2C}(1-\frac{A_i^2}{\alpha_i^2})A_i - \frac{\eta_i}{2Z_0}\right) + \\ & \frac{1}{4CZ_0}\left(A_{i-1}\cos(\phi_{i-1}-\phi_i+\Phi) + A_{i+1}\cos(\phi_{i+1}-\phi_i+\Phi)\right),\end{aligned} \tag{8.7}$$

which also holds for the end elements when $A_0 = A_{N+1} = 0$ is used. The phase θ_i of each VCO is given by

$$\theta_i(t) = \omega_{in}t + \phi_i(t),\ \forall t \in \mathbb{R}, \tag{8.8}$$

which is used to turn the first equation of (8.7) into a differential equation for the phase:

$$\dot{\theta}_i = \omega_{0i} + \frac{\omega_{0i}\epsilon}{2Q_i}\left(\frac{A_{i-1}}{A_i}\sin(\theta_{i-1} - \theta_i + \Phi) + \frac{A_{i+1}}{A_i}\sin(\theta_{i+1} - \theta_i + \Phi)\right), \quad (8.9)$$

where Q_i is the *quality factor* of the i-th parallel resonant circuit given by

$$Q_i := \frac{\omega_{0i}C_i}{G_L}, \quad (8.10)$$

and $\epsilon := \frac{1}{2G_L Z_0}$. The quantities ϵ and Φ are called the coupling strength and coupling phase respectively. When the oscillators are effectively uncoupled $(\epsilon = 0)$, equation (8.7) reduces to a set of independent sinusoidal oscillators with amplitudes $A_i = \alpha_i$ and frequencies ω_{0i}. Under the assumption of weak coupling $(0 < \epsilon << 1)$, the amplitude of each oscillator is assumed to remain close to its constant free-running amplitude $(A_i \approx \alpha_i)$ and the dynamics of the phases θ_i become

$$\dot{\theta}_i = \omega_{0i} - \frac{\omega_{0i}}{2Q_i}\sum_{\substack{j=i-1 \\ j\neq i}}^{i+1} \epsilon\frac{\alpha_j}{\alpha_i}\sin(\Phi + \theta_i - \theta_j), \quad \forall i \in \mathcal{N}. \quad (8.11)$$

A simplification often made [71, 101] is to replace the factor $(\omega_{0i}\epsilon)/(2Q_i)$ in each equation by a common factor $\Delta\omega$, called *the locking range of the oscillator*. This simplification is only valid if the frequency differences are sufficiently small.

The system equations can be further simplified by assuming identical free-running amplitudes α_i of the oscillators [51], which yields a dynamics

$$\dot{\theta}_i = \omega_i - \Delta\omega\sum_{\substack{j=i-1 \\ j\neq i}}^{i+1} \sin(\Phi + \theta_i - \theta_j), \quad \forall i \in \mathcal{N}. \quad (8.12)$$

Equation (8.12) shows that the system equations describing populations of coupled oscillators proposed by Kuramoto [46] are closely related to those arising in antenna array theory.

8.4 Applications

The next two sections present two types of interconnection topologies for a network of voltage controlled oscillators steering an antenna array. The goal of the first application is to perform beam scanning of a linear antenna array without the use of phase shifter technology, as introduced in Section 8.2. The second application demonstrates how a circularly polarized wave is created

from a circular antenna array of linearly polarized antennas. The latter can be analyzed by the unidirectional ring of oscillators presented in Chapter 7. Other applications can be found in [14], [36] and [99].

8.4.1 Beam Scanning with a Linear Antenna Array

In this section we present how the system equations (8.11) yield a solution to the beam scanning problem introduced in Section 8.2, as done in [51]. The antenna array yields a desired radiation pattern when the oscillators oscillate at the same frequency, say ω_f, and the phase difference between the i-th and $(i+1)$-th oscillator is the constant ϕ_0 for all $i = 1, \ldots, N-1$. Furthermore the oscillators are all assumed to have the same amplitude of oscillation ($\alpha_i = \alpha_j, \forall i, j \in \mathcal{N}$), and the oscillators in the array are considered equidistant. Substituting these conditions into (8.11) yields (with $\varepsilon := \frac{\epsilon}{2Q_i}$)

$$\omega_f = \begin{cases} \omega_{0i}[1 - \varepsilon \sin(\Phi + \phi_0)], & i = 1, \\ \omega_{0i}[1 - \varepsilon(\sin(\Phi + \phi_0) + \sin(\Phi - \phi_0))], & 1 < i < N, \\ \omega_{0i}[1 - \varepsilon \sin(\Phi - \phi_0)], & i = N. \end{cases} \tag{8.13}$$

Using the fact that $\frac{1}{1-x} \approx 1 + x,\ x \ll 1$, (8.13) can be approximated by

$$\omega_{0i} = \begin{cases} \omega_f[1 + \varepsilon \sin(\Phi + \phi_0)], & i = 1, \\ \omega_f[1 + 2\varepsilon \sin\Phi \cos\phi_0], & 1 < i < N, \\ \omega_f[1 + \varepsilon \sin(\Phi - \phi_0)], & i = N, \end{cases} \tag{8.14}$$

if $\epsilon \ll 1$. For the special case $\Phi = 0$ this reduces to

$$\omega_{0i} = \begin{cases} \omega_f[1 + \varepsilon \sin\phi_0], & i = 1, \\ \omega_f, & 1 < i < N, \\ \omega_f[1 - \varepsilon \sin\phi_0], & i = N. \end{cases} \tag{8.15}$$

In order to obtain a constant phase shift ϕ_0 between neighboring antennas, the free-running frequencies ω_{0i} of the oscillators are required to satisfy (8.15). The free-running frequencies of the inner elements all take on the value ω_f, which is the frequency of the electric field emitted by the antenna array. The free-running frequencies of the end-elements are connected through $\omega_1 = \omega_N + 2\omega_f \varepsilon \sin\phi_0$. The inter-element phase shift ϕ_0 is controlled by the free-running frequencies of the end elements: the linear array performs beam scanning when the outer frequencies are varied continuously.

8.4.2 Unidirectional Circular Antenna Arrays

By inserting unilateral amplifiers between pairs of electrical oscillators, the respective couplings can be made unidirectional, as explained in [52]. Using this technique it is possible to construct an array of antennas coupled in

a unidirectional ring. The phase equations for this configuration are, from (8.12),

$$\dot{\theta}_i = \omega_i + \Delta\omega \sin(\Phi + \theta_{i+1} - \theta_i), \quad i \in \mathcal{N}.$$

In [23] an antenna array of four *identical* unidirectionally coupled oscillators described by (8.4.2) is investigated. Each antenna is linearly polarized. The spatial topology of the antenna array is such that if the phase locking solution $\phi = [\frac{\pi}{2}\ \frac{\pi}{2}\ \frac{\pi}{2}\ \frac{\pi}{2}]^T$ can be maintained, the antenna array emits a circularly polarized wave. The authors of [23] used ad hoc methods to determine the phase locking solutions and their stability properties. The stability was determined by calculating the eigenvalues of the linearization numerically.

In the previous chapter *all* phase locking solutions of the above oscillator configuration with $\Phi = 0$ and their stability properties are determined *analytically*. All phase locking solutions of (8.4.2) can be analytically obtained using techniques stated in Section 7.2.2. The stability theorems proven in Section 7.3 can be readily adjusted to apply to the above system equations. For instance Theorem 32 changes into:

Theorem 39. *If a phase locking solution of (8.4.2) has only phase differences ϕ_i belonging to $(-\pi/2 + \Phi, \pi/2 + \Phi)$, then it is asymptotically stable.*

The results of the previous chapter show how the setting of [23] can be generalized to nonidentical oscillators, which leads to a robustness result: if the frequencies of the oscillators slightly differ, there exist sufficiently large coupling strengths such that locally stable phase locking solutions exist. Although the travelling wave solutions (7.7) do not belong to the set of solutions, there exist phase locking solutions with phase difference close to those of the travelling wave solutions. This follows from (7.9) and (7.11): a perturbation in the natural frequencies of the originally identical oscillators yields a perturbation of the group velocity Ω via (7.11), which in turn yields a perturbation of the phase differences of the phase locking solutions via (7.9). The polarization of the resulting electromagnetic wave is approximately circular. Once the values of the phase differences are known, Theorem 39 yields a condition on Φ for the corresponding phase locking solution to be stable.

8.5 Conclusions

We have demonstrated how the Kuramoto model naturally arises in the setting of antenna arrays. Each antenna of the array is driven by a voltage controlled oscillator. The oscillators are electrically interconnected; the interconnection topology may differ from the spatial topology of the antenna array. The goal of this set-up is to achieve a desired radiation pattern of the antenna array by tweaking the natural frequencies of the oscillators.

Two applications were presented: beam scanning in a linear antenna array as developed by [51] and the creation of a circularly polarized wave by

means of an antenna array, as devised by [23]. The analysis of the second example as conducted by the authors of [23] is very restricted and uses only ad-hoc methods. The theory developed in the previous chapter provides a general mathematical analysis and allows for an analysis of perturbations of the ideal case with all oscillators identical.

Chapter 9

Vehicle Platoons Formed Through Self-regularization

9.1 Introduction

At first this chapter may seem out of place with the rest of this thesis since it does not treat coupled oscillator systems in any way. It does relate part of the research conducted in the framework of this PhD, however, and therefore merits inclusion into the text. Furthermore, the systems described in this chapter belong to the class of *interconnected systems* and hence are related to the systems of the previous chapters. The building blocks are no longer oscillators, but linear systems modelling vehicles. Inspired by the results of Chapter 7, we decided to investigate the properties of systems of ring-coupled vehicles.

In this chapter systems giving rise to *vehicular platoons* are investigated. Such platoons have gained importance over the years, as they help relieving the congestion of highways. The objective being a capacity increase of the highway, these intelligent vehicle/highway systems (IVHS) form strings of vehicles (so-called *platoons*) moving at a desired speed with desired distances between the vehicles. Several algorithms controlling a string of vehicles have been proposed in the literature.

Ref. [49], [59] and [94] rank among the first to investigate this problem and used an LQR approach controlling an *infinite* string of vehicles. Recently, this approach has been readdressed in [41]. Contrary to [49] and [59], most control strategies use tuning of parameters in order to optimize some proposed controller. In most cases the control is of leader-follower type: the leading vehicle of the platoon moves at a desired speed; the other vehicles receive information from the leading vehicle (position, velocity, acceleration) either directly or indirectly through other vehicles in the platoon. Flow of

information is usually directed from the head of the platoon towards its tail [38, 39, 83].

An important concept regarding the formation of vehicle platoons is *string stability*. A platoon is called string stable if the transient error in the separation distance between vehicles does not grow as one proceeds down the line of vehicles. In [88] the concept of string stability is treated for nonlinear systems. It is proven that for sufficiently weak interactions an ensemble of interconnected exponentially stable nonlinear systems is string stable. In [68] mesh stability is defined, which is an extension of the concept of string stability. In reference [44] one considers a platoon where each vehicle only measures and regulates its distance with its immediate forward neighbor. The leader vehicle drives at a desired speed. It is proven in [44] that the system cannot be string stable when *identical* controllers are applied.

In the present chapter we present a novel interconnection topology using identical controllers. As in [44], only separation distances are measured. The key property of the interconnection is the absence of a master/leader vehicle that determines the overall behavior of the platoon. All vehicles interact with each other trying to satisfy their individual control objective. As a result of this cooperation a platoon formation emerges. This resulting behavior and its stability properties are investigated. Stability regions in parameter space are obtained. Simulations suggest that in practice the system's behavior is string stable, contrary to the behavior in [44]. Furthermore, the control structure renders the platoon robust with respect to malfunctioning vehicles, as shown in Section 9.6 and Section 9.8.4.

9.2 Preliminary: Block Circulant Matrices

In this section some notation and preliminary results on block circulant matrices are introduced which will be used in the description of the dynamics of the platoon and its stability analysis. Consider the block circulant matrix $C \in \mathbb{R}^{Nm \times Nm}$:

$$C = \begin{bmatrix} C_1 & C_2 & \cdots & C_N \\ C_N & C_1 & \cdots & C_{N-1} \\ \vdots & \vdots & \vdots & \vdots \\ C_2 & C_3 & \cdots & C_1 \end{bmatrix} =: \text{circ}(C_1, C_2, \ldots, C_N),$$

where $C_i \in \mathbb{R}^{m \times m}$, $\forall i \in \mathcal{N}$. Define the matrix $F \in \mathbb{C}^{N \times N}$:

$$F := \frac{1}{\sqrt{N}} \begin{bmatrix} 1 & 1 & \cdots & 1 \\ 1 & \omega & \cdots & \omega^{N-1} \\ \vdots & \vdots & \vdots & \vdots \\ 1 & \omega^{N-1} & \cdots & \omega^{(N-1)(N-1)} \end{bmatrix},$$

with $\omega := \exp(2\pi j/N)$, where 'j' represents the imaginary unit. The matrix C can be block diagonalized into a matrix Λ:

$$\Lambda = \text{diag}(\Lambda_1, \ldots, \Lambda_N) = (F \otimes I_m)^* C (F \otimes I_m), \tag{9.1}$$

where '$\otimes$' is the Kronecker product, '$*$' represents complex conjugate, and I_m is the $m \times m$ identity matrix.

The blocks $\Lambda_i \in \mathbb{C}^{m \times m}$ are given by

$$\Lambda_i = C_1 + \omega^{i-1} C_2 + \omega^{2(i-1)} C_3 + \ldots + \omega^{(N-1)(i-1)} C_N, \tag{9.2}$$

for all $i \in \mathcal{N}$.

9.3 System Dynamics

9.3.1 Ring Topology

The idea of coupling agents into a ring has been exploited before in [52], [57], [74] and [82]. In [52] each agent i is represented by a point z_i in the complex plane and the dynamics are

$$\dot{z}_i = (z_{i+1} + c_i) - z_i, \quad i \in \mathcal{N}, \tag{9.3}$$

where $c_i \in \mathbb{C}$, $\forall i \in \mathcal{N}$. It is tacitly assumed that $z_{N+1} \equiv z_1$. This assumption on the indices holds throughout this chapter. If $c_i = 0$, $\forall i \in \mathcal{N}$, then the agents will converge to one point in the complex plane. Choosing values c_i appropriately leads to desired formations of the group of agents. If the centroid of the points $c_1, \ldots, c_N$ is not at the origin, then the centroid of the agents moves off to infinity. This situation is undesired in the setting of [52] and is thus avoided.

In [57] the topology of the interconnection networks is also a unidirectional ring with each agent represented as a kinematic unicycle with nonlinear dynamics. The control strategy is such that agent i tries to reduce the distance between agent $i+1$ and itself to zero. This is done by a proportional feedback of the difference in heading, i.e. orientation, of both vehicles:

$$\begin{bmatrix} \dot{x}_i \\ \dot{y}_i \\ \dot{\theta}_i \end{bmatrix} = \begin{bmatrix} \cos\theta_i & 0 \\ \sin\theta_i & 0 \\ 0 & 1 \end{bmatrix} \begin{bmatrix} s \\ k(\theta_{i+1} - \theta_i) \end{bmatrix},$$

where s and k are positive real constants. The resulting equilibrium motion is that all agents are moving along a circle in one direction as described in Section 7.5. The motion in the physical plane clearly reflects the unidirectional interconnection structure.

Inspired by the examples above, we couple the vehicles in a unidirectional ring at the level of communication. Contrary to [57], the ring topology is not expressed at the level of the geometry of the formation: the equilibrium solution is a *string* of vehicles. The interconnection in the present chapter resembles that of [52] where values for constants c_i have to be chosen. In [52] this choice of c_i determines the shape of the resulting formation in two-dimensional space, while in the present chapter the shape of the formation is a string of vehicles regardless the values of the parameters. The choice of the parameters determines *the separation distances* inside the string. In [52] it is assumed that the centroid of the points $c_1, \ldots, c_N$ is at the origin, since otherwise the formation moves off to infinity. In the present dissertation we deliberately choose the centroid to be different from zero, forcing the string of vehicles to move at a certain constant velocity.

9.3.2 System Equations and Equilibrium Solutions

Each vehicle is represented as a moving mass with second order dynamics:

$$\ddot{x}_i + p\dot{x}_i = u_i, \quad i \in \mathcal{N}, \tag{9.4}$$

where $x_i \in \mathbb{R}$ represents the position of the i-th vehicle, u_i is the input to the i-th vehicle and $p \geq 0$ is a parameter representing the friction/drag coefficient per unit mass. The mass of each vehicle is taken equal to one. We propose the following control:

$$u_i = \omega_i + K(x_{i-1} - x_i - L_i), \quad i \in \mathcal{N}, \tag{9.5}$$

with $K > 0$ the coupling strength and $\omega_i > 0$, $L_1 \leq 0$, $L_i \geq 0$, $i = 2, \ldots, N$, real constants. It is tacitly assumed that $x_0 \equiv x_N$. Each vehicle attempts to keep the distance between itself and its immediate forward vehicle as close as possible to the set point L_i. The leading vehicle tries to obtain a desired distance $|L_1|$ between itself and the last vehicle of the platoon. At the same time, each vehicle aims to drive at an imposed reference speed $v_i := \omega_i/p$. This leads to the dynamical system

$$\begin{cases} \dot{x} = Ax + Kb + \omega, \\ x = \begin{bmatrix} x_1 & \dot{x}_1 & x_2 & \dot{x}_2 & \cdots & x_N & \dot{x}_N \end{bmatrix}^T, \\ A = \text{circ}\left(\begin{bmatrix} 0 & 1 \\ -K & -p \end{bmatrix}, \underbrace{O_2, \ldots, O_2}_{N-2 \text{ times}}, \begin{bmatrix} 0 & 0 \\ K & 0 \end{bmatrix} \right), \\ b = \begin{bmatrix} 0 & L_1 & 0 & L_2 & \cdots & 0 & L_N \end{bmatrix}^T, \\ \omega = \begin{bmatrix} 0 & \omega_1 & 0 & \omega_2 & \cdots & 0 & \omega_N \end{bmatrix}^T \end{cases} \tag{9.6}$$

with O_2 the 2×2 null matrix.

Theorem 40. *Each function $\varphi : \mathbb{R} \to \mathbb{R}^N; t \mapsto \varphi(t)$ defined by*

$$\varphi_i(t) = \alpha t + \beta_i, \quad \forall i \in \mathcal{N}, \tag{9.7}$$

where

$$\begin{aligned} \alpha &= \frac{\omega_m - KL_m}{p}, \\ \beta_{i-1} - \beta_i &= \frac{\omega_m - \omega_i}{K} + L_i - L_m, \end{aligned} \tag{9.8}$$

with $\omega_m := \frac{1}{N}\sum_{j=1}^{N} \omega_j$ and $L_m := \frac{1}{N}\sum_{j=1}^{N} L_j$, is a solution of system (9.4)-(9.5).

Proof. Substitution of (9.7) into the system equations (9.6) yields

$$\alpha p = -K\beta_i + K\beta_{i-1} - KL_i + \omega_i, \quad \forall i \in \mathcal{N}. \tag{9.9}$$

Equation (9.7) represents a solution of (9.4)-(9.5) or, equivalently, (9.6), if and only if α, β_i satisfy (9.9). Adding all N equations (9.9) leads to a value for α:

$$\alpha = \frac{1}{Np} \sum_{j=1}^{N} (\omega_j - KL_j). \tag{9.10}$$

Each equation of (9.9) can be written as

$$\beta_{i-1} - \beta_i = \frac{\alpha p}{K} + L_i - \frac{\omega_i}{K}, \quad \forall i \in \mathcal{N}. \tag{9.11}$$

With (9.10) this changes into

$$\beta_{i-1} - \beta_i = \frac{1}{K}\left(\frac{1}{N}\sum_{j=1}^{N} \omega_j - \omega_i\right) - \left(\frac{1}{N}\sum_{j=1}^{N} L_j - L_i\right), \tag{9.12}$$

for all $i \in \mathcal{N}$. □

Assume each vehicle is given a reference speed v_i close to some value v_0. In the ideal case each vehicle would receive a reference speed perfectly equal to v_0 rendering the coupling structure redundant. In a practical situation however, the reference speeds will differ slightly from each other. If the vehicles remain uncoupled in this situation, the group of vehicles becomes dispersed and/or some vehicles collide. The coupling structure's aim is to keep the vehicles moving together in a highly structured way through self-organization. The interconnections are such that each vehicle abandons its goal to drive at the set speed v_i in order to fall into step with its forward and backward neighbors which move at a speed different from v_i.

Beside the reference speeds, the coupling itself allows control of the platoon's speed by varying the set points L_i: by deliberately choosing the set points L_i such that their mean value L_m is different from zero, the string of

vehicles starts to move at a constant velocity which depends on this mean value and the mean reference speed, according to (9.8). Once the set points have been fixed, the self-regulatory property of the system ensures the resulting motion is a platoon moving at the desired velocity. It can be proven, however, that with fixed coupling strength, the velocity α cannot increase without bound without simultaneously increasing the interdistances $\beta_{i-1} - \beta_i$. This is not desirable since our goal is a fast driving platoon with small interdistances to relieve road congestion. Equation (9.11) shows that by increasing the *coupling strength* appropriately the speed can be increased without increasing the interdistances. Unfortunately, as will be proven in Section 9.4, the coupling strength cannot increase indefinitely without losing stability of the platoon. This leads us to conclude that varying the set points L_i yields a *limited* control of the platoon's speed.

Notice that the platoon behavior, i.e. a string of vehicles moving at a constant velocity with constant interdistances, *emerges* from the interconnections between the *individual* control objectives of the vehicles. This contrasts with the classical look-ahead interconnections where a driver controls the leader vehicle and the consecutive vehicles follow.

9.3.3 Remarks

1. The solutions $t \mapsto \varphi(t)$ of Theorem 40 are called the equilibrium solutions of the system (9.6).

2. The function $t \mapsto \varphi_i(t)$ represents the evolution of the position of the i-th vehicle. Each solution φ represents a string of vehicles moving at a constant velocity given by (9.10) with distances between consecutive vehicles defined by (9.12). The system equations are invariant under the change of coordinates

$$x \to x + \gamma \begin{bmatrix} 1 & 0 & 1 & 0 & \cdots & 1 & 0 \end{bmatrix}^T, \quad \forall \gamma \in \mathbb{R}. \tag{9.13}$$

   In other words, the dynamics are invariant under translations of the origin in the physical space. This invariance is reflected in the spectrum of the system matrix A in (9.6): the matrix A possesses a structural zero-eigenvalue, independent of the parameter values.

3. Notice that the separation distances between consecutive vehicles do not converge to the set points L_i. However, by (9.12) it is possible to compute the distances which the platoon converges to. Conversely, if desired values $\delta_i := \beta_{i-1} - \beta_i$ for the separation distances are given, equation (9.12) allows us to calculate the necessary set points L_i.

9.4 Stability Analysis

In this section the stability of the equilibrium solution as a function of the coupling strength is investigated. In order to establish the stability properties of (9.7), the following change of coordinates is performed:

$$x_i = \alpha t + \beta_i + z_i,$$

where α and β_i are defined by (9.8). This results in a set of system equations

$$\dot{z} = Az, \tag{9.14}$$

with the system matrix A identical to the system matrix of the original system (9.6). Notice that the system (9.14) possesses the same translation invariance (9.13) as the original system.

Theorem 41. *If and only if*

$$K < \frac{p^2}{2\cos^2(\pi/N)}$$

the solution (9.7)-(9.8) of system (9.6) is asymptotically stable.

Proof. System (9.14) has a line of equilibrium points. This can be concluded from the aforementioned translation invariance (9.13). Each equilibrium point on this line corresponds to one of the solutions φ. The system matrix A has a structural zero-eigenvalue which can be discarded from the stability analysis. If and only if the remaining $2N-1$ eigenvalues of A are located in the open left half plane, each initial condition converges to the line of equilibrium points and the solution (9.7)-(9.8) is called asymptotically stable.

Since the matrix A is circulant it can be block diagonalized according to (9.1) and (9.2). The matrices appearing on the diagonal are

$$A_i = \begin{bmatrix} 0 & 1 \\ K(\omega^{(N-1)(i-1)} - 1) & -p \end{bmatrix}, \quad \forall i \in \mathcal{N}, \tag{9.15}$$

with $\omega = \exp(2\pi j/N)$. Since $\exp(j\phi) = \exp(j\phi + j2\pi m)$, $\forall \phi \in \mathbb{R}$, $\forall m \in \mathbb{Z}$, it holds that $\omega^{(N-1)(i-1)} = \omega^{1-i}$. The eigenvalues of A_i are the roots of the characteristic polynomial

$$\lambda^2 + p\lambda - K(\omega^{(1-i)} - 1),$$

which are

$$\lambda_{i(1,2)} = -\frac{p}{2} \pm \frac{1}{2}\left(p^2 + 4K(\omega^{(1-i)} - 1)\right)^{\frac{1}{2}}.$$

Now, the values of K for which the eigenvalues lie in the open left half plane are determined. One immediately notices that A_1 yields the structural zero-eigenvalue and a strictly negative eigenvalue $-p$. Denote the eigenvalues of A_i as

$$\lambda_{i(1,2)} = -\frac{p}{2} \pm \frac{1}{2}(a+jb)^{\frac{1}{2}},$$

with

$$\begin{aligned} a &= p^2 + 4K\cos(2\pi(1-i)/N) - 4K, \\ b &= 4K\sin(2\pi(1-i)/N). \end{aligned}$$

Now set

$$-\frac{p}{2} \pm \frac{1}{2}\Re e(a+jb)^{\frac{1}{2}} < 0. \tag{9.16}$$

With

$$(a+jb)^{\frac{1}{2}} = \sqrt{\frac{|a+jb|+a}{2}} + j\mathrm{sgn}(b)\sqrt{\frac{|a+jb|-a}{2}},$$

(9.16) can be written as

$$-p \pm \sqrt{\frac{|a+jb|+a}{2}} < 0.$$

A simple calculation shows that this is equivalent to

$$\begin{aligned} K < K_{C,i} &:= p^2\left(\frac{1-\cos(2\pi(1-i)/N)}{\sin^2(2\pi(1-i)/N)}\right), \\ &= \frac{p^2}{2\cos^2(\pi(1-i)/N)}. \end{aligned} \tag{9.17}$$

If and only if $K < \min_{i\in\mathcal{N}\setminus\{1\}}\{K_{C,i}\}$, the system is asymptotically stable.

The function

$$f : \mathbb{R} \to \mathbb{R}; x \mapsto \frac{p^2}{2\cos^2 x},$$

is even, convex and has a minimum at the origin. Hence

$$\min_{i\in\mathcal{N}\setminus\{1\}}\{K_{C,i}\} = \frac{p^2}{2\cos^2(\pi/N)}, \tag{9.18}$$

concluding the proof. □

If the number of vehicles tends to infinity, the upper bound on K for stability determined by (9.18) decreases and converges to the value $p^2/2$. This yields a sufficient condition for asymptotic stability.

Theorem 42. *If $0 < K < p^2/2$, system (9.6) is asymptotically stable, irrespective of the number of vehicles in the system.*

Example

Consider system (9.6) with 3 vehicles and drag coefficient $p = 2$. The eigenvalues of the corresponding system matrix A are plotted in Figure 9.1 as a function of K. When the vehicles are uncoupled ($K = 0$), three eigenvalues are located at $-p$; the remaining three eigenvalues are located at the origin. When K increases two of the latter eigenvalues move into the open left half plane while two of the eigenvalues located in $-p$ start to move towards the imaginary axis. The sum of all eigenvalues is $-3p$, irrespective of the value K. As stated before, for all values $K > 0$ there is one eigenvalue at the origin and one in $-p$, corresponding to the matrix A_1 of (9.15). When the coupling strength exceeds the value $p^2/4$ the two rightmost eigenvalues different from zero start to move towards the imaginary axis until at $K = 2p^2$ they cross the imaginary axis simultaneously, rendering the system unstable.

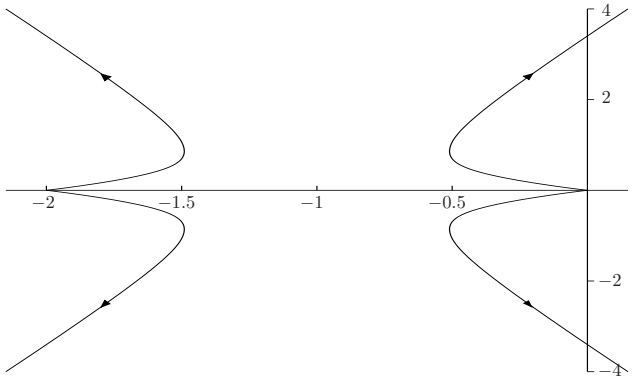

Figure 9.1: The dependence of the spectrum of the three-vehicle-system on the coupling strength K.

9.5 String Stability

In this section *string stability* is discussed with respect to the proposed interconnection structure. For a general treatment of the concept of string stability the reader is referred to [68], [88] and [103] where infinite interconnections of a class of nonlinear systems are considered.

In practice, however, a vehicle platoon always consists of a finite number of vehicles. A string of vehicles is called string stable if disturbances are attenuated as they propagate down the string [69]:

Definition 38. *Let e_i be the distance error between the i-th and $(i-1)$-th vehicle:*

$e_i := x_i - x_{i-1} - (\beta_i - \beta_{i-1})$. *The platoon is called string stable if*

$$\|e_i(t)\|_\infty < \|e_{i-1}(t)\|_\infty, \quad \forall i > 1,$$

where $\|e_i(t)\|_\infty$ *denotes* $\sup_{t\geq 0} |e_i(t)|$.

In the literature concerned with leader-follower control of vehicle strings, string stability of the platoon is determined by assuming zero initial conditions and introducing some linear input-output model to express the relation between consecutive distance errors [78,83,98]:

$$e_i = h_i * e_{i-1}, \quad \forall i > 1,$$

or in the Laplace-domain:

$$E_i(s) = H_i(s)E_{i-1}(s), \quad \forall i > 1.$$

Then a criterium for string stability can be established:

Theorem 43. *If* $|H_i(j\omega)| < 1$, $\forall i > 1, \forall \omega \in \mathbb{R}$, *the platoon is string stable.*

The configuration of the present chapter does not allow the assumption of zero initial conditions. The error dynamics can be written as a linear system $\dot{z} = Az$ without an input: applying the change of coordinates

$$e_i := x_i - x_{i-1} - (\beta_i - \beta_{i-1}), \quad \forall i \in \mathcal{N},$$

the system equations (9.6) change into

$$\ddot{e}_i + p\dot{e}_i = K(e_{i-1} - e_i), \quad \forall i \in \mathcal{N}. \tag{9.19}$$

which in turn can be rewritten, using $z_i := [e_i \; \dot{e}_i]^T$, into

$$\dot{z}_i = \begin{bmatrix} 0 & 1 \\ -K & -p \end{bmatrix} z_i + \begin{bmatrix} 0 & 0 \\ -K & 0 \end{bmatrix} z_{i-1}, \quad \forall i \in \mathcal{N}. \tag{9.20}$$

Starting at zero initial conditions means starting at the equilibrium. The platoon is controlled by changing the parameters L_i, K, ω_i of the system. The state of the system (9.20) stays at the equilibrium, regardless how these parameters vary over time. Contrary to the classical look-ahead configuration where the state of the leader vehicle can be seen as an input to the platoon, it is not possible to construct an input-output model equivalent to (9.19), where the control can be implemented as the input.

Theorem 44. *The platoon described by (9.6) is not string stable for arbitrary initial conditions.*

Proof. Consider the error dynamics (9.19) corresponding to the system (9.6). Let $e : t \mapsto e(t) = [e_1(t) \cdots e_N(t)]^T$ be the solution of (9.19) with initial condition $e(0) = [e_{10} \cdots e_{N0}]^T$. Assume the system is string stable, i.e. $\|e_i(t)\|_\infty < \|e_{i-1}(t)\|_\infty, i > 1$. This implies $\|e_1(t)\|_\infty > \|e_N(t)\|_\infty$. Introduce the operator $\sigma : \mathbb{R}^n \to \mathbb{R}^n$ which returns a cyclic permutation of a vector. Because of the circular symmetry of the system (the system matrix of (9.20) is a circulant), $\sigma(e)$ is also a solution of (9.19), corresponding to the initial condition $(\sigma e)(0)$. This solution has the property that $\exists j > 1 : \|e_j(t)\|_\infty > \|e_{j-1}(t)\|_\infty$. This contradicts the assumption of string stability, which implies the assumption is invalid. □

However, this does not imply that system (9.6) does not possess the desired string stability property in practice, where the initial conditions have to satisfy some restrictions:

- First, from the definition of e_i it follows that

$$\sum_{j=1}^{N} e_j(t) = 0, \quad \forall t \in \mathbb{R}.$$

- Second, each equilibrium solution of (6) has $x_{i-1}(t) > x_i(t), i \neq 1$. Necessary to avoid collisions, only initial conditions are considered with vehicle positions satisfying $x_{i-1}(0) > x_i(0),\ i \neq 1$.

- Third, we impose the extra assumption that control by resetting the values L_i is applied to a platoon driving at constant velocity, i.e., $\dot{e}_i(0) = 0, \forall i \in \mathcal{N}$. By adjusting the parameters L_i, the platoon is steered from one equilibrium solution to another. The manoeuvres included are speeding up, slowing down and starting from a standstill.

- Fourth, we consider only set points L_i for which $L_m < 0$ so that the platoon velocity α is positive.

Example

For simplicity, it is assumed that $\omega_i = 0,\ \forall i \in \mathcal{N}$. Assume that for time $t < 0$ the platoon is behaving according to an equilibrium solution, i.e. $x_i(t) - x_{i-1}(t) = L_m - L_i,\ \forall i \in \mathcal{N},\ \forall t < 0$. At $t = 0$ the set point L_1 is replaced by $\tilde{L}_1$. For positive time the platoon behavior can be described by

$$\ddot{e}_i + p\dot{e}_i = K(e_{i-1} - e_i), \quad \forall i \in \mathcal{N}, \tag{9.21}$$

with

$$e_i := x_i - x_{i-1} - \tilde{L}_m + \tilde{L}_i, \quad i \in \mathcal{N},$$

where $\tilde{L}_i = L_i, \forall i \in \mathcal{N} \setminus \{1\}$. The corresponding initial condition is given by

$$\begin{cases} e_1(0) = \dfrac{N-1}{N}(\tilde{L}_1 - L_1), \\ e_i(0) = \dfrac{L_1 - \tilde{L}_1}{N}, \quad \forall i \in \mathcal{N} \setminus \{1\}, \\ \dot{e}_i(0) = 0, \ \forall i \in \mathcal{N}. \end{cases}$$

In Figure 9.2, system (9.6) is simulated with $N = 39$, $L_1 - \tilde{L}_1 = -5$, $p = 10$, $K = 10$. This corresponds to a slowing down manoeuvre. The figure presents the evolution of the distance errors $e_i(t)$ over time. For reasons of clarity, half of the distance errors, namely those with even index, are omitted from the picture. The figure suggests that the maximum distance error between pairs of consecutive vehicles does not grow when proceeding towards the tail of the platoon. This is made explicit by the separate plots of Figure 9.3, where the first 4 separation distance errors are displayed.

Figure 9.4 shows the distance error e_4 over a longer time period compared to Figure 9.3 and illustrates a typical feature of the interconnection topology: each distance error rises quickly to its maximum value and then decreases to a value close to zero, but, contrary to leader-follower control, after some time the distance error starts to rise again. It then decreases again to some value near zero. This rising and decreasing is repeated periodically over time. As time evolves, the time it takes for an error to rise and fall down increases, while the peak value decreases. This may be interpreted as if there is a Mexican wave in the error value moving around in the platoon: when the wave reaches the tail of the platoon, it reappears at the leader vehicle. Notice that the Mexican wave continually decreases in amplitude while moving around in the platoon.

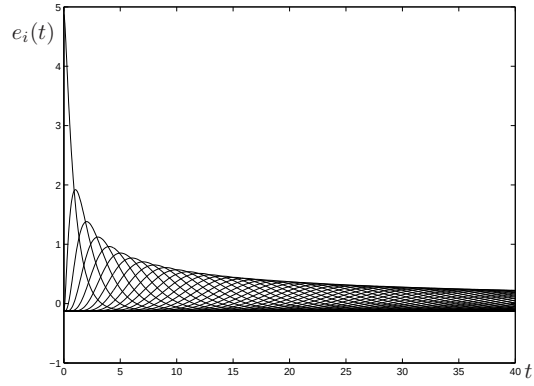

Figure 9.2: Evolution of the separation distance errors for a platoon of 39 vehicles.

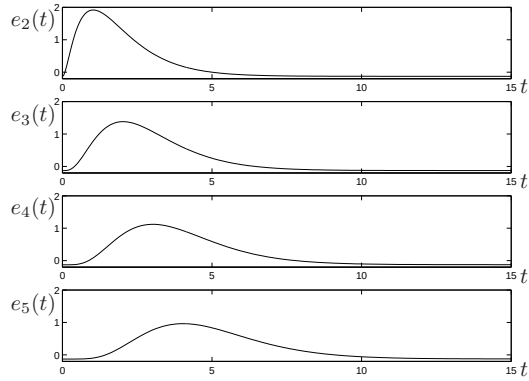

Figure 9.3: Separation distance errors of the first 5 vehicles.

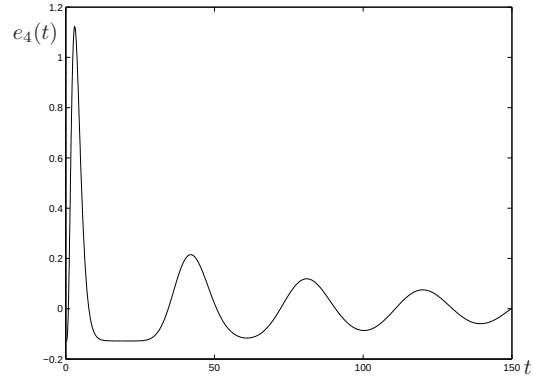

Figure 9.4: Evolution of the separation distance error e_4.

9.6 Robustness

Assume that one of the vehicles starts to malfunction and cannot attain the velocity required by the platoon at that moment. In the case of leader-follower control this causes the leading group of vehicles to abandon the group with the malfunctioning vehicle as first vehicle, and therefore a splitting of the platoon. The distance between both groups increases without bound.

With the interconnection topology of the present chapter all vehicles adapt to the "weakest link" and the platoon starts to drive at the maximum velocity attainable by the malfunctioning vehicle. This is illustrated on the right hand side plot of Figure 9.5: at $t = 80$ s the speed of one of the vehicles becomes bounded by 0.3 m/s. The distance between the first and the second group remains bounded. There is a splitting of the platoon but no aban-

doning. The left hand side plot shows the evolution of the platoon without malfunctions. Again, only the positions of the vehicles with an odd index are plotted, for reasons of clarity.

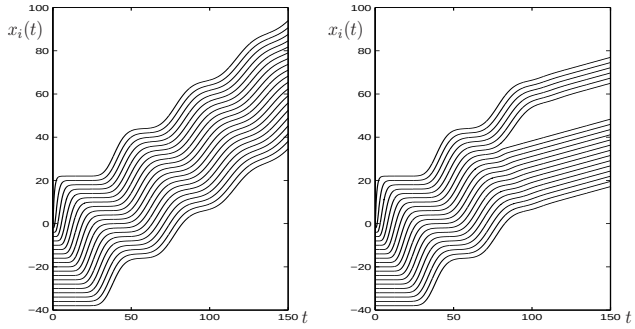

Figure 9.5: Evolution of the position for a platoon of 39 vehicles. Left hand side figure: no malfunctions. Right hand side figure: at $t = 80$ s, the 12-th vehicle starts malfunctioning and cannot drive faster than 0.3 m/s.

9.7 Disadvantages of Unidirectional Ring Coupling

The unidirectional ring coupling (9.6) has some undesirable properties. First, the equilibrium solutions are only stable for sufficiently small coupling strengths K (see Section 9.4). This results in an undesirable slow decay of the transient behavior. Furthermore, it determines an upper bound on the difference in reference speeds v_i. The interconnections regulate the interdistances to constant values. They need to be sufficiently strong to avoid collisions between consecutive vehicles with different reference speeds. The more the values v_i differ, the larger the coupling strength has to be to avoid collisions. Since the coupling strength has an upper bound for stability, the differences $v_{i-1} - v_i$ which do not result in collisions are bounded from below.

Second, the platoon is not robust to malfunctions where one of the vehicles possesses a lower bound on its velocity. Since each vehicle only regulates its interdistance with its immediate forward neighbor, it is not aware of the behavior of its immediate backward neighbor. Assume the string of vehicles drives according to an equilibrium solution. If a vehicle starts to malfunction by driving faster than the required velocity of the platoon, its backward neighbors will respond by trying to catch up. Through the link between the first and last vehicle of the platoon, the first part of the platoon responds likewise. However, due to a delay, by the time the immediate forward neighbor

of the malfunctioning vehicle starts to speed up, the malfunctioning vehicle might already have collided with it. Remark that this behavior is inherent to all leader-follower strategies as well. It is not an exclusive disadvantage of the unidirectional ring coupling.

Clearly the above robustness problem can be solved by adding interconnections directed opposite to the original interconnections. This is the topic of Section 9.8. The coupling structure presented in Section 9.8 is also suited to remove the upper bound on the coupling strength.

9.8 Bidirectional Ring Topology

The main disadvantage of system (9.6) is that the equilibrium solutions are only stable for sufficiently small coupling strengths, resulting in a slowly decaying transient behavior. This situation is amended by adding a coupling ring directed opposite to the first ring of the coupling structure. The control is:

$$u_i = \omega_i + K_1(x_{i-1} - x_i - L_{i1}) - K_2(x_i - x_{i+1} - L_{i2}), \quad \forall i \in \mathcal{N}, \tag{9.22}$$

$K_1 > 0$, $K_2 > 0$ the coupling strengths, $L_{i2}, L_{i1} \in \mathbb{R}$ the set points and with $\omega_i > 0$. Each vehicle attempts to keep its distance with its immediate forward and backward vehicles as close as possible to the given set points with the additional aim to drive at the reference speed $v_i = \omega_i/p$.

9.8.1 System Equations

The differential equations governing the system are

$$\begin{cases} \dot{x} = Ax - K_1 b_1 + K_2 b_2 + \omega, \\ x = \begin{bmatrix} x_1 & \dot{x}_1 & x_2 & \dot{x}_2 & \cdots & x_N & \dot{x}_N \end{bmatrix}^T, \\ A = \operatorname{circ}\left(\begin{bmatrix} 0 & 1 \\ -(K_1+K_2) & -p \end{bmatrix}, \begin{bmatrix} 0 & 0 \\ K_2 & 0 \end{bmatrix}, \underbrace{O_2, \ldots, O_2}_{N-3 \text{ times}}, \begin{bmatrix} 0 & 0 \\ K_1 & 0 \end{bmatrix} \right), \\ b_i = \begin{bmatrix} 0 & L_{1i} & 0 & L_{2i} & \cdots & 0 & L_{Ni} \end{bmatrix}^T, \\ \omega = \begin{bmatrix} 0 & \omega_1 & 0 & \omega_2 & \cdots & 0 & \omega_N \end{bmatrix}^T. \end{cases} \tag{9.23}$$

Theorem 45. *Let $K_1 > K_2$. Each function $\varphi : \mathbb{R} \to \mathbb{R}^N; t \mapsto \varphi(t)$ defined by*

$$\varphi_i(t) = \alpha t + \beta_i, \quad \forall i \in \mathcal{N}, \tag{9.24}$$

with

$$\begin{aligned}\alpha &= \frac{1}{Np}\sum_{j=1}^{N}\left(-K_1L_{j1}+K_2L_{j2}+\omega_j\right),\\ \beta_i-\beta_{i-1} &= \frac{\sum_{j=1}^{N}\left(\frac{K_2}{K_1}\right)^{j-1}\xi_{j+i-1}}{1-\left(\frac{K_2}{K_1}\right)^{N}}, \quad i\in\mathcal{N},\\ \xi_j &= -\alpha p+\omega_j-K_1L_{j1}+K_2L_{j2}, \quad j\in\mathcal{N}.\end{aligned} \tag{9.25}$$

is a solution of system (9.23).

The proof is similar to the proof of Theorem 40. Similar results can be obtained for the cases $K_1 = K_2$ and $K_1 < K_2$.

9.8.2 Stability Results

Theorem 46. *If and only if*

$$\frac{(K_1-K_2)^2}{K_1+K_2} < \frac{p^2}{2\cos^2(\pi/N)}$$

the solution (9.24)-(9.25) of system (9.23) is asymptotically stable.

The proof is similar to the proof of Theorem 41.

Theorem 47.

$$\forall\epsilon>0, \exists\delta : |K_1-K_2|<\delta \Rightarrow \frac{(K_1-K_2)^2}{K_1+K_2}<\epsilon. \tag{9.26}$$

Proof. Let $\delta < \sqrt{\epsilon(K_1+K_2)}$. Then

$$|K_1-K_2|<\delta \Rightarrow \frac{(K_1-K_2)^2}{K_1+K_2} < \frac{\delta^2}{K_1+K_2} < \epsilon. \tag{9.27}$$

□

From Theorem 46 and Theorem 47 it is concluded that if the coupling strengths K_1 and K_2 are sufficiently close to each other the system is asymptotically stable. For $K_1 = K_2$ the system is always stable, regardless the size of the drag coefficient $p > 0$. The coupling strengths can be taken arbitrarily large without endangering the stability of the system, which is the main advantage over system (9.6): the region of stability has been enlarged considerably. The larger the coupling strengths, the larger the equilibrium speed α can be depending on the values of the set points L_{i1}, L_{i2}, according to (9.25). By carefully choosing the set points L_{i1}, L_{i2} the platoon can be made to drive at a desired velocity.

In Section 9.4 the drag coefficient determined the maximum stable coupling strength: a small p-value implied a small maximum K-value yielding stability. This restriction is removed by the bidirectional coupling. The decay of the transient can be made much faster compared to vehicles strings with unidirectional ring coupling by choosing sufficiently large K_1 and K_2-values. This is demonstrated in Figure 9.6, with the parameter values given by

$$\begin{array}{lll} K_1 = 0.16 & L_{11} = 20.6 & L_{i1} = .6,\ i = 2, \ldots, 10, \\ K_2 = 0.14 & L_{N2} = 21 & L_{i2} = 1,\ i = 1, \ldots, 9, \\ p = 0.2 & & \omega_i = 0,\ i = 1, \ldots, 10. \end{array}$$

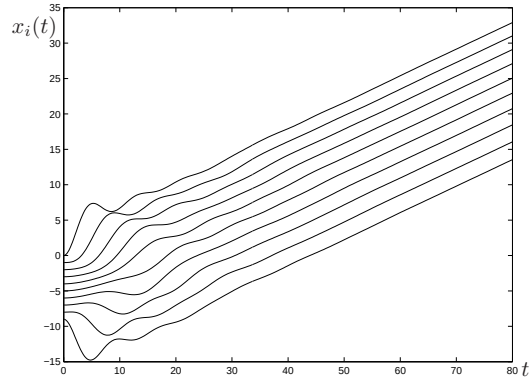

Figure 9.6: Simulation of a ten vehicle platoon with double ring coupling.

9.8.3 String Stability

As stated in Section 9.5, string stability of a platoon ensures that errors decrease as they propagate upstream through the platoon. It was proved that in general unidirectional ring coupling does not produce string stable platoons. However, using simulations we showed that in practical situations the errors indeed attenuate when moving from the head towards the tail of the platoon. From the analysis in traditional leader-follower strategies it follows that if a platoon is not string stable and identical controllers are used, errors grow as they propagate through the platoon. The larger the platoon, the larger the errors become at the platoon's tail.

In the present section the interconnection topology is a *bi*directional ring and identical controllers are implemented. Simulations show that in the case of bidirectional coupling the platoon is not string stable (cfr. Figure 9.7). Contrary to leader-follower control this does *not* imply that errors continuously grow when propagating from the head of the platoon towards its tail.

Figure 9.7 presents 4 consecutive separation distance errors e_5 to e_8. Clearly, $||e_6(t)||_\infty < ||e_7(t)||_\infty < ||e_8(t)||_\infty$ which implies that the system is not string stable. On the other hand, $||e_6(t)||_\infty < ||e_5(t)||_\infty$, showing that the error does not grow between *every* pair of consecutive interdistances. (The same simulation showed that $||e_i(t)||_\infty < ||e_{i-1}(t)||_\infty$, $i = 2, 3, 4, 5$). We conclude that although the platoon is not string stable, it exhibits a desirable behavior.

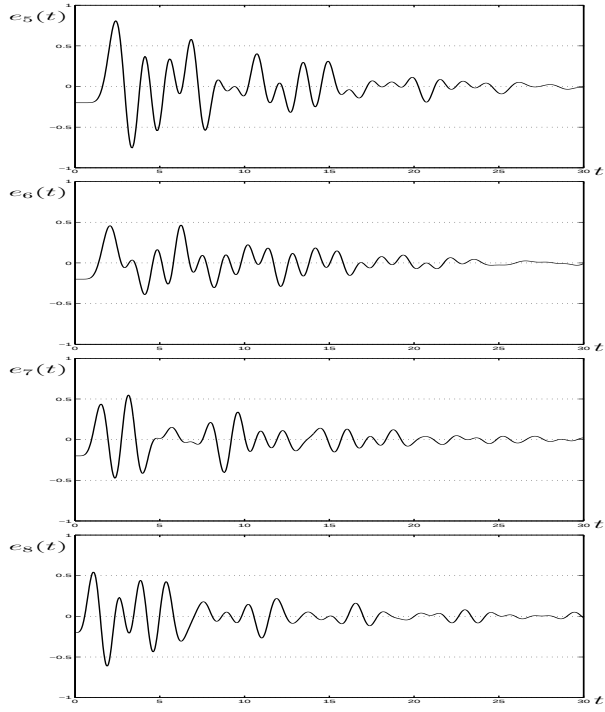

Figure 9.7: Evolution of the separation distances e_5 to e_8 of a ten vehicle platoon with bidirectional ring coupling.

9.8.4 Robustness

In this section robustness of the bidirectional ring coupling against malfunctions is investigated. Let us first consider the situation where one of the vehicles receives an upper bound on its velocity. It can no longer drive at the speed required by the equilibrium solution. This situation was also considered in Section 9.6 for the unidirectional ring coupling. The parameter

values are given by

$$\begin{array}{llll} K_1 = 10 & L_{11} = -18 & L_{i1} = 2, & i = 2, \ldots, 10, \\ K_2 = 10 & L_{N2} = -18 & L_{i2} = 2, & i = 1, \ldots, 9, \\ p = 0.2 & N = 10 & \omega_i = 1, & i = 1, \ldots, 10. \end{array}$$

From (9.25) the velocity of the equilibrium solution is 5 m/s. At $t = 50$ s the maximum velocity of the sixth vehicle becomes 2 m/s. This situation is simulated in Figure 9.8. The simulation shows that the platoon reacts to

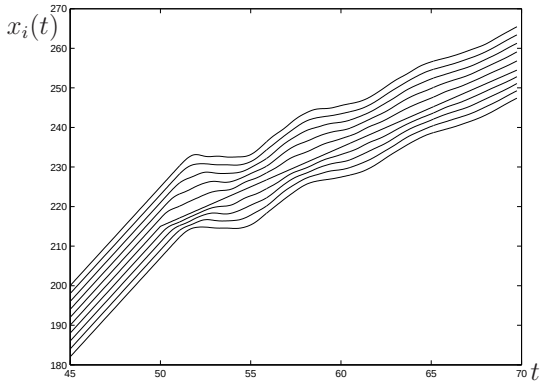

Figure 9.8: Evolution of the position for a platoon of 10 vehicles. At $t = 80$ s, the 6-th vehicle starts malfunctioning and cannot drive faster than 2 m/s

the malfunction as desired. All vehicles adapt their speed to the slow vehicle and the platoon does not split. Compared to Figure 9.5 representing the same malfunction in a platoon with unidirectional ring coupling, there is no gap between the malfunctioning vehicle and its immediate forward neighbor. This is simply the result of the different choice of set points L_{ij}: in the present section they have been chosen such that $\sum_{i=1}^{10} L_{ij} = 0,\ j = 1, 2$.

Now consider the situation where one of the vehicles receives a lower bound on its velocity and is forced to drive faster than the speed required by the equilibrium solution. The parameter values are the same as above, except for the reference speeds, which are given by $\omega_i = 0.1, i = 1, \ldots, 10$. At $t = 50$ s the minimum velocity of the fifth vehicle becomes 6 m/s. Figure 9.9 presents a simulation. As explained in Section 9.6 the unidirectional ring coupling and leader-follower strategies are not able to avoid collisions when this type of malfunctions occur. The simulation of Figure 9.9 clearly shows that with bidirectional ring coupling the platoon responds as desired.

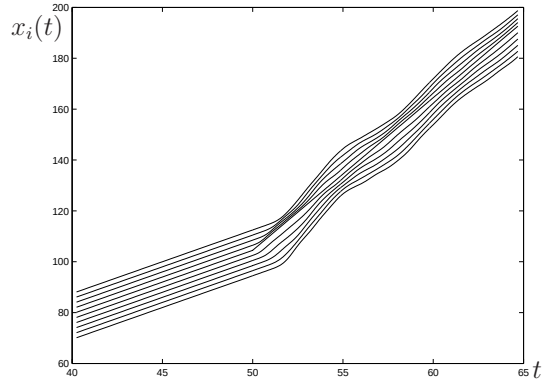

Figure 9.9: Evolution of the position for a platoon of 10 vehicles. At $t = 50$ s, the 5-th vehicle starts malfunctioning and cannot drive slower than 6 m/s

9.9 Conclusions

In the present chapter several control strategies for strings of vehicles are proposed. All strategies have a self-organizing property in common; there is no leader/master vehicle present. The coupling structures are uni- or bidirectional ring couplings. We prove that the resulting behavior of the system is a platoon of vehicles moving at a constant velocity with a constant distance separating consecutive vehicles. In the case of unidirectional ring coupling it is proven that for a class of identical controllers the system is asymptotically stable for sufficiently small coupling strength. An upper bound of this coupling strength is calculated, below which the system is asymptotically stable, independent of the number of vehicles in the platoon. The concept of string stability of a platoon is discussed and applied to the proposed interconnection. We present some simulations supporting the claim that the system is well-behaved with respect to string stability. For the bidirectional ring case it is shown that the platoon is stable if the coupling strengths in forward and backward direction are sufficiently close to each other. This yields an improvement over the unidirectional ring case, since the coupling strengths may be large, resulting in a fast decay of the transient behavior. Furthermore, the platoon's response to malfunctions is improved.

Chapter 10

Conclusions

In Chapters 1 and 8 it is explained how systems of interacting oscillators possess a wide area of application. The Kuramoto model, introduced in the second chapter, is presented as a model suited for describing such systems: it retains the common characteristics between the systems while discarding all particularities. It is a simplified model capable of explaining the different types of behavior observed in networks (also called populations) of coupled oscillators. Due to the simplifications, a detailed mathematical analysis is made possible. It is important to notice that, although the Kuramoto model can be applied more generally, the interconnection topology originally used is all-to-all coupling: each oscillator interacts with all the other oscillators in the population.

At the time of the research presented in this dissertation, the analysis of the Kuramoto model for infinitely large populations was already well known, but there was still a need for an analysis of *finite populations*. All oscillator systems encountered in the physical world are finite. Infinite systems can be thought of as a mathematical idealization of finite systems and may be easier to analyze, revealing some properties of their finite counterparts, but a finite analysis provides more precise information on the system under consideration.

Thus, the first novel result in this dissertation is the sought-for analysis of **finite networks of all-to-all coupled oscillators** described by the Kuramoto model. The oscillators need not be identical, i.e. they may possess different natural frequencies ω_i. Our results reveal qualitative differences with the infinite analysis. Both analyses make use of an auxiliary quantity called the complex order parameter. The amplitude of this parameter gives information on the type of behavior exhibited by the system. In the infinite case this amplitude always tends to a constant r_∞. If the interactions between the oscillators are weak, $r_\infty = 0$ and it is concluded that the oscillators act as if uncoupled. When the coupling strength exceeds some critical value K_T,

$r_\infty \neq 0$ and the population is said to exhibit *partial synchronization*: one group of oscillators *phase locks* (i.e. all oscillators of the group oscillate at the same frequency with constant mutual phase differences), while a second group consisting of the remaining oscillators still acts as if uncoupled. The phase locking group grows continuously with increasing coupling strength until the entire population is phase locking for infinitely large coupling strength.

The behavior of a finite population is quite different. The amplitude r of the order parameter does not always converge to a constant. Convergence depends on the size of the coupling strength. If the coupling strength is small, the oscillators act as if uncoupled, similarly to the infinite case, but r varies with time. If the coupling strength exceeds a threshold value K_P, the population splits into two or more groups: some oscillators start to *entrain* each other (i.e. their mutual phase difference becomes bounded), while the remaining oscillators still behave as if they were uncoupled. This type of behavior is called *partial entrainment*; the corresponding amplitude of the order parameter varies with time. The number of oscillators entraining each other increases in discrete steps with increasing coupling strength. When the coupling strength increases even further and becomes larger than some value K_T, r tends to a constant r_∞ and the entire population phase locks.

We present an algorithm to compute the value of K_T. A necessary and sufficient condition for phase locking is obtained in Theorem 30. The main result of our analysis is the establishment of stability of *each* phase locking solution for general frequency distributions:

- If the amplitude r_∞ satisfies the consistency condition (6.14) containing minus signs, the corresponding phase locking solution is *locally unstable*.

- The phase locking solution with r_∞ satisfying the consistency condition (6.14) containing only plus signs is *locally asymptotically stable* if and only if condition (6.39) is satisfied.

Results on partial entrainment of a generic population of N oscillators are hard to obtain. We found the following results for the three oscillator network:

- The onset of partial entrainment K_P satisfies $K_P \in (1.5\Delta\omega, 1.7044\Delta\omega]$, with $\Delta\omega = \min W$, where $W = \{\omega_{ij} \mid \omega_{ij} = |\omega_i - \omega_j|,\ i \neq j\}$.

- Proof of existence: let $\omega_1 < \omega_2 < \omega_3$ and $|\omega_2 - \omega_1| = \min W$. If $K > 4.065(\omega_2 - \omega_1)$ then $\theta_2 - \theta_1$ is bounded.

- If the natural frequencies are such that $\omega_1 = \omega_2$, then there exist solutions with $(\theta_2 - \theta_1)(t) = 0,\ \forall t \in \mathbb{R}$ and these solutions are locally stable.

A separate chapter discusses all-to-all coupled *identical* oscillators. This class of systems exhibits phase locking for every non-zero coupling strength. The phase locking solutions are explicitly determined. Every phase locking solution

- has a corresponding amplitude $r_\infty = 0$, or
- is an elementary solution, i.e. the phase difference between each pair of oscillators is either π or 0, or
- is the synchronized solution, i.e. all phase differences zero.

The above cases are not exclusive, since some elementary solutions have zero amplitude of the order parameter. It is proven that the synchronized solution is asymptotically stable almost everywhere.

After the analysis of all-to-all coupled networks, we decided to investigate other types of interconnection topologies, still using the Kuramoto model. We chose to examine the **unidirectional ring** topology: the oscillators are coupled in a ring; each oscillator is coupled to exactly one other oscillator and the couplings are either all directed clockwise or counterclockwise. Unidirectional ring coupling has some interesting applications in biology and antenna theory. Furthermore the interconnection possesses some extra structure which the analysis can benefit from. We did not consider investigation of the bidirectional ring coupling, since it had already been extensively described in the literature, albeit not in the setting of the Kuramoto equations. As in the case of all-to-all coupling, a ring of *identical* oscillators exhibits phase locking for every non-zero coupling strength. Each phase locking solution belongs to exactly one of the following classes:

- the class of travelling wave solutions, i.e. equal phase differences between consecutive oscillators,
- the class of elementary solutions,
- the synchronized solution.

For *nonidentical* oscillators it is proven that there exist phase locking solutions for sufficiently strong coupling. An algorithm to obtain all phase locking solutions is constructed. The phase locking solutions can be classified into classes, each with its own stability properties according to Table 7.1. The stability properties are obtained by means of a novel extension of Gershgorin's theorem. We proved that a phase locking solution is locally asymptotically stable if and only if

- all phase differences between neighboring oscillators, denoted by ϕ_i, are contained in $(\frac{-\pi}{2}, \frac{\pi}{2})$, or

- exactly one of the phase differences between neighboring oscillators is contained in $(\frac{\pi}{2}, \frac{3\pi}{2})$ and $\sum_{j=1}^{N} \prod_{k=1,\, k\neq j}^{N} \cos\phi_k > 0$ is satisfied.

Applying these stability results to a ring of identical oscillators, it follows that the synchronized solution is stable, together with the travelling wave solutions for which $\phi_i := \theta_i - \theta_{i-1} < \frac{\pi}{2}$. The remaining travelling wave solutions are unstable, as are all the elementary solutions. To conclude the examination of unidirectional ring coupling, the stability results are extended from sinusoidal interconnections to a class of odd functions.

Inspired by the results of the unidirectional ring coupling of oscillators, we transposed this interconnection structure to a different domain of application, where the interconnected systems are vehicles. In Chapter 9 several control strategies for **strings of vehicles** are proposed. All strategies have a self-organizing property in common; there is no leader/master vehicle present. The vehicles are coupled on the control level, with a uni- or bidirectional ring coupling. In the unidirectional ring, each vehicle measures the distance with its immediate forward neighbor and the lead vehicle in the platoon receives information on the position of the last vehicle in the platoon. In the bidirectional case each vehicle receives information on the position of both forward and backward neighboring vehicles; the first and last vehicle in the string exchange information on their positions as well, establishing a ring structure. We prove that the resulting behavior of the system is a platoon of vehicles moving at a constant velocity with a constant distance separating consecutive vehicles. In the case of unidirectional ring coupling it is proven that for a class of identical controllers the system is asymptotically stable for sufficiently small coupling strength. An upper bound of this coupling strength is calculated, below which the system is asymptotically stable, independent of the number of vehicles in the platoon. The concept of string stability of a platoon is discussed and applied to the proposed interconnection. A string of vehicles is called string stable if disturbances are attenuated as they propagate down the string. We present some simulations supporting the claim that the system is well-behaved with respect to string stability. For the bidirectional ring case it is shown that the platoon is stable if the coupling strengths in forward and backward direction are sufficiently close to each other, thus yielding an improvement over the unidirectional ring case: the decay of the transient behavior is much faster. Furthermore, the control structure renders the platoon robust with respect to malfunctioning vehicles. Assume one of the vehicles receives a lower bound on its velocity, that is larger than the equilibrium velocity. Simulations show that the platoon will adapt to the malfunctioning vehicle without collisions. Similarly, when one of the vehicles has an upper bound on its velocity, that is smaller than the equilibrium velocity, the platoon will adapt to this weakest link by assuming the maximum velocity attainable by the malfunctioning vehicle.

Appendix A

Definitions and Theorems

The following definitions are found in [26] and/or [43]. Consider the nonlinear autonomous system

$$\dot{x} = f(x), \qquad x \in \mathbb{R}^n, f : \mathbb{R}^n \to \mathbb{R}^n. \tag{A.1}$$

We assume that f is locally Lipschitz in $\mathbb{R}^n$ in order to ensure that (A.1) has a unique solution through every point in $\mathbb{R}^n$.

Definition 39. *Let the subset $X \in \mathbb{R}^n$ be open and connected and let $I \subset \mathbb{R}$ be an interval. The function $\phi : I \to \mathbb{R}^n$ is called* a solution *of system (A.1) if $\forall t \in I : \phi(t) \in X$, $\phi \in C^1(I)$ and*

$$\frac{d\phi}{dt}(t) = f(\phi(t)), \quad \forall t \in I,$$

with $C^1(I)$ denoting the class of continuously differentiable functions on I.

Definition 40. *Let the subset $X \in \mathbb{R}^n$ be open and connected and let $[0, \alpha] \subset \mathbb{R}$ be an interval, with $\alpha > 0$. The function $\phi(., x_0) : [0, \alpha] \to \mathbb{R}^n$, $x_0 \in \mathbb{R}^n$ is called* the solution of system (A.1) starting in x_0, *if $\forall t \in I : \phi(t, x_0) \in X$, $\phi \in C^1(I)$ and*

$$\frac{d\phi}{dt}(t, x_0) \equiv f(\phi(t, x_0)) \quad \textit{and} \quad \phi(0, x_0) = x_0.$$

Definition 41. *A solution ϕ starting at x_0 is called an* equilibrium point *or* fixed point *of system (A.1), when $\phi(t, x_0) = x_0$, $\forall t > 0$.*

Definition 42. *The set of initial states converging along solutions to the equilibrium point x_0 as $t \to \infty$ is called the* stable manifold of x_0.

Definition 43. *A solution is called* nontrivial periodic *if there exists a $T \in \mathbb{R} : T > 0$ such that $\phi(t + T) = \phi(t)$, $\forall t \geq 0$ and if it is not a constant solution.*

Definition 44. *Let $\phi(t, x_0)$ denote the solution of (A.1) starting in x_0 as defined above. Then for $t \in I$, the mapping $\phi_t : \mathbb{R}^n \to \mathbb{R}^n$; $\phi_t(y) := \phi(t, y)$ is a C^1-diffeomorphism from $Y \subset \mathbb{R}^n$ to $\phi_t(Y) \subset \mathbb{R}^n$. This mapping, or also the mapping from $\mathbb{R} \times \mathbb{R}^n \to \mathbb{R}^n$ defined by $(t, y) \mapsto \phi(t, y)$ is called the* flow *of the vector field f.*

Definition 45. *Let $\phi : I \to \mathbb{R}^n$ denote a solution of (A.1). The* trajectory or orbit *γ of $\phi(t)$ is defined by*

$$\gamma := \{x \in \mathbb{R}^n \mid x = \phi(t),\ t \in I\}.$$

A trajectory is called closed *if it is the trajectory of a nontrivial periodic solution.*

Whenever we refer to a periodic solution it is tacitly assumed to be nontrivial.

Definition 46. *The point $p \in \mathbb{R}^n$ is called a* positive limit point *or* omega limit point *of the trajectory γ of a solution $\phi(t)$ if there is a sequence $\{t_n\}$, with $t_n \to \infty$ as $n \to \infty$, such that $\phi(t_n) \to p$ as $n \to \infty$. The set of all positive limit points of γ is* the positive limit set *or* omega limit set *of γ.*

Definition 47. *One defines the* negative or alpha limit set *by replacing $t_n \to \infty$ by $t_n \to -\infty$ in the preceding definition.*

Definition 48. *The* positive semiorbit *through x_0 is the set*

$$\gamma^+(x_0) = \{\phi(t, x_0) \mid t \in \mathbb{R}^+\}.$$

The negative semiorbit *through x_0 is the set*

$$\gamma^-(x_0) = \{\phi(t, x_0) \mid t \in \mathbb{R}^-\}.$$

Definition 49. *A* limit cycle *is a closed orbit Γ such that Γ is the positive limit set of a positive semiorbit $\gamma^+(y)$ or the negative limit set of a negative semiorbit $\gamma^-(y)$ for some $y \notin \Gamma$.*

Define an ϵ-neighborhood U_ϵ of the trajectory γ by

$$U_\epsilon = \{x \in \mathbb{R}^n \mid \text{dist}(x, \gamma) < \epsilon\}, \tag{A.2}$$

where

$$\text{dist}(x, \gamma) = \inf_{y \in \gamma} \|x - y\|.$$

Definition 50. *The solution $\phi(., x_0)$ of (A.1) is said to be* orbitally stable *if for every $\epsilon > 0$ there exists a $\delta(\epsilon) > 0$ such that*

$$x_1 \in U_\delta \Rightarrow \phi(t, x_1) \in U_\epsilon, \forall t \geq 0.$$

Definition 51. *The solution $\phi(., x_0)$ of (A.1) is said to be* asymptotically orbitally stable *if it is orbitally stable and if a δ can be chosen such that*

$$x_1 \in U_\delta \Rightarrow \lim_{t\to\infty} dist(\phi(t, x_1), \gamma) = 0.$$

Definition 52. *If a periodic solution $\phi(., x_0)$ is asymptotically orbitally stable, then its trajectory γ is called a* stable limit cycle.

Definition 53. *The solution $\phi(., x_0)$ of (A.1) is said to have the* asymptotic phase property *if there exists a $\delta > 0$ such that to each initial value x_1 satisfying $dist(x_1, \gamma) < \delta$ there corresponds an* asymptotic phase $\alpha(x_1) \in \mathbb{R}$ *with the property*

$$\lim_{t\to\infty} |\phi(t + \alpha(x_1), x_1) - \phi(t, x_0)| = 0. \tag{A.3}$$

Definition 54. *The non-constant periodic solution p with period $T > 0$ and trajectory γ of system (A.1) is* non-isolated *if for each $\epsilon > 0$ there exists an $x_0 \in \mathbb{R}^n$ such that*

1. $0 < dist(x_0, \gamma) < \epsilon$,
2. $\phi(t, x_0)$ *is a periodic solution with period* $\tau(x_0)$,
3. $|\tau(x_0) - T| < \epsilon$.

If the above conditions are not *satisfied, then the solution p is said to be* isolated.

Theorem 48. *Denote the eigenvalues of a symmetric matrix $M \in \mathbb{R}^{n\times n}$ by $\lambda_1(M) \geq \lambda_2(M) \geq \ldots \geq \lambda_n(M)$. Let $\tilde{A}$ and $\tilde{B}$ be symmetric matrices in $\mathbb{R}^{n\times n}$, with $\tilde{B}$ positive semidefinite. Then*

$$\lambda_k(\tilde{A} + \tilde{B}) \geq \lambda_k(\tilde{A}), \qquad k = 1, 2, \ldots, n. \tag{A.4}$$

If $\tilde{B}$ is positive definite then

$$\lambda_k(\tilde{A} + \tilde{B}) > \lambda_k(\tilde{A}), \qquad k = 1, 2, \ldots, n. \tag{A.5}$$

Theorem 49 (Gershgorin's theorem)**.** *For a matrix $A = (a_{ij}) \in \mathbb{C}^{n\times n}$, define*

$$R_i := \sum_{j=1,\, j\neq i}^{n} |a_{ij}|.$$

Each eigenvalue of A is contained in at least one of the disks $D_i \subset \mathbb{C}$, defined by

$$D_i := \{z \in \mathbb{C} : |z - a_{ii}| \leq R_i\}.$$

It is important to note that not necessarily all Gershgorin disks contain at least one eigenvalue. The following theorem gives some more detailed information regarding the eigenvalues of A [60].

Theorem 50. *If* $\left(\cup_{j=1}^{m} D_j\right) \cap \left(\cup_{j=m+1}^{n} D_j\right) = \emptyset$*, then* $\cup_{j=1}^{m} D_j$ *contains exactly* m *eigenvalues of* A*, with each eigenvalue being counted according to its algebraic multiplicity. The remaining eigenvalues are in* $\cup_{j=m+1}^{n} D_j$*.*

We extended this theorem as follows.

Theorem 51. *If* $\left(\cup_{j=1}^{m} D_j\right) \cap \left(\cup_{j=m+1}^{n} D_j\right) = \{p\}, p \in \mathbb{C}$*, then* $\cup_{j=1}^{m} D_j$ *contains at least* m *eigenvalues of* A*, with each eigenvalue being counted according to its algebraic multiplicity. The region defined by* $\cup_{j=m+1}^{n} D_j$ *contains at least* $n - m$ *eigenvalues.*

Proof. Define $A_D = \text{diag}(a_{11}, a_{22}, \ldots, a_{nn})$ and let $A = A_D + B$. For $t \in [0, 1]$ define $A_t = A_D + tB$. Then $A_0 = A_D$ and $A_1 = A$. Call the eigenvalues of A_t, λ_t. Let $D_{j,t}$ denote a disk with center a_{jj} and radius $r_{j,t}$. Because of Theorem 50, for $t \in [0, 1)$ $\cup_{j=1}^{m} D_{j,t}$ contains m eigenvalues and $\cup_{j=m+1}^{n} D_{j,t}$ contains the remaining eigenvalues.

Suppose that for $t = 1$, $\cup_{j=1}^{m} D_{j,t}$ contains $k < m$ eigenvalues. This implies that

$$\exists j \in \{1, \ldots, m\}, \exists \lambda_t : \begin{cases} |\lambda_t - a_{jj}| \leq r_{j,t} \text{ for } t \in [0, 1), \\ |\lambda_t - a_{jj}| > r_{j,t} \text{ for } t = 1, \end{cases}$$

or equivalently, that there exists a continuous function $g(t) := |\lambda_t - a_{jj}| - r_{j,t}$:

$$\begin{cases} g(t) \leq 0 \text{ for } t \in [0, 1), \\ g(t) > 0 \text{ for } t = 1. \end{cases}$$

This is not possible, so the assumption was incorrect. Similarly it can be proven that $\cup_{j=m+1}^{n} D_j$ contains at least $n - m$ eigenvalues.

Suppose $\cup_{j=1}^{m} D_j$ contains $k > m$ eigenvalues. It then follows that at least $k - m$ eigenvalues are located in p. □

Bibliography

[1] R. Abraham, J. E. Marsden, and T. Ratiu. *Manifolds, Tensor Analysis, and Applications*. Springer, 1988.

[2] R. Adler. A study of locking phenomena in oscillators. *Proceedings of the IEEE*, 61(10):1380–1385, 1973.

[3] D. Aeyels and J. A. Rogge. Existence of partial entrainment and stability of phase locking behavior of coupled oscillators. *Progress of Theoretical Physics*, 112(6):921–942, 2004.

[4] D. Aeyels and J. A. Rogge. *Liber Amicorum: Richard Delanghe, een veelzijdig wiskundige*, chapter Networks of dynamical systems, pages 1 – 13. Academia Press, 2005.

[5] D. Aeyels and J. Rogge. Stability of phase locking and existence of partial entrainment in networks of globally coupled oscillators. In *6th IFAC-Symposium on Nonlinear Control Systems*, volume 3, pages 1031–1036, 2004.

[6] T. Apostol. *Calculus*. John Wiley and sons, 1967.

[7] E. Armstrong. Some recent developments in the audion receiver. *IRE Proceedings*, 3:215 – 247, 1915.

[8] J. Baillieul and C. I. Byrnes. Geometrical critical point analysis of lossless power system models. *IEEE Transactions on Circuits and Systems*, 29(11):724–737, 1982.

[9] J. Baillieul and C. I. Byrnes. The load flow equations for a 3-node electrical power system. *Systems & Control Letters*, 2:321–329, 1983.

[10] J. Baillieul and C. I. Byrnes. The singularity theory of the load flow equations for a 3-node electrical power system. *Systems & Control Letters*, 2:330–340, 1983.

[11] W. M. Boothby. *An Introduction To Differentiable Manifolds and Riemannian Geometry*. Academic Press, 1986.

[12] W. C. Bray. A periodic reaction in homogeneous solution and its relation to catalysis. *Journal of the American Chemical Society*, 43(6):1262–1267, 1921.

[13] E. Brown, P. Holmes, and J. Moehlis. *Perspectives and Problems in Nonlinear Science*, chapter Globally Coupled Oscillator Networks. Springer Verlag, 2003.

[14] O. M. Bucci, G. Mazzarella, and G. Panariello. Reconfigurable arrays by phase-only control. *IEEE Transactions on Antennas and Propagation*, 39(7):919–925, 1991.

[15] J. Buck and E. Buck. Synchronous fireflies. *Scientific American*, 234:74, 1976.

[16] C. C. Canavier, R. J. Butera, R. O. Dror, D. A. Baxter, J. W. Clark, and J. H. Byrne. Phase response characteristics of model neurons determine which patterns are expressed in a ring circuit model of gait generation. *Biological Cybernetics*, 77:367–380, 1997.

[17] J. Carr. *Applications of Centre Manifold Theory*. Springer, New York, 1982.

[18] B. Chance, E. K. Pye, A. K. Gosh, and B. Hess, editors. *Biological and biochemical oscillators*. Academic Press, New York, 1973.

[19] H-C. Chang, E. S. Shapiro, and R. A. York. Influence of the oscillator equivalent circuit on the stable modes of parallel-coupled oscillators. *IEEE Transactions on Microwave Theory and Techniques*, 45(8):1232–1239, 1997.

[20] J. J. Collins and I. Stewart. Coupled nonlinear oscillators and the symmetries of animal gaits. *Journal of Nonlinear Science*, 3(3):349–392, 1993.

[21] D. E. N. Davies. *The handbook of Antenna Design*, volume 2, chapter 12: Circular arrays, pages 298–329. IEEE, 1983.

[22] R. O. Dror, C. C. Canavier, R. J. Butera, J. W. Clark, and J. H. Byrne. A mathematical criterion based on phase response curves for stability in a ring of coupled oscillators. *Biological Cybernetics*, 80:11–23, 1999.

[23] L. Dussopt and J. M. Laheurte. Coupled oscillator array generating circular polarization. *IEEE Microwave and Guided Wave Letters*, 9(4):160–162, 1999.

[24] B. Ermentrout. The behavior of rings of coupled oscillators. *Journal of Mathematical Biology*, 23:55–74, 1985.

[25] G. B. Ermentrout and N. Kopell. Frequency plateaus in a chain of weakly coupled oscillators. *SIAM Journal of Mathematical Analysis*, 15(2):215–237, 1984.

[26] M. Farkas. *Periodic Motions*. Springer, New York, 1994.

[27] R. J. Field and M. Burger, editors. *Oscillations and Traveling Waves in Chemical Systems*. Wiley, 1985.

[28] R. J. Field, R. M. Noyes, and E. Körös. Oscillations in chemical systems 2. Thorough analysis of temporal oscillation in bromate-cerium-malonic acid system. *Journal of the American Chemical Society*, 94(25):8649, 1972.

[29] R. J. Field and R. M. Noyes. Explanation of spatial band propagation in Belousov reaction. *Nature*, 237(5355):390, 1972.

[30] R. J. Field and R. M. Noyes. Oscillations in chemical systems 4. Limit cycle behavior. *Journal of Chemical Physics*, 60(5):1877–1884, 1974.

[31] H. Fujii and Y. Sawada. Phase-difference locking of coupled oscillating chemical systems. *Journal of Chemical Physics*, 69(8):3830–3832, 1978.

[32] M. Golubitsky, I. Stewart, P-L. Buono, and J. J. Collins. A modular network for legged locomotion. *Physica D*, 115:56–72, 1998.

[33] M. Golubitsky and I. Stewart. *Singularities and Groups in Bifurcation Theory, Vol. II*. Springer-Verlag, 1988.

[34] R. L. De Haan. *Factors influencing myocardial contractility*, chapter Spontaneous activity of cultured heart cells: an introduction, pages 217–230. Academic press, 1967.

[35] P. Hadley, M. R. Beasley, and K. Wiesenfeld. Phase locking of Josephson-junction series arrays. *Physical Review B*, 38(13):8712–8719, 1988.

[36] R. L. Haupt. Phase-only adaptive nulling with a genetic algorithm. *IEEE Transactions on Antennas and Propagation*, 45(6):1009–1015, 1997.

[37] U. Helmke and J. B. Moore. *Optimization and Dynamical Systems*. Springer, London, 1994.

[38] P. A. Ioannou and C. C. Chien. Autonomous intelligent cruise control. *IEEE Transactions on Vehicular Technology*, 42(4):657–672, 1993.

[39] Z. Jin and R. M. Murray. Double-graph control strategy of multi-vehicle formations. In *Proceedings of the 43rd IEEE Conference on Decision and Control*, 2004.

[40] B. D. Josephson. Possible new effects in superconductive tunnelling. *Physics Letters*, 1:251 – 253, 1962.

[41] M. R. Jovanović and B. Bamieh. On the ill-posedness of certain vehicular platoon control problems. In *Proceedings of the 43rd IEEE Conference on Decision and Control*, 2004.

[42] J. Keener and J. Sneyd. *Mathematical Physiology*. Springer, New York, 1998.

[43] H. K. Khalil. *Nonlinear Systems*. Macmillan Publishing Company, 1992.

[44] M. E. Khatir and E. J. Davison. Bounded stability and eventual string stability of a large platoon of vehicles using non-identical controllers. In *Proceedings of the 43rd IEEE Conference on Decision and Control*, 2004.

[45] Y. Kuramoto. *Chemical Oscillations, Waves and Turbulence*. Springer Berlin, 1984.

[46] Y. Kuramoto. Cooperative dynamics of oscillator community. *Progress of Theoretical Physics Supplement*, 79:223–240, 1984.

[47] K. Kurokawa. Noise in synchronized oscillators. *IEEE Transactions on Microwave Theory and Techniques*, MTT-16(4):234–240, 1968.

[48] C. R. Laing. Rotating waves in rings of coupled oscillators. *Dynamics and Stability of Systems*, 13(4):305–318, 1998.

[49] W. S. Levine and M. Athans. On the optimal error regulation of a string of moving vehicles. *IEEE Transactions on Automatic Control*, AC-11(3):355–361, 1966.

[50] A. J. Lewy, V. K. Bauer, S. Ahmed, K. H. Thomas, N. L. Cutler, C. M. Singer, M. T. Moffit, and R. L. Sack. The human phase response curve (PRC) to melatonin is about 12 hours out of phase with the PRC to light. *Chronobiology International*, 15(1):71 – 83, 1998.

[51] P. Liao and R. A. York. A new phase-shifterless beam-scanning technique using arrays of coupled oscillators. *IEEE Transactions on Microwave Theory and Techniques*, 1993.

[52] Z. Lin, M. Broucke, and B. Francis. Local control strategies for groups of mobile autonomous agents. *IEEE Transactions on Automatic Control*, 49(4):622–629, 2004.

[53] Z. Lin, B. Francis, and M. Maggiore. Necessary and sufficient graphical conditions for formation control of unicycles. *IEEE Transactions on Automatic Control*, 50(1):121–127, 2005.

[54] S. Lubkin. Unidirectional waves on rings: models for chiral preference of circumnutating plants. *Bulletin of Mathematical Biology*, 56(5):795, 1994.

[55] C. Luo, J. W. Clark, C. Canavier, D. A. Baxter, and J. H. Byrne. Multimodal behavior in a four neuron ring circuit: mode switching. *IEEE Transactions on Biomedical Engineering*, 51(2):205–218, 2004.

[56] M. Marek and I. Stuchl. Synchronization in two interacting oscillatory systems. *Biophysical Chemistry*, 4:241–248, 1975.

[57] J. A. Marshall, M. E. Broucke, and B. A. Francis. Formations of vehicles in cyclic pursuit. *IEEE Transactions on Automatic Control*, 49(11):1963–1974, 2004.

[58] J. Marshall, M. Broucke, and B. Francis. A pursuit strategy for wheeled-vehicle formations. In *Proceedings of the 42nd IEEE Conference on Decision and Control*, 2003.

[59] S. M. Melzer and B. C. Kuo. Optimal regulation of systems described by a countably infinite number of objects. *Automatica*, 7:359–366, 1971.

[60] C. D. Meyer. *Matrix Analysis and Applied Linear Algebra*. SIAM, 2000.

[61] D. S. Minors, J. M. Waterhouse, and A. Wirzjustice. A human phase response curve to light. *Neuroscience Letters*, 133(1):36 – 40, 1991.

[62] R. E. Mirollo and S. H. Strogatz. Stability of incoherence in a population of coupled oscillators. *Journal of Statistical Physics*, 63:613–635, 1991.

[63] L. Moreau. Stability of multiagent systems with time-dependent communication links. *IEEE Transactions on Automatic Control*, 50(2):169 – 182, 2005.

[64] J. D. Murray. *Mathematical Biology*. Springer, Berlin Heidelberg, 1993.

[65] S. Nichols and K. Wiesenfeld. Ubiquitous neutral stability of splay-phase states. *Physical Review A*, 45(12):8430 – 8435, 1992.

[66] R. M. Noyes, R. J. Field, and E. Körös. Oscillations in chemical systems 1. Detailed mechanism in a system showing temporal oscillations. *Journal of the American Chemical Society*, 94(4):1394, 1972.

[67] R. Olfati-Saber and R. M. Murray. Consensus problems in networks of agents with switching topology and time-delays. *IEEE Transactions on Automatic Control*, 49(9):1520–1533, 2004.

[68] A. Pant, P. Seiler, and K. Hedrick. Mesh stability of look-ahead interconnected systems. *IEEE Transactions on Automatic Control*, 47(2):403–407, 2002.

[69] L. E. Peppard. String stability of relative-motion pid vehicle control systems. *IEEE Transactions on Automatic Control*, AC-19(10):579–581, 1974.

[70] A. Pikovsky, M. Rosenblum, and J. Kurths. *Synchronization, a universal concept in nonlinear sciences*. Cambridge University Press, 2001.

[71] R. J. Pogorzelski, P. F. Maccarini, and R. A. York. A continuum model of the dynamics of coupled oscillator arrays for phase-shifterless beam scanning. *IEEE Transaction on Microwave Theory and Techniques*, 47(4):463–469, 1999.

[72] I. Prigogine and R. Lefever. Symmetry breaking instabilities in dissipative systems II. *Journal of Chemical Physics*, 48:1695–1700, 1968.

[73] J. A. Rogge and D. Aeyels. Stability of phase locking in a ring of unidirectionally coupled oscillators. In *Proceedings of the 43rd IEEE Conference on Decision and Control*, 2004.

[74] J. A. Rogge and D. Aeyels. Stability of phase locking in a ring of unidirectionally coupled oscillators. *Journal of Physics A: Mathematical and General*, 37:11135–11148, 2004.

[75] J. A. Rogge and D. Aeyels. Vehicle platoons formed through self-regularisation. In *Proceedings of the 2005 International Symposium on Nonlinear Theory and its Applications*, 2005.

[76] J. Rogge and D. Aeyels. Decentralized control of vehicle platoons with interconnection possessing ring topology. In *Proceedings of the 44th IEEE Conference on Decision and Control and European Control Conference ECC 2005*, 2005.

[77] W. Sarlet. *Differentiaalmeetkundige structuren en mechanica*. Universiteit Gent.

[78] P. Seiler, A. Pant, and K. Hedrick. Disturbance propagation in vehicle strings. *IEEE Transactions on Automatic Control*, 49(10):1835–1841, 2004.

[79] R. Seydel. *Practical Bifurcation and Stability Analysis*. Springer New York, 1994.

[80] K. R. Sharma and R. M. Noyes. Oscillations in chemical systems 13. Detailed molecular mechanism for Bray-Liebhafsky reaction of iodate and hydrogen-peroxide. *Journal of the American Chemical Society*, 98(15):4345–4361, 1976.

[81] J. Silber, L. Fabiny, and K.Wiesenfeld. Stability results for in-phase and splay-phase states of solid-state laser arrays. *Journal of the Optical Society of America B*, 10(6):1121, 1993.

[82] S. L. Smith, M. E. Broucke, and B. A. Francis. A hierarchical cyclic pursuit scheme for vehicle networks. *Automatica*, 2005.

[83] S. S. Stanković, M. J. Stanojević, and D. Šiljak. Decentralized overlapping control of a platoon of vehicles. *IEEE Transactions on Control Systems Technology*, 8(5):816–832, 2000.

[84] K. D. Stephan and W. A. Morgan. Analysis of interinjection-locked oscillators for integrated phased arrays. *IEEE Transactions on Antennas and Propagation*, AP-35(7):771–781, 1987.

[85] K. D. Stephan. Interinjection-locked oscillators for power combining and phased arrays. *IEEE Transactions on Microwave Theory and Techniques*, MTT-34(10):1017–1025, 1986.

[86] S.H. Strogatz. *Sync*. Hyperion, 2003.

[87] S. H. Strogatz. From Kuramoto to Crawford: Exploring the onset of synchronization in populations of coupled oscillators. *Physica D*, 143:1–20, 2000.

[88] D. Swaroop and J. K. Hedrick. String stability of interconnected systems. *IEEE Transactions on Automatic Control*, 41(3):249–356, 1996.

[89] C. J. Távora and O. J. M. Smith. Equilibrium analysis of power systems. *IEEE Transactions on Power Apparatus and Systems*, 91:1131–1137, 1972.

[90] T. Van Duzer and C. W. Turner. *Principles of Superconducting Devices and Circuits*. Elsevier, New York, 1981.

[91] J. L. van Hemmen and W. F. Wreszinski. Lyapunov function for the Kuramoto model of nonlinearly coupled oscillators. *Journal of Statistical Physics*, 72(1–2):145–166, 1993.

[92] T. Vicsek, A. Czirók, E. Ben-Jacob, I. Cohen, and O. Shochet. Novel type of phase transition in a system of self-driven particles. *Physical Review Letters*, 75(6):12261229, 1995.

[93] N. Wiener. *Nonlinear Problems in Random Theory*. MIT Press, 1958.

[94] J. L. Willems. Optimal control of a uniform string of moving vehicles. *Ricerche di automatica*, 2(2):184–192, 1971.

[95] A. T. Winfree. Spiral waves of chemical activity. *Science*, 175(4022):634, 1972.

[96] A. T. Winfree. *The Geometry of Biological Time*. Springer, New York, 1980.

[97] D. E. Woodward. Synthesis of phase-locking patterns in networks with cyclic group symmetries. *SIAM Journal of Applied Mathematics*, 50(4):1053–1072, 1990.

[98] D. Yanakiev and I. Kanellakopoulos. Nonlinear spacing policies for automated heavy-duty vehicles. *IEEE Transactions on Vehicular Technology*, 47(4):1365–1377, 1998.

[99] R.A. York and T. Itoh. Injection- and phase-locking techniques for beam control. *IEEE Transaction on Microwave Theory and Techniques*, 46(11):1920–1929, 1998.

[100] R. A. York, P. Liao, and J. J. Lynch. Oscillator array dynamics with broadband N-port coupling networks. *IEEE Transactions on Microwave Theory and Techniques*, 42(11):2040–2045, 1994.

[101] R. A. York. Nonlinear analysis of phase relationships in quasi-optical oscillator arrays. *IEEE Transactions on Microwave Theory and Techniques*, 41(10):1799–1809, 1993.

[102] M. Yoshimoto, K. Yoshikawa, and Y. Mori. Coupling among three chemical oscillators: synchronization, phase death, and frustration. *Physical Review E*, 47(2):864–874, 1993.

[103] J. Zhang, Y. Suda, T. Iwasa, and H. Komine. Vector Liapunov function approach to longitudinal control of vehicles in a platoon. *JSME international journal series C - Mechanical systems, machine elements and manufacturing*, 47(2):653–658, 2004.